PONTIFICIA UNIVERSIDAD CATÓLICA DE CHILE
PHYSICS FACULTY
PHYSICS INSTITUTE

NON-EQUILIBRIUM THERMOELECTRIC TRANSPORT THROUGH A HYBRID NANO-JUNCTION

by

Manuel Lautaro Álamo Ulloa

Thesis submitted to the Faculty of Physics
of Pontificia Universidad Católica de Chile, as one of the requirements
to qualify for the academic Master's degree in Physics.

Supervisor : Dr. Enrique Muñoz T. (PUC Chile)
Committee : Dr. Marcelo Loewe (PUC Chile)
Dr. Sebastián Reyes (PUC Chile)

January, 2018
Santiago, Chile

To my grandparents.

Acknowledgments

Since my bachelor thesis I have been working with Dr. Enrique Muñoz. In these almost four years I have learned what it means to be a scientist thanks to his teaching and the way he showed me how to perform a good and serious research. Thanks to him I acquired all the physical knowledge to prepare the work I here present and I found the exciting world of non-equilibrium many body physics. During all this time he has kept his door open to listen my concerns, even the simplest question I had he was willing to answer. He always had time to share his knowledge with me in order to guide me to be a better physicist. No matter the circumstances I always counted with his advice, support and sincerity, making the time I worked with him even more fruitful. For all of this I am most grateful.

I would also like to thank Dr. Marcelo Loewe for all the years of constant support. Since I was a bachelor student he was always there if I had any question or I needed any help. He was in every moment kind to me and willing to give me helpful advises. I also want to thank Dr. Rafael Benguria for all the considerations he had to my in all these years as bachelor and master student. No matter how fleeting it may have been a conversation with him, I could always find a valuable learning in his words.

I would like to thank to my friends in the Institute of Physics Christian Díaz, Daniel Pérez, Ricardo Rojas, Vicente Valenzuela, Ignacio Alvizú and Mauricio Sarabia for all the stimulating, intense and meaningful conversations we had, trying to better understand what and why we were doing what we were doing.

Finally I want to thank my family, specially my parents Alex and Cecilia, my brother Daniel and my girlfriend Carlita for all their love, patience and energy they always and constantly have gave to me.

Abstract

This thesis is focused in the study of transport phenomena in strongly correlated systems. Particularly we have evaluated the non-equilibrium thermoelectric transport current and thermoelectric transport coefficients of a hybrid system, composed by a quantum dot connected to a normal s-wave superconductor and a topological superconductor leads, using the Keldysh formalism and Floquet theory.

Due the non-conventional terminals, these system presents interesting correlations between different kind of quasi-particles, in particular, Cooper pairs and Majorana Fermions. The later are characterized by a non-abelian statistics and its discover in strongly correlated systems has opened new research horizons for the condensed matter community.

Our results show a non-linear electrical current for different magnetic fields, whose peaks are signatures of Majorana Bound States. We also show that the transport processes are highly mediated by Andreev reflections and Andreev bound states, which are the principal mechanism present in the superconducting proximity effect of these kind of systems.

Starting from the electrical current, we have evaluated the thermoelectric performance of the system for different magnetic fields, characterized by the Seebeck coefficient S, electrical and thermal conductivities σ, κ, Lorenz number L and the figure of merit ZT, which reaches its maximum value $ZT = 0.02\Delta/k_B$ at a finite magnetic field $H = 0.3\Delta$ at an applied bias voltage $0.7eV/\Delta$. We also found that this system has a Lorenz number which achieves a maximum and minimum values far apart to those reported for Fermi liquids, violating the Wiedemann-Franz law.

Contents

Abstract **iv**

1 Introduction **1**

1.1 Structure of the Thesis 2

2 Transport phenomena in topological and normal superconductors **3**

2.1 Majorana fermions and Majorana zero modes 4

2.2 Detection of Majorana Fermions 7

2.3 Andreev reflections 9

2.4 Thermoelectric transport 11

3 Non-equilibrium Green's function formalism **15**

3.1 Closed-time path contour 18

3.2 Fermionic Green's functions: functional integral approach 28

3.3 Fermionic Green's functions and Keldysh rotation 37

3.4 Non-equilibrium Dyson equation 43

4 The model: A superconductor-semiconductor QD-Topological superconductor nano-junction **45**

4.1 Our system 48

4.2 Current operator 50

4.3 Keldysh Green's functions 50

4.4 Green's functions in Floquet space 59

4.5 The tunneling current 62

5 Results and discussion **66**

5.1 Electric current 66

5.2 Thermoelectric performance 73

6 Conclusions and further work **80**

6.1 Conclusions 80

6.2 Further work 81

A Superconductor Green's function in the quasiclassical approximation **82**

B Superconductor Green's function rotation **94**

C Fourier Transform of the Keldysh Green's Functions **97**

D The Structure of the Keldysh component **102**

E Real part of the Current **104**

F Coulomb interaction **108**

Bibliography **111**

Chapter 1

Introduction

In the last decade, our understanding of the electronic band structure of solids has been drastically changed by the incorporation of topological effects and the realization of topological materials, like topological insulators and topological superconductors [1, 2]. It is based on the realization that spin-orbit interaction in materials can lead to such electronic phases which has been observed in real materials [3, 4, 5].

One of the most interesting features of topological insulators is the bulk-boundary correspondence, which means that for nontrivial topological invariants, there are gapless surface modes (edge states) despite of the insulating bulk behavior (similar to an ordinary insulator) away from the surface. These modes turn out to be Dirac fermions. Similarly, in topological superconductors there is typically a bulk gap for quasi-particle excitation, but nontrivial value of corresponding topological invariant again implies the existence of gapless surface modes, but in this case, these modes correspond to Majorana fermions [6].

Since one of the compelling criteria of material to be topological is that the system ought to have an energy gap, the topological concept extends over any gapped system, such as superconductors and superfluids.

Recently, there is an attempt to formulate the thermoelectric transport in topological-like systems theoretically [7]. The intersection of topology and thermoelectricity would open doors for novel phenomena and new opportunities for energy harvesting that are not available in conventional systems. This thesis aims to contribute in this new frontier of

condensed matter physics.

1.1 Structure of the Thesis

In chapter 2 we present a general introduction on the main concepts and processes relevant to the study of thermoelectric transport in topological systems. The mathematical foundations of non-equilibrium situations we are dealing with are described carefully in chapter 3, where the Keldysh formalism is derived from first principles. Further, in chapter 4, we present our nano junction model and calculate the non-equilibrium transport current through the system. Numerical results for the electric current and thermoelectric performance are presented in chapter 5. The work we present here concludes in chapter 6 where conclusions and further work are discussed.

Chapter 2

Transport phenomena in topological and normal superconductors

In this chapter we will present an introduction to important topics required to understand the problem of thermoelectric transport through a system where a conventional superconductor and a topological superconductor are involved, in which we will find different particles (or quasi-particles) like Cooper pairs and Majorana fermions. In particular, we will center our attention in the interesting appearance of the last one. In section 2.1, we will begin by giving a brief look at their history and a mathematical introduction of their most important properties. Despite their origin as an idea from fundamental particles, a possible realization in the form of quasi-particles in solid state systems was found much later. In section 2.2 we will look at the simplest model in order to find these quasi-particles in one dimension, the so called Kitaev model. Experimental realizations of the Kitaev model are also discussed. An important process which occurs at the interface between a metal and a superconductor, known as Andreev reflections is presented briefly in section 2.3. Finally section 2.4 presents a brief overview of thermoelectric processes which underlie many practical and technological applications.

2.1 Majorana fermions and Majorana zero modes

After Schrödinger found the nonrelativistic wave equation for fundamental particles, Paul Dirac in 1928 developed a relativistic wave equation, whose solutions are a four-component vector that describes spin 1/2 particles, which admits positive and negative energy solutions. Dirac proposed that the vacuum state is such that all negative energy states are filled up. Since we are dealing with fermions, it is impossible for any such state to be further occupied. This is called the Dirac sea. If we add fermions they only occupy a positive energy state. Further there is a gap $2m$ (considereing $c = 1$) between the highest negative energy state and the lowest possible energy state. If we inject energy to the system it is possible to promote one of the negative energy states to positive energy. We have thus produced a *particle* with positive energy and a *hole* in the sea of negative energy. This is an *antiparticle*. The particle and antiparticle are related by a symmetry operation that takes the complex conjugate of the wave function. When a particle and its antiparticle interact, they annihilate, producing a pair of photons. In 1937 an italian physicist, Ettore Majorana, recognized a specific representation of the complex Dirac equation. He noted that the Dirac equation can be separated into a pair of real wave equations, each of which describes a real fermionic field without the distinction of particles and antiparticles [8]. There are numerous examples of elementary particles described by the Dirac's equation and Dirac's solution, but none have been found that obeys that of Majorana. The discovery of fundamental particles or quasi-particles governed by Majorana's solution would have significant consequences in physics, from cosmology to condensed matter: one of the most interesting potential outcomes of the existence of Majorana fermions are leptogenesis [9, 10] in particle physics and quantum computing in solid-state physics [11].

Even though in solid state physics the only fermionic particles that matter for practical purposes are electrons, one can find different emergent quasi-particles, which are defined as collective excitations of the quantum many-body state, describing the interacting electron system. Some examples are phonons, polarons, magnons, plasmons, etc. In the condensed matter physics this quasi-particles act like elementary particles and it is possible to study their properties and symmetries.

If Dirac's fermions are described by operators written in terms of creation and annihilation operators $\hat{c}_j^\dagger$, $\hat{c}_j$ respectively, then one can perform a canonical transformation of these operators to a new basis

$$\hat{c}_j = \frac{1}{2}(\gamma_{j1} + i\gamma_{j2}) \qquad \text{and} \qquad \hat{c}_j^\dagger = \frac{1}{2}(\gamma_{j1} - i\gamma_{j2}), \tag{2.1}$$

where one can associate the operator $\gamma_{j\alpha}$ as the real and imaginary part of the electron operator. Indeed, inverting the above transformation we get

$$\gamma_{j1} = \hat{c}_j^\dagger + \hat{c}_j \qquad \text{and} \qquad \gamma_{j2} = i(\hat{c}_j^\dagger - \hat{c}_j), \tag{2.2}$$

and we can see that the Majorana operators $\gamma_{j\alpha}$ satisfy

$$\{\gamma_{i\alpha}, \gamma_{j\beta}\} = 2\delta_{ij}\delta_{\alpha\beta} \qquad \text{and} \qquad \gamma_{i\alpha}^\dagger = \gamma_{i\alpha}. \tag{2.3}$$

It follows that $\gamma_i^2 = 1$, i.e., acting twice with a Majorana operator, we get back the same state we started with and therefore there is no Pauli exclusion principle for Majorana fermions. On the other hand, the relations above say that a particle created by the operator γ is equal to its antiparticle. One can try to construct a number operator for Majorana fermions in a traditional way

$$n_i^\gamma = \gamma_i^\dagger \gamma_i = 1 = \gamma_i \gamma_i^\dagger, \tag{2.4}$$

thus a Majorana mode is in a sense always empty and always filled and counting does not make any sense.

The transformation (2.1) tells us that any electron system can be written in a Majorana representation, but this fact is only a mathematical trick and brings no benefit to physical situations. The reason for that is that two Majorana fermions are spatially localized very close to each other, i.e. they overlap in a significant manner and make no sense to describe them as individual particles.

However, there is a novel class of systems, called topological superconductors, in which

one can find two Majorana fermions spatially separated. In this kind of systems, described by the BCS theory, coherent superpositions of electron and holes as indicate Eq.(2.2) occur naturally. On the other hand, an operator defined by Eq.(2.2) can act only non-trivially on a ground state with uncertain total number of particles; such ground state is characteristic of superconducting systems. The electron-hole excitation of the superconductor plays the role of particle and anti-particle. Electrons, which are filled states at energy ϵ above the Fermi level E_F, and holes, representing empty states at $-\epsilon$ below the Fermi level, have opposite charge, but the charge difference $2e$ can be absorbed as a Cooper pair in the superconducting condensate. We can immediately see that in superconductors charge is no longer conserved. The superconductor, in effect, shields the electric field and confines the magnetic field. Therefore, it seems plausible that particles or quasi-particles in the superconductor would be invariant to charge conjugation, leading to Majorana fermions described by operators with the structure presented in Eq.(2.2).

At the Fermi level $\epsilon = 0$, in the middle of the superconducting gap, the eigenstates are charge-neutral superpositions of electrons and holes. Because of the electron-hole symmetry one can associate a midgap excitation to Majorana fermions: the creation and annihilation operators $\gamma_i^\dagger(\epsilon)$, $\gamma_i(\epsilon)$ for an excitation at energy ϵ are related by

$$\gamma_i(\epsilon) = \gamma_i^\dagger(-\epsilon). \tag{2.5}$$

In other words, creating a quasi-particle with energy $-\epsilon$ or removing one with energy ϵ are identical operations. *At the Fermi level* $\gamma(\epsilon) = \gamma(0) \equiv \gamma_0 = \gamma_0^\dagger$ *the particle and antiparticle coincide.* So, the BCS theory predicts that Majorana fermions should exist in superconductors. The excitation at zero energy is known as **Majorana zero mode** and it is important to mention some important points [12]

1. Because of the fact that creating a particle with the operator $\gamma_0^\dagger$ costs zero energy, in the presence of a Majorana zero mode the ground state of the system must be degenerate. Naturally, if $|0\rangle$ is the ground state then so is $\gamma_0^\dagger|0\rangle$, but it is not possible to label the degenerate ground state by the number of Majorana zero modes because $n_i^\gamma = 1$ as we mentioned above.

2. If a Majorana zero mode exists, then it is topologically protected, provided that there is an energy gap separating it from all other states. The reason is that the zero mode cannot acquire a nonzero energy E_0 by any continuous deformation of the Hamiltonian that does not close the gap.

3. A single unpaired Majorana zero mode can exist only in an infinite system, because in systems of finite size Majorana modes always appear in pairs, reflecting the fact that such systems always contain an integral number of electrons. Nevertheless, a situation of interest arises when two Majorana zero modes are spatially separated so that their individual wave functions have a negligible overlap. In this case the systems exhibit an unpaired Majorana zero mode. Also, in this situation Majorana modes can be moved away from zero energy without closing the gap by simply bringing them close together so that the wave functions overlap. The two zero modes thus evolve into a pair of levels $(E_0, -E_0)$ with a splitting proportional to the overlap.

4. Majorana zero modes are non-abelian anyons [13, 14, 15], which means that particle exchanges are non-trivial operations which in general do not commute. It is a crucial ingredient for non-abelian statistics to have a degenerate ground state, which is separated from all excited states by a gap. Then adiabatic operations, such as the slow exchange of quasiparticles positions, can in priniciple bring the system from one ground state to another. Ivanov [16] provided a simple proof of the non-abelian statistics for Majorana zero modes in $p_x \pm ip_y$ superconductors.

2.2 Detection of Majorana Fermions

The first model realizing Majorana fermions was proposed by Kitaev in 2000 [17] and is known as the Kitaev model, described by the Hamiltonian

$$\hat{H} = -t \sum_{j=1}^{N-1} \left(\hat{c}_j^\dagger \hat{c}_{j+1} + \text{h.c} \right) - \mu \sum_{j=1}^{N} \hat{c}_j^\dagger \hat{c}_j + \sum_{j=1}^{N-1} \left(\Delta \hat{c}_j \hat{c}_{j+1} + \Delta^* \hat{c}_{j+1}^\dagger \hat{c}_j^\dagger \right), \tag{2.6}$$

where Δ represents the nearest-neighbor pairing amplitude, the simplest allowed possibility for superconducting order parameter with spinless fermions, and we are considering a chain

with N sites and open boundary conditions. Because of the fact that the system describes a one dimensional system of spinless fermions, Kitaev himself describes this model as a toy model. Since spins are not considered in the Kitaev model, the electron pairs have to live on neighboring sites instead on to respect the Pauli exclusion principle. This connection of neighboring sites corresponds to a discretized derivative of a momentum operator and shows a momentum dependency in the superconducting term. So we know that we do not have the common s-wave superconductivity, which must be isotropic and hence independent of momentum. Instead, we have much rater p-wave superconductivity. This model picks the basic necessary ingredients to realize Majorana fermions, knowing that the result is not an accurate description of an arbitrary one dimensional real wire. Providing an experimental setup for a wire or different system that would behave similar to this toy Hamiltonian, is a challenge that he leaves open. Recent experiments have found signatures of Majorana fermions in one-dimensional nanowires [18, 19]. It was made of a superconducting material that has strong spin-orbit interactions. When a magnetic field is placed along the axis of the wire, a gap opens up between the two spin-orbit bands. If the Fermi energy is within the gap, then the degeneracy is two-fold, while if the Fermi energy is outside the gap, then it is four-fold. Connecting this nanowire to a superconductor causes electron states of opposite momenta and spins to pair together, producing a gap. Combining the degeneracy with an induced gap creates what is known as a *topological superconductor*. On the ends of this construction, a zero-energy bound state appeared, which is thought to be a Majorana fermion.

The accelerated interest and quick development of further ideas to realize Majorana fermions in solid state physics was sparked not only by theoretical interest but also by possible applications that were pointed out by Kitaev: such states could be used as particularly decoherence resistant qubits for quantum computers and because of their non-Abelian exchange statistics, they could be used for quantum computations. A quantum computer following this concept is called a topological quantum computer [20].

2.3 Andreev reflections

Andreev reflection is defined as the conversion of electrons into hole excitations in a metal at the interface with a superconductor [21]. We will not describe the complete process in this section, or give the entire mathematical formulation, but we will only mention some of its characteristics and the role they play in the tunneling current in a junction with a superconductor. When electrons coming from a normal metal impinges the normal-superconductor interface, some of them are reflected specularly (or normally) and others suffer a different process, in which they cross to the superconducting metal, creating a Cooper pair. However, since the superconducting condensate can emit or absorb electrons in pairs, therefore the creation of a Cooper pair requires another electron. This second electron is taken from the normal region, creating a hole, which travels in the direction opposite to the original electron, as is shown in figure (2.1). While the electron excitation is a filled state at energy ϵ above the Fermi energy E_F, the hole excitation is an empty state at energy ϵ below E_F. This process is possible for $\epsilon < \Delta_0$, with Δ_0 the energy gap of the superconductor. Due to this feature, Andreev reflections provide a mechanism for current flow through the normal metal-superconductor interface. There are important differences between the two reflection processes [22]

1. **Charge is conserved in normal reflection, but not in Andreev reflection**: The hole is a quasiparticle excitation that has opposite charge as the electron therefore a charge of $2e$ is lost in the electron-hole conversion process. However, this missing charge is absorbed into the superconducting ground state as a Cooper pair, i.e., it is missing only with respect to the excitations.

2. **Andreev reflections conserve momentum but normal reflections do not**: This assumption is valid when the superconducting energy gap is much smaller than the Fermi energy of the normal metal. If this is the case, the energy of the incoming electron is much bigger compared to Δ_0 and the superconductor cannot affect it significantly. Nevertheless, there are no excited states within a range Δ_0 from the Fermi level and so the superconductor has to find another mechanism to reflect the electron, but without changing its momentum. In order to deal with this difficult

task, the superconductor transform the electron into a quasiparticle excitation whose velocity is opposite to its momentum, i.e., a hole. This is a process that only a superconductor can do, so, in a normal reflection, where an electron impinges an interface between two normal metals or between a normal metal and an insulator, the electron is reflected, changing its trajectory and therefore, its momentum.

3. **Both Andreev and normal reflection conserve energy**: As the electron has an excitation energy ϵ above the Fermi energy, and the hole an excitation energy ϵ below the Fermi level, Andreev reflection is an elastic scattering process, because both particles have the same energy.

4. **Both Andreev and normal reflections conserve spin**: In order to conserve spin in the scattering process, the hole and the electron should have opposite spin. However, if the scattering properties of the normal metal are spin-independent, then this spin-flip can be ignored

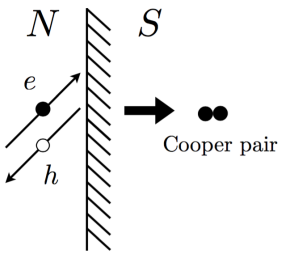

Figure 2.1: Schematic drawing of an Andreev reclection in a normal metal-superconductor interface.

If we now change the junction, considering a superconductor-normal metal-superconductor device, an interesting situation arises. If we have no voltage applied between the superconductors, an electron from the normal region, with energy within the gap, can be partially specularly reflected into another electron or can suffer Andreev reflections. Let's assume that Andreev reflections dominate the process. If this is the case, then the electron from the normal region is reflected as a hole at one interface, say, the right one. It is then Andreev reflected as an electron at the left interface. Therefore, it is possible that multiple reflections can lead to the formations of Andreev bound states, as is shown in the first

draw in figure (2.2). In this process a Cooper pair is emitted into the right superconductor for every reflection at the right interface, and conversely, a Cooper pair is absorbed from the left superconductor for every reflection in the left interface. This corresponds to a supercurrent through the device. Therefore Andreev bound states give a microscopic description for the Josephson effect in this kind of junctions.

A complete different story occurs if we apply a finite voltage V. If an electron, moving to the right for example, increases its kinetic energy by eV due this bias voltage, an Andreev reflected hole traveling to the left also increases its kinetic energy by eV since it carries the opposite charge. An electron/hole Andreev reflected multiple times can thus gain arbitrarily high energies for any non-vanishing bias voltage. In particular, an electron-like quasiparticle from an occupied state below the gap in, say, the left superconductor, can after multiple reflections emerge in a previously unoccupied state above the gap in the right superconductor (figure 2.2b). A new transport channel becomes available whenever the full gap $2\Delta_0$ is an odd integer multiple of eV:

$$2\Delta_0 = (2n+1)eV \Rightarrow eV = \frac{\Delta_0}{n+\frac{1}{2}}, \tag{2.7}$$

for $n = 0, 1, 2, \ldots$. The special case $n = 0$ corresponds to direct quasiparticle transfer from one superconductor to the other, similar to quasiparticle tunneling in a superconductor-insulator-superconductor junction. The opening of new transport channels for $n = 0, 1, 2, \ldots$, i.e., at

$$eV = \frac{2}{3}\Delta_0, \quad \frac{2}{5}\Delta_0, \quad \frac{2}{7}\Delta_0, \quad \ldots \tag{2.8}$$

leads to structures in the current-voltaje characteristic below the gap, specifically to peaks in the differential conductance $\frac{dI}{dV}$.

2.4 Thermoelectric transport

The broad topic of thermoelectricity describes the direct relationship between heat and electrical energy. In this section we present a brief review of the main concepts needed to understand the basic notions of themoelectric transport in nanoscale systems. For a more

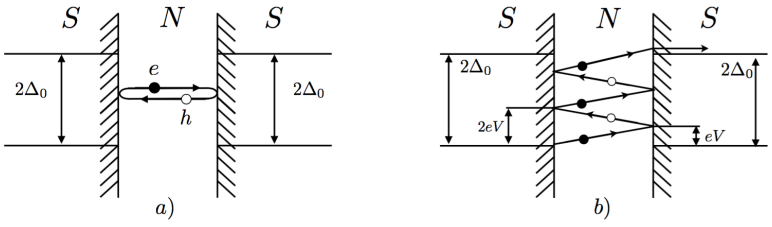

Figure 2.2: a) Andreev bound states in a SNS junction, **b)** Andreev reflections at non zero bias voltage.

complete description of such processes, refer to [23, 24].

In attempting to understand transport properties of a nano-system, one generally applies an external force to the material or device and measures the response of the system to such perturbation. In the linear response regime, by applying a potential gradient $\vec{E} = -\vec{\nabla}V$, one can measure the electrical current $\vec{J}_E$, that flows and calculate the electrical conductance σ, governing the electron transport in the system. On the other hand, by applying a temperature gradient $\vec{\nabla}T$, one can measure the heat $\vec{J}_Q$ which flows and calculate the thermal conductance κ, from the relation

$$\vec{J}_Q = -\kappa\vec{\nabla}T, \tag{2.9}$$

governing thermal transport in the system. The equations whose relates the generalized forces and their corresponding current can be written in a matrix form [24, 25]

$$\begin{pmatrix} \vec{J}_E \\ \vec{J}_Q \end{pmatrix} = \begin{pmatrix} L_{EE} & L_{ET} \\ L_{TE} & L_{TT} \end{pmatrix} \begin{pmatrix} \vec{\nabla}V \\ \vec{\nabla}T \end{pmatrix}. \tag{2.10}$$

Here V represents the electric potential and L_{ij} are transport coefficients, independent of V and T, evaluated at equilibrium i.e. for $\vec{\nabla}V = 0$ and $\vec{\nabla}T = 0$. Although all these coefficients are tensors, we consider that our system is essentially one dimensional and therefore we can treat them as scalars. If we keep the device at constant temperature and we apply an electric field $\vec{E}$, then the electrical conductivity σ is defined according to

$$\vec{J}_E = \sigma\vec{E}. \tag{2.11}$$

In this scenario $\vec{\nabla}T = 0$ and therefore

$$\sigma = L_{EE}. \tag{2.12}$$

On the other hand, if the material is electrically insulated, eliminating any electric current flowing through it, but maintained a thermal gradient, then we can measure the thermal conductivity κ, determined by Eq.(2.9) which, in the zero-electrical current regime, is given by

$$\kappa = -\left(L_{TT} - \frac{L_{TE}L_{ET}}{L_{EE}}\right). \tag{2.13}$$

Lets suppose we can generate a temperature difference ΔT across some material. It is easy to note that a voltage difference ΔV develops in response on the temperature gradient. The ratio of voltage to the applied temperature difference is called the thermoelectric power (TEP) or Seebeck coefficient S

$$S = -\left.\frac{\Delta V}{\Delta T}\right|_{J_E=0}. \tag{2.14}$$

The origin of the voltage which develops across the sample can be easily understood: the application of a temperature gradient causes the charge carriers at each end of the sample to have different energies. It can be argued that on average the higher energy electrons will also have a higher velocity, and they will tend to diffuse toward the colder end of the sample. Thus, initially an electric current, say $\vec{J_E}$, begins to flow. However, since we experimentally restrict current from flowing, charge collects until the electric field is large enough that $\vec{J_E}$ becomes zero. The Seebeck effect was discovered in 1821 and in parallel in 1834 the Peltier effect was discovered. This effect occurs when a current is allowed to flow in the system, with both end fixed at same temperature T. It was noticed that along with the electrical current $\vec{J_E}$, a thermal current $\vec{J_Q}$ also flows, so that the temperature at one end of the system decreases and the other increases in order to preserve continuity of $\vec{J_Q}$. The transport quantity

$$\Pi = \frac{L_{TE}}{L_{EE}} \tag{2.15}$$

is called the Peltier coefficient . Since an amount of heat energy Q in absorbed at one of the

ends (or junctions if we consider a structure involving different materials) the Peltier effect can be used to transfer heat from one end to another, which can be utilized for thermoelectric refrigeration. Nevertheless, in typical conducting systems Joule heating dominates, making efficient Peltier cooling a very difficult task. Besides Peltier cooling, there is an additional means of generating reversible heat in a medium, which is the Thomson effect. It was predicted in 1854 and found experimentally in 1856, and it occurs when a temperature gradient is applied across two ends of a current carrying conductor. In this case heat is emitted or absorbed in addition to Joule heat. The Thomson coefficient μ describes the rate of heat generation per unit current flow per unit temperature gradient.

The three thermoelectric properties provide the basis for modern direct energy conversion devices and their explotation has been the subject of considerable research[26]. The strength of these effects and suitability for applications are determined by their thermoelectric figure of merit Z,commonly presented as a dimensionless quantity

$$ZT = \frac{S^2\sigma}{\kappa}T. \tag{2.16}$$

Therefore, the thermopower, S, describes how much heat is carried per unit charge. Higher TEP yields higher TE efficiency. The electrical conductivity, σ, determines how much energy is lost due to Joule heating. The larger σ, the less Joule heat is produced and the more efficient the material. κ governs thermal transport in the system. A temperature gradient is built up by electronic transport of heat, but thermal energy will tend to leak back across the conductor. The more thermally resistive is the sample, the better its candidacy for thermoelectric application.

Chapter 3

Non-equilibrium Green's function formalism

So far we have introduced the relevant quasi-particles we are working with, such as Majorana fermions and Cooper pairs. In order to describe the collective phenomena due the interaction between them or their correlations in a physical system such as nanojunctions, we need a powerful mathematical toolbox, provided by quantum field theoretical methods. In this chapter, we provide a systematic introduction to the non-equilibrium many-body formalism, particularly, the Keldysh functional integral approach, which is the proper technical tool to accomplish transport phenomena in non-equilibrium quantum systems.

With the advent of nanoscale physics and ultrafast lasers, it became possible to probe correlations between particles in excited quantum states. New fields of research, like, e.g., molecular transport, nanoelectronics, ultracold atomic gases in optical traps, optimal control theory, Josephson nanojunctions, attosecond physics, non-equilibrium phase transitions, kinetics of Bose condensates, quantum computation, etc. added to the already existing fields in mesoscopic physics and nuclear physics. In this context, the Green's function method is probably one of the most powerful and versatile formalisms in physics, and its non-equilibrium version has already proven to be extremly useful in several of the aforementioned contexts. We will adopt the integral formulation of quantum field theory, which corresponds to the modern framework to understand many-particle problems in

thermodynamic equilibrium. Additionally it provides us with a well-developed toolbox of techniques, such as diagrammatic perturbation theory, including sophisticated resummation schemes. But it also encompasses non-perturbative approaches, which often capitalize on the flexibility of the functional integral when it comes to picking the relevant degrees of freedom for a given problem. Another important advantage of the functional integral approach is that it allows us to leverage the power of symmetries in the system. Is well known that it is in quantum field theory relations among Green's functions often follow as consequences of a symmetry of the action. They are known as Ward-Takahashi identities associated with the symmetry [27, 28].

Even though the field of non-equilibrium phenomena is in principle much broader than equilibrium thermodynamics, it is by far less studied. The reason for this is the remarkable universality of equilibrium systems, whose properties depend only on very few parameters. In contrast, the characterization of a non-equilibrium state usually requieres detailed knowledge about its preparation. The purpose of this chapter is to give a clear mathematical definition of non-equilibrium problems that will be discussed in the remainder of this thesis, and introduce the theoretical tools that are needed to study them from a microscopic point of view.

Problems in non-equilibrium physics may be classified according to:

(i) Whether they deal with **open** or **closed** systems, and

(ii) whether the focus is on the **transient time evolution** during and after some perturbation, or on the **stationary state** that possibly develops when a system is driven by external fields.

Open systems are coupled to a dissipative environment, while the dynamics of a closed system is completely described in terms of its time-dependent Hamiltonian $\hat{H}(t)$. The latter may include external fields that act on the system, but there is no coupling to a heat bath.

Although equilibrium properties are not the main subject of this chapter, it is important to understand the effect of correlations in simple cases. The first reason is that the thermodynamic equilibrium state is often the end point of relaxation processes of a

system that is externally excited. In this case, a key requirement for the theory of the non-equilibrium dynamics should be that it guarantees that the evolution converges to the correct thermodynamic state. It is the main subject of non-equilibrium theories to understand this relaxation process and to predict how the final state will look like. Based on this knowledge, one may suggest a specific form of excitation which allows to reach a well-defined desired state.

Following this idea, non-equilibrium theories have to solve two problems [29]

(i) What are the properties of various external excitations, what are their characteristic time scales, how do they interact with particle systems, and how much energy in what spectral composition do they allow to *feed* into the system?

(ii) What are the dominant mechanisms in a given many-particle system, how can they be activated, how much momentum and energy do they allow to transform?

Obviously, both questions are closely related and require a detailed knowledge of the microscopic properties of the many-particle system and of the character of the interaction of the particles with the excitation under non-equilibrium conditions.

The non-equilibrium Green's function method is an extension of the standard equilibrium formulation on the imaginary-time axis, as is described in classics textbooks as Kadanoff and Baym [30] and Abrikosov, Gorkov and Dzyaloshinski [31]. The firts steps to introduce quantum field-theoretical methods in non-equilibrium statistical mechanics were made by Martin and Schwinger in 1959 [32] and by Schwinger in 1961 [33]. Later Kadanoff and Baym [30] contributed with significant developments. At the same time in USSR a big work was done by Konstatinov and Perel in 1960 [34], Dzyaloshiski in 1962 [36], Keldysh (1964) [37], Abrikosov [31] and Eliashberg [38]. Since then, non-equilibrium Green's functions have become in a standard tool for the study of different quantum transport models at different levels of sophistication.

In section 3.1, we will define the non-equilibrium problem in the context of this thesis and we will describe the standard procedure for constructing a non-equilibrium situation. Also we will introduce the closed-time path contour, which is the central idea in the Keldysh formalism, and we will derive the evolution of any operator along this two time-branch

contour. We will further see in sections 3.2 and 3.3 how to construct the Keldysh functional integral for fermionic systems and at the end of this chapter there will be a brief overview of the Dyson equation in the non-equilibrium context in section 3.4.

3.1 Closed-time path contour

Non-equilibrium time evolution from a thermal initial state

Let's consider a general quantum system described by the time-independent Hamiltonian

$$\hat{H} = \hat{H}_0 + \hat{H}_I, \tag{3.1}$$

where $\hat{H}_0$ is the free particle Hamiltonian and $\hat{H}_I$ includes all the interactions and static potentials between the particles. The Hamiltonian $\hat{H}$ acts on the multi-particle state space consisting of product of multi-particle spaces for the species involved.

In order to construct our non-equilibrium situation, we employ a standard preparation device (figure 3.1) as follows:

1. Far in the past, for $t < t_0$, the system has been brought to the equilibrium state, characterized by a temperature T. In thermal equilibrium, the system is assumed to be in a mixed state described by a density matrix or statistical operator $\hat{\rho}_{\text{eq}}$ given by

$$\hat{\rho}_{\text{eq}}(H) \equiv \hat{\rho}_{\text{eq}} = \sum_{\nu} p_\nu |\psi_\nu\rangle\langle\psi_\nu| = \frac{1}{Z_H} e^{-\beta H} = \frac{e^{-\beta H}}{\text{Tr}\,(e^{-\beta H})}, \tag{3.2}$$

   where Tr denotes the trace on the multi-particle state of the system, $\beta = \frac{1}{k_B T}$ corresponds to the inverse temperature and Z_H the thermal equilibrium partition function, corresponding to the Hamiltonian $\hat{H}$.

2. At time $t = t_0$, the system is isolated or disconnected from the reservoir and exposed to a time-dependent perturbation or driving field, and the system starts to evolve from its initial state. Now the dynamics of the system is governed by the full time-dependent Hamiltonian

$$\hat{\mathcal{H}}(t) = \hat{H} + \hat{H}'(t) \tag{3.3}$$

and the statistical operator $\hat{\rho}(t)$, such that $\hat{\rho}(t = t_0) = \hat{\rho}_{\text{eq}}$ and the information of the thermal reservoir is stored in the initial condition.

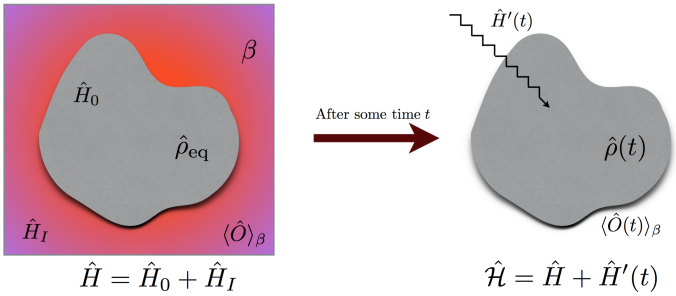

Figure 3.1: Sketch of the preparation device in non-equilibrium situations.

It is well known that the time evolution of the density matrix is determined by the Von Neumann equation

$$i\hbar\frac{d}{dt}\hat{\rho}(t) = [\hat{\mathcal{H}}(t), \hat{\rho}(t)], \tag{3.4}$$

with $[\hat{A}, \hat{B}] = \hat{A}\hat{B} - \hat{B}\hat{A}$ the commutator between the operators $\hat{A}$ and $\hat{B}$. The solution for the equation (3.4) is generally written as

$$\hat{\rho}(t) = \hat{\mathcal{U}}_{\mathcal{H}}(t, t_0)\hat{\rho}(t_0)\hat{\mathcal{U}}^{\dagger}_{\mathcal{H}}(t, t_0), \tag{3.5}$$

where the evolution operator corresponding to the Hamiltonian $\hat{\mathcal{H}}(t)$ has the form

$$\hat{\mathcal{U}}_{\mathcal{H}}(t, t') = \begin{cases} \hat{T}e^{-\frac{i}{\hbar}\int_{t'}^{t} d\bar{t}\hat{\mathcal{H}}(\bar{t})} & \text{for} \quad t > t' \\ \\ \hat{\tilde{T}}e^{-\frac{i}{\hbar}\int_{t'}^{t} d\bar{t}\hat{\mathcal{H}}(\bar{t})} & \text{for} \quad t < t' \end{cases}, \tag{3.6}$$

and ($\hat{\tilde{T}}$) $\hat{T}$ denotes the (anti-)time ordering operator, i.e., it arranges the operators so that an operator with time argument t comes (right)left to operators with earlier time argument $t' < t$. It is important to note that the time-dependent perturbation Hamiltonians at different times do not commute with each other, $[\hat{\mathcal{H}}(t), \hat{\mathcal{H}}(t')] \neq 0$. As a consequence, $\hat{\mathcal{U}}(t, t')$ has to be understood as an infinite product of incremental evolution operators with instantaneous locally constant Hamiltonians, resulting in a Trotter decomposition of the

evolution operator

$$\begin{aligned}\hat{\mathcal{U}}_{\mathcal{H}}(t,t') &= \lim_{N\to\infty} e^{-\frac{i}{\hbar}\hat{\mathcal{H}}(t-\delta_t)\delta_t} e^{-\frac{i}{\hbar}\hat{\mathcal{H}}(t-2\delta_t)\delta_t} \cdots e^{-\frac{i}{\hbar}\hat{\mathcal{H}}(t-N\delta_t)\delta_t} e^{-\frac{i}{\hbar}\hat{\mathcal{H}}(t')\delta_t} \\ &= \lim_{N\to\infty} (\hat{1} - \frac{i}{\hbar}\delta_t \hat{\mathcal{H}}(t)), \end{aligned} \tag{3.7}$$

with $\delta_t = \frac{t-t_0}{N}$ an infinitesimal time step. Once defined this operator, it is clear that the time evolution operator satisfies the semi-group property

$$\hat{\mathcal{U}}(t,t')\hat{\mathcal{U}}(t',t'') = \hat{\mathcal{U}}(t,t'') \tag{3.8}$$

and becomes unitary

$$\hat{\mathcal{U}}(t,t')\hat{\mathcal{U}}^{\dagger}(t,t') = \hat{\mathcal{U}}(t,t')\hat{\mathcal{U}}(t',t) = \hat{\mathcal{U}}(t,t) = 1 \quad \Rightarrow \quad \hat{\mathcal{U}}^{\dagger}(t,t') = \hat{\mathcal{U}}(t',t). \tag{3.9}$$

The non-equilibrium average values of operator $\hat{\mathcal{O}}$ representing physical observables in the Schrödinger picture for times $t > t_0$ is given by

$$\langle \hat{\mathcal{O}}(t) \rangle = \mathrm{Tr}\left(\hat{\rho}(t)\hat{\mathcal{O}}\right) = \frac{\mathrm{Tr}\left(e^{-\beta\hat{H}(t)}\hat{\mathcal{O}}\right)}{Z_{\mathcal{H}}}, \tag{3.10}$$

where $Z_{\mathcal{H}} = \mathrm{Tr}\left(e^{-\beta\hat{\mathcal{H}}(t)}\right)$ is the partition function corresponding to the time-dependent Hamiltonian $\hat{\mathcal{H}}$. Using the time-dependent density matrix given in Eq.(3.5), the expectation value of any observable $\hat{\mathcal{O}}$ measured at time t is given by

$$\langle \hat{\mathcal{O}}(t) \rangle = \mathrm{Tr}\left(\hat{\rho}(t)\hat{\mathcal{O}}\right) = \mathrm{Tr}\left(\hat{\mathcal{U}}_{\mathcal{H}}(t,t_0)\hat{\rho}(t_0)\hat{\mathcal{U}}_{\mathcal{H}}(t_0,t)\hat{\mathcal{O}}\right) \tag{3.11a}$$

$$= \mathrm{Tr}\left(\hat{\rho}(t_0)\hat{\mathcal{O}}_{\mathcal{H}}(t)\right) \tag{3.11b}$$

$$= \frac{\mathrm{Tr}\left(e^{-\beta\hat{H}}\hat{\mathcal{O}}_{\mathcal{H}}(t)\right)}{Z_{\mathcal{H}}} \tag{3.11c}$$

where $\hat{\mathcal{O}_{\mathcal{H}}}(t)$ denotes the operator of the physical quantity in question in the Heisenberg picture with respect to the time-dependent Hamiltonian $\mathcal{H}$, and we have used the cyclic property of the trace. Hereinafter one can proceed in two different (but analogous) ways:

1. Using an operator formalism (taking as starting point Eq.(3.11c)), in which, one has to define different Green's functions as correlators between operators in the Heisenberg picture and keeping track of matrix Green's functions and tensor vertices, or

2. using Eq.(3.11a) and adopting a modern framework using a functional approach, in which one has to construct a scalar action obtaining from then, using the powerful toolbox from quantum field theory, the different non-equilibrium Green's functions.

We will adopt the functional approach during the calculations, following the references [39, 40, 41, 42], whereas the operator formalism is extensively discussed in classics references [43, 30, 44, 45]. Our starting point is therefore Eq.(3.11a), in which the operator representing a physical observable $\hat{\mathcal{O}}$ is in the Schrödinger picture. Noting that the equilibrium statistical operator can be written as

$$\hat{\rho}(t_0) = \frac{e^{-\beta H}}{Z_H} = \frac{e^{-\frac{i}{\hbar}\int_{t_0}^{t_0-i\beta} d\bar{t}\hat{H}}}{Z_H} \tag{3.12}$$

$$= \frac{\hat{\mathcal{U}}_H(t_0 - i\beta, t_0)}{Z_H}, \tag{3.13}$$

in other words, we can consider $\hat{\rho}_{\text{eq}} = \hat{\rho}(t_0)$ as the time evolution along the imaginary time-axis from t_0 to $t_0 - i\beta$ (with imaginary-time ordering). This allows us to write Eq.(3.11a) as

$$\begin{aligned}\langle\hat{\mathcal{O}}(t)\rangle &= \frac{1}{Z_{\mathcal{H}}}\text{Tr}\left(\hat{\mathcal{U}}_{\mathcal{H}}(t,t_0)\hat{\mathcal{U}}_H(t_0-i\beta,t_0)\hat{\mathcal{U}}_{\mathcal{H}}(t_0,t)\hat{\mathcal{O}}\right)\\ &= \frac{1}{Z_H}\text{Tr}\left(\hat{\mathcal{U}}_H(t_0-i\beta,t_0)\hat{\mathcal{U}}_{\mathcal{H}}(t_0,t)\hat{\mathcal{O}}\hat{\mathcal{U}}_{\mathcal{H}}(t,t_0)\right).\end{aligned} \tag{3.14}$$

It should not surprise that in the last equation appears the thermal equilibrium partition function. That is because we have also considered that, according to the Von Neumann equation (3.4), the trace of the initial density matrix is invariant under unitary evolution.

If one reads the operators from right to left, one can see that the operators follow the time ordering of $t_0 \to t \to t_0 \to -i\beta$. This motivates us to introduce a contour $\mathcal{C}$ with three branches, as shown in the figure 3.2: γ^+: $t_0 \to t_{\max}$; γ^-: $t_{\max} \to t_0$ and γ^M: $t_0 \to t_0 - i\beta$, where we have called $t_{\max}$ the maximal time up to which one wants to let the system evolve.

This contour is exact and is known as the *Konstantinov-Perel' contour*. Konstantinov and Perel' [34] developed a diagrammatic technique, based on the time contour containing two branches in the real time direction and an imaginary time appendix of length β.

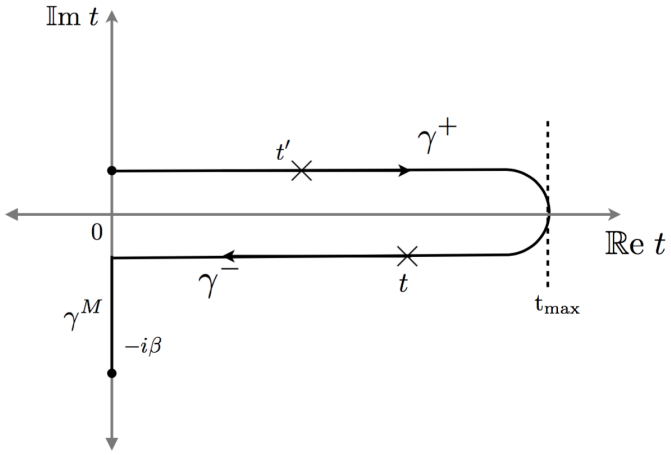

Figure 3.2: Contour $\mathcal{C} = \gamma^+ \oplus \gamma^- \oplus \gamma^M$, considering $t_0 = 0$

One must be very careful with expression (3.14). Note that the operator $\hat{\mathcal{U}}_H(t_0 - i\beta, t_0)$ is the time evolution operator with respect to the time-independent Hamiltonian $\hat{H}$, while the two other evolution operators include the full time-dependent Hamiltonian $\hat{\mathcal{H}}(t)$. However, the time-dependent contribution $\hat{H}(t)$ along the forward (γ^+) and backward (γ^-) contour cancels if no other operator is inserted, so that we can extend the contour of $\hat{\mathcal{U}}_H(t_0 - i\beta, t_0)$ to the complete contour described where $\hat{\mathcal{H}}$ acts:

$$\hat{\mathcal{U}}_H(t_0 - i\beta, t_0) \longrightarrow \hat{\mathcal{U}}_{\mathcal{H}}(t_0 - i\beta, t_0). \tag{3.15}$$

In order to simplify our calculation, we have to make some assumptions. The first one is that we will consider an *adiabatic assumption*, based on the idea that one can generate a density matrix $\hat{\rho}_{\text{eq}}$ starting from the density matrix $\hat{\rho}_0$ governed by time-independent Hamiltonians $\hat{H}$ and $\hat{H}_0$ (according with Eq.(3.1)), respectively, switching on the interaction $\hat{H}_I$ adiabatically[35], i.e.,

$$\hat{\rho}_{\text{eq}} = \frac{e^{-\beta\hat{H}}}{Z_H} = \hat{\mathcal{U}}_\epsilon(t_0, -\infty)\hat{\rho}_0\hat{\mathcal{U}}_\epsilon(-\infty, t_0), \tag{3.16}$$

where $\hat{\mathcal{U}}_\epsilon$ corresponds to the real-time evolution operator with Hamiltonian

$$\hat{H} \to \hat{H}_\epsilon(t) = \hat{H}_0 + e^{-\epsilon|t-t_0|}\hat{H}_I. \tag{3.17}$$

and ϵ a real positive infinitesimal number. This poweful assumption is supported by the Gell-Mann and Low theorem [46, 47], which is extremely relevant in the zero and finite temperature formalism (refer to section 3.1 for more details). A schematic representation of the new contour is presented in figure 3.3.

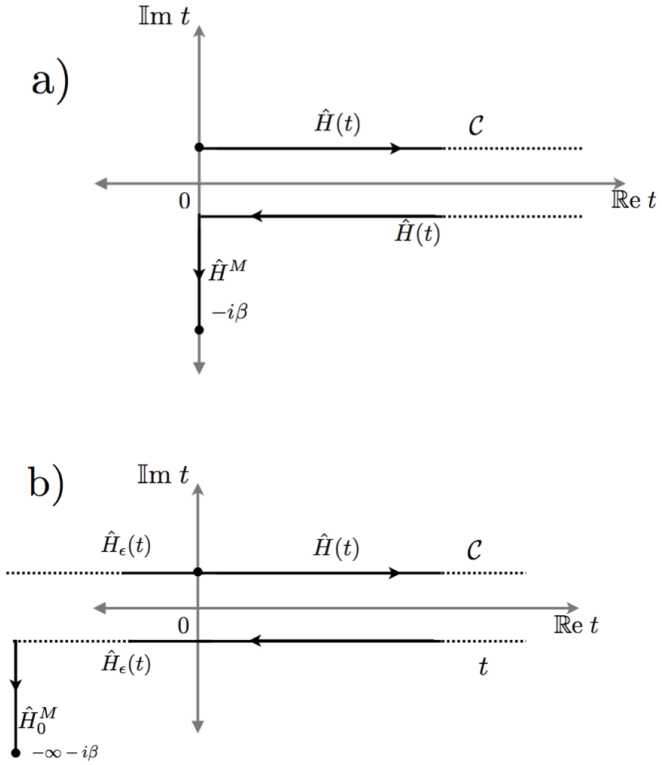

Figure 3.3: a) Exact Contour, **b)** Adiabatic assumption

With the adiabatic assumption, Eq.(3.14) acquires the form

$$\langle\hat{\mathcal{O}}(t)\rangle = \frac{1}{Z_{-\infty}}\mathrm{Tr}\left(\hat{\mathcal{U}}_{\mathcal{H}}(-\infty - i\beta, -\infty)\hat{\mathcal{U}}_{\mathcal{H}}(-\infty, t)\hat{\mathcal{O}}\hat{\mathcal{U}}_{\mathcal{H}}(t, -\infty)\right). \tag{3.18}$$

The second assumption is that it is more convenient to extend the time evolution towards $t \to \infty$ and to neglect the imaginary-time contribution $i\beta$. Inserting $\hat{1} = \hat{\mathcal{U}}_{\mathcal{H}}(t, \infty)\hat{\mathcal{U}}_{\mathcal{H}}(\infty, t)$

and using the semi-group property $\hat{\mathcal{U}}_{\mathcal{H}}(-\infty,t)\hat{\mathcal{U}}_{\mathcal{H}}(t,\infty) = \hat{\mathcal{U}}_{\mathcal{H}}(-\infty,\infty)$ one gets

$$\langle\hat{\mathcal{O}}(t)\rangle = \frac{\mathrm{Tr}\left(\hat{\mathcal{U}}_{\mathcal{H}}(-\infty,\infty)\hat{\mathcal{U}}_{\mathcal{H}}(\infty,t)\hat{\mathcal{O}}\hat{\mathcal{U}}_{\mathcal{H}}(t,-\infty)\hat{\rho}(-\infty)\right)}{Z_{-\infty}}. \tag{3.19}$$

This last equation is the central object in the Keldysh formalism. It describes an evolution along a closed contour $\mathcal{C}$, depicted in figure 3.4, with a forward branch γ^+ going from $t = -\infty$ to $t = \infty$ and then goes back along the backward branch γ^- along the time axis from $t = \infty$ to $t = -\infty$. The observable $\hat{\mathcal{O}}$ is inserted at time t, somewhere along forward branch of the contour $\mathcal{C}$[1] and $Z_{-\infty}$ denotes the thermal equilibrium partition function at $t = -\infty$.

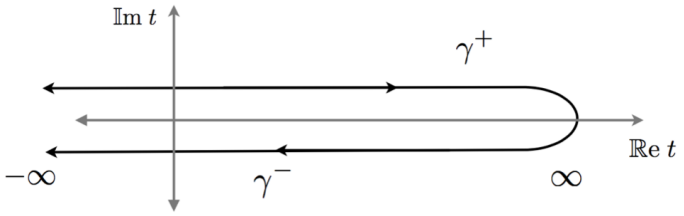

Figure 3.4: closed time contour $\mathcal{C} = \gamma^+ \oplus \gamma^-$, considering $t_0 = 0$

In general, initial correlations are supposed to be relevant in a realistic situation, since interactions are always present in the initial state. However, in a dissipative system coupled to an external thermal bath the initial correlations are expected to disappear in the long-time limit, since the large number of degrees of freedom in the heat bath would influence the long-range dynamics, and wipe out the information of the initial state and initial transcient dynamics. In this case, *Keldysh formalism is applicable to the nonequilibrium steady state without the use of adiabatic switching of interactions* [48]. For this reason we do not consider the contour extending in the imaginary time axis. It is important to note that in the functional derivative method, the imaginary-time contour doesn't appear also. The boundary condition, in which the system is assumed to be in equilibrium before external perturbation is turned on, can be imposed directly on the Dyson equation in integral form [44].

[1] If one wants to insert a operator in the backward branch of the contour, the identity $\hat{1} = \hat{\mathcal{U}}_{\mathcal{H}}(t,\infty)\hat{\mathcal{U}}_{\mathcal{H}}(\infty,t)$ have to be inserted on the right side of $\hat{\mathcal{O}}$ in Eq.(3.18).

An important consequence of the closed path contour is that in non-equilibrium situations we have **the double number of degrees of freedom** compared to thermal equilibrium (or zero temperature) situations, one from each branch of the contour.

To conclude this section, we have to mention two important remarks:

1. Let's consider the evolution operator along the closed contour

$$\hat{\mathcal{U}}_{\mathcal{C}} \equiv \hat{\mathcal{U}}(-\infty,-\infty) = \hat{\mathcal{U}}(-\infty,\infty)\hat{\mathcal{U}}(\infty,-\infty) = \hat{1}. \tag{3.20}$$

   If there is no differences in the Hamiltonians of the two branches of the closed-time contour, then the evolution along the contour of any state brings it back exactly to the original state. If there is a phase factor accumulated in the forward evolution (as in the equilibrium situation), it will be canceled by the accumulative phase factor coming from the backward evolution. Therefore, the partition function is identical to the unit, i.e.,

$$\mathcal{Z}_{\mathcal{C}} \equiv \frac{\mathrm{Tr}\left(\hat{\mathcal{U}}_{\mathcal{C}}\hat{\rho}(-\infty)\right)}{Z_{-\infty}} = 1. \tag{3.21}$$

2. In order to obtain the expectation value of an observable, using Eq.(3.18), it is necessary to insert an observable somewhere in the contour, either in the forward or backward branch. The most convenient way to do it is to modify the time-dependent Hamiltonian adding a source term α

$$\hat{\mathcal{H}}(t) \to \hat{\mathcal{H}}(t) \pm \frac{1}{2}\hat{\mathcal{O}}\alpha(t), \tag{3.22}$$

   where the plus (minus) sign refers to the (backward) forward branch of the contour. With this modification, the evolution along the two branches is no longer symmetric (since the Hamiltonain is quite different in the two branches), and then it follows that the evolution operator along the closed contour $\hat{\mathcal{U}}_{\mathcal{C}}[\alpha] \neq \hat{1}$ and the generating functional becomes non-trivial

$$\mathcal{Z}_{\mathcal{C}}[\alpha] \equiv \frac{\mathrm{Tr}\left(\hat{\mathcal{U}}_{\mathcal{C}}[\alpha]\hat{\rho}(-\infty)\right)}{Z_{-\infty}}. \tag{3.23}$$

Using this new generating functional, the expectation value of the observable may be generated as the result of a functional differentiation

$$\langle \hat{\mathcal{O}}(t) \rangle = \frac{\delta}{\delta \alpha(t)} \mathcal{Z}_{\mathcal{C}}[\alpha] \Big|_{\alpha \to 0}. \tag{3.24}$$

This is not intuitive. One would expect that the observables should be given by variational derivatives of the *logarithmic* of the generating function, as one finds in the equilibrium context

$$\langle \hat{\mathcal{O}}(t) \rangle = \frac{\delta}{\delta \alpha(t)} \ln \mathcal{Z}_{\mathcal{C}}[\alpha] \Big|_{\alpha \to 0}, \tag{3.25}$$

but as was noted above, since $\mathcal{Z}_{\mathcal{C}} = \mathcal{Z}_{\mathcal{C}}[0] = 1$, the presence of the **logarithm is optional in the theory of closed-time contour**.

Non-equilibrium vs zero temperature formalism

To end this section is convenient to comment very quickly the relation between the non-equilibrium formulation and the one used in field theories in equilibrium, where one usually works with a single-branch time axis ranging from $-\infty$ to ∞.

It is well known that the latter is posible due to a clever trick: the Gell-Mann and Low's theorem [46, 47]. It states that the ground state of the interacting system at $t = 0$ $|\Psi(0)\rangle$ and the ground state of the non-interacting one in the far past $t \to -\infty$ $|0\rangle$ are related by

$$|\Psi(0)\rangle = \hat{\mathcal{U}}_H(0, -\infty)|0\rangle. \tag{3.26}$$

Since we are dealing with equilibrium situations, the time dependence of the Hamiltonian has to be an adiabatic switching of the interaction, which turned on from $t \to -\infty$ to $t = 0$, say by the substitution presented in Eq.(3.17). The ground state is assumed nondegenerate and is evolved by the full adiabatic evolution operator into the ground state of the interacting system at $t = 0$. Its follows that the expectation value of any

operator is given by

$$\langle\hat{\mathcal{O}}(t)\rangle = \frac{\langle 0|\hat{\mathcal{U}}_H(-\infty, t_{\max})\hat{\mathcal{U}}_H(t_{\max}, t)\hat{\mathcal{O}}(t)\hat{\mathcal{U}}_H(t, -\infty)|0\rangle}{\langle 0|\hat{\mathcal{U}}(-\infty, t_{\max})|0\rangle}. \tag{3.27}$$

We can similarly assume that the interaction is adiabatically switched off in the far future and let $t_{\max} \to \infty$. Then the wavefunction goes back to the noninteracting ground state $|0\rangle$ up to the phase factor $e^{i\varphi}$, with φ a real number, i.e., $\hat{\mathcal{U}}_H(\infty, -\infty)|0\rangle = e^{i\varphi}|0\rangle$. This statement is based on the belief that adiabatic perturbation keeps the system in its (evolving) ground state at all times. Taking its Hermite conjugate and inserting it to Eq.(3.27) gives an expression for the expectation value

$$\langle\hat{\mathcal{O}}(t)\rangle = \frac{\langle 0|\hat{\mathcal{U}}(\infty, t)\hat{\mathcal{O}}(t)\hat{\mathcal{U}}_H(t, -\infty)|0\rangle}{\langle 0|\hat{\mathcal{U}}_H(\infty, -\infty)|0\rangle} \tag{3.28a}$$

$$= \frac{\langle 0|\hat{T}e^{-i\int_{-\infty}^{\infty} d\bar{t}\mathcal{H}(\bar{t})}\hat{\mathcal{O}}(t)|0\rangle}{\langle 0|\hat{T}e^{-i\int_{-\infty}^{\infty} d\bar{t}\mathcal{H}(\bar{t})}|0\rangle} \tag{3.28b}$$

in which the time argument $t \in (-\infty, \infty)$ moves on a single branch of the real time axis.

However, for general non-equilibrium systems one cannot use Eq.(3.28b), since the initial state $|0\rangle$ would be driven into excited states and never return after the whole time evolution, i.e., $\hat{\mathcal{U}}(\infty, -\infty)|0\rangle \neq e^{i\varphi}|0\rangle$. This forces one to use the analogy of Eq.(3.18) instead of Eq. (3.28b) with a round trip ($-\infty \to \infty \to -\infty$) and Tr instead of $\langle 0|\cdots|0\rangle$. On the other hand, the elimination of the backward evolution comes with a tremendous consequence, very important in perturbation theory and diagrammatic formulation of the non-equilibrium problem: in the non-equilibrium formalism there is no need for canceling disconnected diagrams. The phase accumulative factor $e^{i\varphi}$ from the non-interacting ground states is compensated in the two branches (as we already mentioned above). Therefore, in the closed loop evolution, only the identity term corresponding to no evolution coming from the perturbative expansion of the denominator survives, whereas all other terms come in two, one with a plus sign corresponding to the forward branch and other with a minus sign coming from the backward one, and the sum along the contour cancels.

3.2 Fermionic Green's functions: functional integral approach

The construction of a functional path integral for any field operator consists on the idea of making a partition of the time evolution many-body Hamiltonian into infinitesimal time slices, absorbing as much as possible the quantum dynamical phase accumulated during the propagation into a set of suitably chosen eigenstates. It is well known that in the single-particle quantum mechanics context, the perfect choice is to use a Hamiltonian representation in terms of coordinate and momentum eigenstates. But in the many-particle quantum mechanics formalism, any Hamiltonian can be expressed in terms of creation and annihilation operators, following the second quantization procedure. Therefore, in this case the most appropriate choice will be the eigenstates of these creation and annihilation operators, i.e., coherent states. In this section, we present a quick introduction to fermionic coherent states. For more details refer to [49, 50].

Grassmann variables and fermionic coherent states

Let's assume that a fermionic coherent state $|\xi\rangle$ is already constructed, defined as

$$\hat{c}_\alpha|\xi\rangle = \xi_\alpha|\xi\rangle, \tag{3.29}$$

where $\hat{c}_\alpha$ is a annihilation operator where $\alpha = 1, \dots n$. Due the Pauli exclusion principle, the wavefunction of N Fermions is anti-symmetric under exchange of any pair of particles, satisfying the idea that two Fermions cannot occupy the same state. Because of the anti-symmetric property of fermionic states, two annihilation operators of fermionic states anti-commute

$$\{\hat{c}_\mu, \hat{c}_\nu\} = 0, \tag{3.30}$$

where $\{\hat{A}, \hat{B}\} = \hat{A}\hat{B} + \hat{B}\hat{A}$ denotes the anti-commutator between operators $\hat{A}$ and $\hat{B}$. Since fermionic eigenvalues anti-commute, it is necessary to introduce anti-commuting variables called Grassmann numbers. According to Eq.(3.30)

$$\xi_\alpha\xi_\beta + \xi_\beta\xi_\alpha = 0, \tag{3.31}$$

it follows

$$\xi_\alpha^2 = 0. \tag{3.32}$$

We will denote ξ_α a generator of the Grassmann algebra $\mathcal{G}$ according to Eq.(3.29). In an algebra with even number of generators $n = 2p$, a conjugation operation is defined: for each generator ξ_α another generator $\bar{\xi}_\alpha$ is associated according to

$$(\xi_\alpha)^* = \bar{\xi}_\alpha \qquad \text{and} \qquad (\bar{\xi}_\alpha)^* = \xi_\alpha. \tag{3.33}$$

It follows that

$$\langle \xi_\alpha | \hat{c}_\alpha^\dagger = \langle \xi_\alpha | \bar{\xi}_\alpha. \tag{3.34}$$

Here $\bar{\xi}_\alpha$ represents a complete different Grassmann variable (it is a generator by itself), which is used to parametrize the left states. In order to simplify notation we will consider only two generators $\xi, \bar{\xi}$ and therefore $\mathcal{G}$ is generated by the set of numbers

$$\{1, \xi, \bar{\xi}, \bar{\xi}\xi\}. \tag{3.35}$$

According to Eq.(3.32), if there is an arbitrary analytic function f on this algebra it has to be linear

$$f(\xi) = f_0 + f_1 \xi, \tag{3.36}$$

where f_0, f_1 are Taylor expansion coefficients. For functions of two variables, we have

$$f(\bar{\xi}, \xi) = f_{00} + f_{10}\bar{\xi} + f_{01}\xi + f_{11}\bar{\xi}\xi. \tag{3.37}$$

It is natural to introduce a derivative for Grassmann functions analogously to complex functions, with the exception that variables $\bar{\xi}$ and ξ anti-commute. Derivatives of Grass-

mann functions satisfy

$$\frac{\partial}{\partial\bar{\xi}}f(\bar{\xi},\xi) = f_{10}+f_{11}\xi \tag{3.38a}$$

$$\frac{\partial}{\partial\xi}f(\bar{\xi},\xi) = f_{01}-f_{11}\bar{\xi} \tag{3.38b}$$

$$\frac{\partial}{\partial\bar{\xi}}\frac{\partial}{\partial\xi}f(\bar{\xi},\xi) = \frac{\partial}{\partial\bar{\xi}}(f_{01}-f_{11}\bar{\xi}) = -f_{11} = -\frac{\partial}{\partial\xi}\frac{\partial}{\partial\bar{\xi}}f(\bar{\xi},\xi), \tag{3.38c}$$

i.e. Grassmann derivatives anti-commute. There is no analog of the Riemann summation using Grassmann variables, so a traditional integration operation is not possible. So integration over Grassmann variables is defined as a linear mapping with the fundamental property that integral of exact differential form is zero over functions vanishing at infinity, i.e.,

$$\int d\xi = 0 \tag{3.39a}$$

$$\int \xi\, d\xi = 1. \tag{3.39b}$$

Applying these rules to an arbitrary function, we have

$$\int f(\bar{\xi},\xi)\, d\bar{\xi} = f_{10}+f_{11}\xi \tag{3.40a}$$

$$\int f(\bar{\xi},\xi)\, d\xi = f_{01}-f_{11}\bar{\xi} \tag{3.40b}$$

$$\int f(\bar{\xi},\xi)\, d\bar{\xi}\, d\xi = -f_{11} = -\int f(\bar{\xi},\xi)\, d\xi\, d\bar{\xi} \tag{3.40c}$$

Another convenient requirement is that Grassmann variables anti-commutes with fermionic annihilation and creation operators

$$\{\xi,\hat{c}\} = \{\xi,\hat{c}^\dagger\} = \{\bar{\xi},\hat{c}\} = \{\bar{\xi},\hat{c}^\dagger\} = 0. \tag{3.41}$$

We have constructed the Grassmann algebra $\mathcal{G}$ in which we associate a generator ξ with each annihilation operator $\hat{c}$ and a generator $\bar{\xi}$ with each creator operator $\hat{c}^\dagger$. Now we are able to construct a generalized Fock space as the linear combination of states of the

fermionic Fock space $\mathcal{F}$ with coefficients in the Grassmann algebra $\mathcal{G}$. Any vector $|\varphi\rangle$ in $\mathcal{F}$ can be expanded as

$$|\varphi\rangle = \sum_{\alpha} \chi_\alpha |\psi_\alpha\rangle, \tag{3.42}$$

where χ_α are Grassmann numbers, in our case, of the set (3.35) and $|\psi_\alpha\rangle$ vectors of the Fock space. Let's consider a single quantum level occupied by fermionic particles. This level may have either zero or one fermion in such state, and therefore the complete many-body Hilbert space is spanned by two orthonormal basis states, say $|0\rangle$ and $|1\rangle$, obeying the following standard relations

$$\hat{c}|0\rangle = 0 \qquad ; \qquad \hat{c}^\dagger|0\rangle = |1\rangle \tag{3.43a}$$

$$\hat{c}|1\rangle = |0\rangle \qquad ; \qquad \hat{c}^\dagger|1\rangle = 0. \tag{3.43b}$$

Since the Hilbert space has only two basis vectors, the coherent state must be a linear superposition of $|0\rangle$ and $|1\rangle$, for example

$$|\xi\rangle = |0\rangle - \xi|1\rangle = (1 - \xi\hat{c}^\dagger)|0\rangle = e^{-\xi\hat{c}^\dagger}|0\rangle. \tag{3.44}$$

Indeed, this parametrization corresponds to the explicit form of a coherent state:

$$\hat{c}|\xi\rangle = \hat{c}|0\rangle - \hat{c}\xi|1\rangle \tag{3.45a}$$

$$= 0 + \xi\hat{c}|1\rangle = \xi|0\rangle, \tag{3.45b}$$

where we have used Eq.(3.41) and

$$\xi|\xi\rangle = \xi|0\rangle - \xi^2|1\rangle \tag{3.46a}$$

$$= \xi|0\rangle. \tag{3.46b}$$

It follows that a fermionic coherent state has the form

$$|\xi\rangle = e^{-\xi\hat{c}^\dagger}|0\rangle = e^{\hat{c}^\dagger\xi}|0\rangle, \tag{3.47}$$

and for the left eigenstates

$$\langle\xi| = \langle 0|e^{-\hat{c}\bar{\xi}} = \langle 0|e^{\bar{\xi}\hat{c}} = \langle 0| - \langle 1|\bar{\xi}. \tag{3.48}$$

Using this parametrization is easy to verify that the set of coherent states is not orthonormal. In effect, for any two fermionic coherent states

$$\langle\xi|\xi'\rangle = (\langle 0| - \langle 1|\bar{\xi})(|0\rangle - \xi'|1\rangle) = 1 + \bar{\xi}\xi' = e^{\bar{\xi}\xi'}. \tag{3.49}$$

The resolution of the unity in this representation is given by

$$\hat{1} = \int d\bar{\xi}\, d\xi e^{-\bar{\xi}\xi}|\xi\rangle\langle\xi| \tag{3.50}$$

and the scalar product for two Grassmann functions of one variable is defined as

$$\langle f|g\rangle = \int d\bar{\xi}\, d\xi \bar{f}(\xi)g(\bar{\xi}) = \bar{f}_0 g_0 + \bar{f}_1 g_1. \tag{3.51}$$

Finally, the trace of an operator $\hat{\mathcal{O}}$ in the coherent state basis can be calculated according to

$$\begin{aligned}
\mathrm{Tr}(\hat{\mathcal{O}}) &= \sum_{n=0,1}\langle n|\hat{\mathcal{O}}|n\rangle = \sum_{n=0,1}\int d[\bar{\xi},\xi]e^{-\bar{\xi}\xi}\langle n|\xi\rangle\langle\xi|\hat{\mathcal{O}}|n\rangle \\
&= \int d[\bar{\xi},\xi]e^{-\bar{\xi}\xi}\sum_{n=0,1}\langle\xi|\hat{\mathcal{O}}|n\rangle\langle n| - \xi\rangle \\
&= \int d[\bar{\xi},\xi]e^{-\bar{\xi}\xi}\langle\xi|\hat{\mathcal{O}}| - \xi\rangle,
\end{aligned} \tag{3.52}$$

and because of the matrix element $\langle\varphi_i|\xi\rangle$ and $\langle\xi|\varphi\rangle$ between states $|\varphi\rangle$ in the Fock space and coherent states contain Grassmann numbers, it follows from the anti-commutation relations that

$$\langle\varphi_i|\xi\rangle\langle\xi|\varphi_j\rangle = \langle\xi|\varphi_j\rangle\langle\varphi_i| - \xi\rangle, \tag{3.53}$$

with $|-\xi\rangle = |0\rangle + \xi|1\rangle$.

Fermionic generating functional

Let's consider again the generating functional along the closed-time contour

$$\mathcal{Z}_{\mathcal{C}} = \frac{\mathrm{Tr}\left(\hat{\mathcal{U}}_{\mathcal{C}}\hat{\rho}(-\infty)\right)}{Z_{-\infty}}, \tag{3.54}$$

where $\hat{\rho}(-\infty)$ is the density matrix in the thermal equilibrium situation according to a standard Hamiltonian $\hat{H} = \epsilon_0\hat{c}^\dagger\hat{c} - \mu\hat{N}$. Since an arbitrary external perturbation may be switched on (and off) at later time, the choice of equilibrium initial density matrix does not prevent one from treating non-equilibrium dynamics. For fermions we have

$$Z_{-\infty} = \mathrm{Tr}\left(e^{-\beta(\epsilon_0-\mu)\hat{N}}\right) = 1 + e^{-\beta(\epsilon_0-\mu)}. \tag{3.55}$$

As in equilibrium theories, we proceed to divide the contour into equal infinitesimal time intervals of length $\delta_t \propto \frac{1}{N} \to 0$, but in our our case the number of intervals is $(2N-2)$ with $2N$ discrete time-points due the two branch contour as shown in figure 3.5. Then one has to insert the fermionic resolution of the identity

$$\hat{1} = \int d[\bar{\xi_j}, \xi_j] e^{-\bar{\xi_j}\xi_j} |\xi_j\rangle\langle\xi_j| \tag{3.56}$$

at each point $j = 1, \ldots, 2N$ along the contour between each pair of factors of the Trotter descomposition in Eq.(3.7), such that $t_1 = t_{2N} = -\infty$ and $t_N = t_{N+1} = \infty$, then

$$\begin{aligned}
\mathrm{Tr}\left(\hat{\mathcal{U}}_{\mathcal{C}}\hat{\rho}(-\infty)\right) &= \langle\xi_{2N}|\hat{\mathcal{U}}_H^{-\delta_t}|\xi_{2N-1}\rangle\cdots\langle\xi_{N+1}|\hat{\mathcal{U}}_H|\xi_N\rangle\cdots\langle\xi_2|\hat{\mathcal{U}}_H^{+\delta_t}|\xi_1\rangle\langle\xi_1|\hat{\rho}(-\infty)|-\xi_{2N}\rangle \\
&= \langle\xi_{2N}|\hat{\mathcal{U}}_H^{-\delta_t}|\xi_{2N-1}\rangle\cdots\langle\xi_{N+1}|\hat{1}|\xi_N\rangle\cdots\langle\xi_2|\hat{\mathcal{U}}_H^{+\delta_t}|\xi_1\rangle\langle\xi_1|\hat{\rho}(-\infty)|-\xi_{2N}\rangle.
\end{aligned}$$

Here $\hat{\mathcal{U}}^{\pm\delta_t}$ is the time evolution operator during time interval δ_t in the positive (negative) time direction, and we have considered in the last step that the time evolution operator between intervals t_N and t_{N+1} is equal to the identity, because these two time-points are physically indistinguishable.

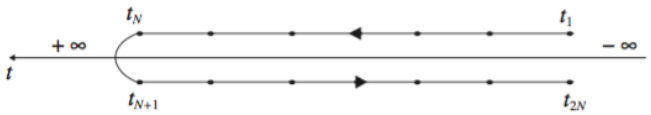

Figure 3.5: 2N discrete time points on the contour $\mathcal{C}$.

The matrix elements are

$$\begin{aligned}\langle\xi_j|\hat{\mathcal{U}}_H^{\pm\delta_t}|\xi_{j-1}\rangle &= \langle\xi_j|e^{\mp\frac{i}{\hbar}\hat{H}(\hat{c}^\dagger,\hat{c})\delta_t}|\xi_{j-1}\rangle \\ &\approx \langle\xi_j|1\mp\frac{i}{\hbar}\hat{H}(\hat{c}^\dagger,\hat{c})\delta_t|\xi_{j-1}\rangle = \langle\xi_j|\xi_{j-1}\rangle(1\mp\frac{i}{\hbar}H(\bar{\xi}_j,\xi_{j-1})\delta_t) \\ &\approx e^{\bar{\xi}_j\xi_{j-1}}e^{\mp\frac{i}{\hbar}H(\bar{\xi}_j,\xi_{j-1})\delta_t}, \end{aligned} \tag{3.57}$$

where the approximation are valid up to linear order in δ_t. In order to find the explicit form of the last matrix element, it is recommended to introduce an operational identity [41]

$$f(\hat{a}^\dagger\hat{a})\hat{a} = \hat{a}f(\hat{a}^\dagger\hat{a}-1), \tag{3.58}$$

with $\hat{a}^\dagger, \hat{a}$ any creation and annihilation operator respectively and f an arbitrary function. Using this identity one can prove that

$$M(\varrho) = \langle\xi|\varrho^{\hat{c}^\dagger\hat{c}}|\xi'\rangle = e^{\bar{\xi}\xi'\varrho}. \tag{3.59}$$

Indeed

$$\partial_\varrho M(\varrho) = \langle\xi|\hat{c}^\dagger\hat{c}\varrho^{\hat{c}^\dagger\hat{c}-1}|\xi'\rangle = \langle\xi|\hat{c}^\dagger\varrho^{\hat{c}^\dagger\hat{c}}\hat{c}|\xi'\rangle = \bar{\xi}\xi' M(\varrho), \tag{3.60}$$

i.e., we obtain a differential equation. Integrating this equation and considering as initial condition $M(1) = e^{\bar{\xi}\xi'}$, according to Eq.(3.49), one obtains the relation in Eq.(3.59). Using this identity over the term that involves the density matrix $\hat{\rho}(-\infty)$ one has

$$\langle\xi_1|e^{-\beta(\epsilon_0-\mu)\hat{c}^\dagger\hat{c}}|-\xi_{2N}\rangle = \exp\{\bar{\xi}_1\xi_{2N}\rho(-\infty)\}, \tag{3.61}$$

where $\rho(-\infty) = -\exp\{-\beta(\epsilon_0-\mu)\} \equiv -\rho(\epsilon_0)$.

Collecting all the matrix elements, one obtain finally the fermionic generating functional

$$\mathcal{Z}_{\mathcal{C}} = \frac{1}{Z_{-\infty}} \int\int \prod_{j=1}^{2N} [\, d\bar{\xi}_j \, d\xi_j] \exp\left(i \sum_{j,j'=1}^{2N} \bar{\xi}_j \underline{G}^{-1}_{jj'} \xi_{j'} \right), \tag{3.62}$$

where the the $2N \times 2N$ matrix $\underline{G}^{-1}_{jj'}$ is called the inverse Green's function and its discrete structure is as follows

$$i\underline{G}^{-1}_{jj'} = \left[\begin{array}{cccc|cccc} -1 & & & & & & & -\rho(\epsilon_0) \\ h_+ & -1 & & & & & & \\ & \ddots & \ddots & & & & & \\ & & h_+ & -1 & & & & \\ \hline & & & 1 & -1 & & & \\ & & & & h_- & -1 & & \\ & & & & & \ddots & \ddots & \\ & & & & & & h_- & -1 \end{array}\right]. \tag{3.63}$$

The diagonal elements comes from the resolution of the identity in the coherent state representation Eq.(3.56), while the lower sub-diagonal elements $h_\pm = 1 \mp i\epsilon_0\delta_t$ corresponds to the brackets of the time evolution operator $\hat{\mathcal{U}}_H^{\pm\delta_t}$ in Eq.(3.57) and the upper-right element comes from the matrix element involving the density matrix operator. Explicitly, the action acquires the form

$$\mathcal{S}[\bar{\xi}, \xi] = \sum_{j=2}^{2N} \delta_{t_j} \left[i\bar{\xi}_j \frac{\xi_j - \xi_{j-1}}{\delta_t} - \epsilon_0 \bar{\xi}_j \xi_{j-1} \right] + i\bar{\xi}_1 \left[\xi_1 + \rho(\epsilon_0)\xi_{2N} \right], \tag{3.64}$$

where $\delta_{t_j} = t_j - t_{j-1} = \pm\delta_t$, with $\pm$ signs corresponding to the forward and backward branches of the contour, respectively. In order to write the generating functional in a continuum notation, we have to take the limit $N \to \infty$ and $(\bar{\xi}_j, \xi) \to (\bar{\xi}(t), \xi(t))$ and therefore

$$\mathcal{Z}_{\mathcal{C}} = \int \mathcal{D}[\bar{\xi}(t, \xi(t)] \exp\left(i \int_{\mathcal{C}} dt [\bar{\xi}(t) \underline{G}^{-1} \xi(t)] \right) = \int \mathcal{D}[\bar{\xi}(t), \xi(t)] e^{i\mathcal{S}[\bar{\xi}, \xi]}. \tag{3.65}$$

Is then clear that in the continuum notation, the inverse Green's function for a non-

interacting Hamiltonian, is given by

$$G^{-1} = i\partial_t - \omega_0. \tag{3.66}$$

One can easily verify, using the identity of Grassmann Gaussian integrals, that in the limit $N \to \infty$

$$\mathcal{Z}_{\mathcal{C}} = \frac{\det[i\underline{G}^{-1}]}{Z_{-\infty}} = 1 \tag{3.67}$$

as was mentioned previously.

One would like to avoid the contour integration and work with time. In order to do that, we can split the integration contour into two time branches

$$\int_{\mathcal{C}=\gamma^+\oplus\gamma^-} d\tau = \int_{-\infty}^{\infty} dt + \int_{\infty}^{-\infty} dt = \int_{-\infty}^{\infty} dt - \int_{-\infty}^{\infty} dt. \tag{3.68}$$

Therefore it is also convenient to split the Grassmann field in two components

$$\xi(t) \to \begin{pmatrix} \xi^+(t) \\ \xi^-(t) \end{pmatrix}, \tag{3.69}$$

where the indices $(\pm)$ denote the field which reside on the forward and backward parts of the contour, respectively. Therefore, the final expression for the continuum action is

$$\begin{aligned} \mathcal{S}[\bar{\xi}(t), \xi(t)] &= \int_{-\infty}^{\infty} dt \left[\bar{\xi}^+(t)(i\partial_t - \epsilon_0)\xi^+(t) - \bar{\xi}^-(t)(i\partial_t - \epsilon_0)\xi^-(t)\right] \\ &= \int_{-\infty}^{\infty} dt \bar{\xi}(t)\hat{\sigma}_z(i\partial_t - \epsilon_0)\xi(t), \end{aligned} \tag{3.70}$$

where $\hat{\sigma}_z$ is the third Pauli matrix acting on Keldysh space and it contain the minus sign from the splitting of the contour.

Defining the inverse Green's function in the continuum representation Eq.(3.66), we are ignoring the boundary term. As a consequence, we are loosing the information stored in the initial density operator. However, the field theory is defined by its correlation functions and they must be calculated with proper boundary conditions, i.e., according to the boundary information stored in the density matrix operator $\hat{\rho}(-\infty)$. Even though one

might consider this information in a proper boundary condition to the continuum action, the safest way to take into account this information is by restoring the discrete formulation showed in Eq.(3.63). We will see in the next section that part of this information appears in the continuum limit of some propagators, storing in the equilibrium Fermi distribution functions. Therefore as long as we interpret these Green's functions as propagators of the action Eq.(3.70), the boundary conditions have been taken care of.

3.3 Fermionic Green's functions and Keldysh rotation

In order to calculate expectation values using Wick's theorem we need to know the structure of elementary contraction between two fields

$$\underline{G}_{i,j}^{\alpha,\beta} = -i\langle \psi_i^{\alpha} \bar{\psi}_j^{\beta} \rangle, \tag{3.71}$$

where the indices $\alpha, \beta = \pm$ indicate if the field is in the forward or backward branch of the contour, respectively. This motivates us to write the $2N \times 2N$ matrix Green's function and the inverse Green's function in a block decomposition of the form

$$\underline{G} = \frac{1}{\det[-i\underline{G}^{-1}]} \begin{bmatrix} G^{++} & G^{+-} \\ G^{-+} & G^{--} \end{bmatrix}, \tag{3.72}$$

where the determinant is

$$\begin{aligned} \det[i\underline{G}^{-1}] &= 1 + \rho(\omega_0)(h_+ h_-)^{N-1} = 1 + \rho(\omega_0)(1 + \omega_0^2 \delta_t^2)^{N-1} \\ &\approx 1 + \rho(\omega_0) e^{\omega_0^2 \delta_t^2 (N-1)} \xrightarrow{N\to\infty} 1 + \rho(\omega_0) = Z_{-\infty}, \end{aligned} \tag{3.73}$$

which is the result one would expect due Eq.(3.67) and we have considered that $\delta_t^2 N \to 0$ if $N \to \infty$. Indeed, we divided the contour in a way to keep $\delta_t N = \text{const}$ and as a result $\delta_t^2 \sim N^{-2}$[41]. Using the general formulae for the inversion of a 2×2 block matrices one

obtains the following results for the fermionic Green's functions

$$G^{\mathbb{T}}_{ij} \equiv G^{++}_{ij} = \frac{-ih_+^{i-j}}{\det[-i\underline{G}^{-1}]} \begin{cases} 1 & i \geqslant j \\ \rho(\omega_0)(h_-h_+)^{N-1} & i < j \end{cases} \tag{3.74a}$$

$$G^{\tilde{\mathbb{T}}}_{ij} \equiv G^{--}_{ij} = \frac{-ih_-^{j-i}}{\det[-i\underline{G}^{-1}]} \begin{cases} 1, & i \leqslant j \\ \rho(\omega_0)(h_-h_+)^{N-1} & i > j \end{cases} \tag{3.74b}$$

$$G^{<}_{ij} \equiv G^{+-}_{ij} = \frac{-i\rho(\omega_0)h_-^{j-1}h_+^{i-1}}{\det[-i\underline{G}^{-1}]} \tag{3.74c}$$

$$G^{>}_{ij} \equiv G^{-+}_{ij} = \frac{-ih_-^{N-i}h_+^{N-j}}{\det[-i\underline{G}^{-1}]}, \tag{3.74d}$$

where $j = 1, \ldots, N$ and the $2N \times 2N$ matrix must be read as index as $1, \ldots, N, N, \ldots 1$. The symbols $\mathbb{T}$ and $\tilde{\mathbb{T}}$ stand for time ordering and anti-ordering, respectively, and $<$ ($>$) indicates that the first argument is taken before (after) the second argument in the contour[2].

Since $h_+^* = h_-$ we have the following relations

$$[G^{\mathbb{T}}]^\dagger = -G^{\tilde{\mathbb{T}}} \qquad \text{and} \qquad [G^{<,>}]^\dagger = -G^{<,>}. \tag{3.75}$$

Taking the continuum limit we note that $(h_+h_-)^{N-1} \xrightarrow{N\to\infty} 1$ and $h_\pm^j \xrightarrow{N\to\infty} \exp[\mp i\omega_0 t]$,

[2]Let's take some time and analize an example trough an intiutive example, from Atland and Simonn's book[39]. For instance consider the matrix G^{++} which corresponds to the amplitude between two discrets points i, j in the upper branch contour γ^+. If we want to get from j to i, we may either go directly, which is complete possible if $i > j$. In this case, we pick up $i - j$ hopping amplitudes h_+, corresponing to the first term in the equation above. Alternatively, we may go via round-trips through the γ^- part of the contour. In this particular case, and no matter what the chronological ordering between i and j, we first go from j to N, i.e. $(N - j)$ amplitudes h_+. Then proceed from 1 to N on the bottom part ($N - 1$ amplitudes h_-), go back to the upper part (multiplying by a factor $\rho(\omega_0)$), and finally make it form 1 to i, giving $(i - 1)$ ampltudes h_+. That is the reason of the $\rho(\omega_0)$ term in the above expression.

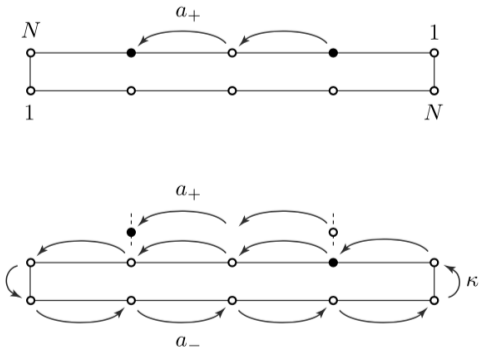

Figure 3.6: The two possibilities to go from j to i.

where t stands for $t = \delta_t j$ and therefore

$$G^{\mathbb{T}}(t,t') = -i\exp\left[-i\epsilon_0(t-t')\right](\Theta(t-t') - n_F(\omega_0)) \tag{3.76a}$$

$$G^{\tilde{\mathbb{T}}}(t,t') = -i\exp\left[-i\epsilon(t-t')\right](\Theta(t'-t) - n_F(\omega_0)) \tag{3.76b}$$

$$G^{<}(t,t') = i\exp\left[-i\epsilon_0(t-t')\right]n_F(\omega_0) \tag{3.76c}$$

$$G^{>}(t,t') = -i\exp\left[-i\epsilon_0(t-t')\right](1 - n_F(\omega_0)), \tag{3.76d}$$

where

$$n_F(\omega_0) = \frac{1}{1+e^{\beta(\omega-\mu)}} \tag{3.77}$$

corresponds to the Fermi distribution function in thermal equilibrium and $\Theta(t)$ is the Heaviside step function.

In general, one can shift the operator with the largest real-time argument from γ^+ to γ^- (and vice-versa), because of the time evolution along γ^+ and γ^- to the right of that operator cancels. This kind of redudancy implies the following relations among components of the matrix in Eq.(3.72):

$$G^{++}(t,t') = G^{+-}(t,t') \qquad (\text{for } t \leqslant t') \tag{3.78}$$

$$G^{++}(t,t') = G^{-+}(t,t') \qquad (\text{for } t > t') \tag{3.79}$$

$$G^{--}(t,t') = G^{-+}(t,t') \qquad (\text{for } t < t') \tag{3.80}$$

$$G^{--}(t,t') = G^{+-}(t,t') \qquad (\text{for } t \geqslant t'). \tag{3.81}$$

These equations can be summarized as

$$G^{++}(t,t') + G^{--}(t,t') = G^{+-}(t,t') + G^{-+}(t,t'). \tag{3.82}$$

The violation of this relation at $t = t'$ in the normal ordering convention is negligible under time integration used below.

This redundancy can be avoided by performing the so-called Keldysh rotation for fermionic fields ψ [51] by defining new fields according to

$$\psi_1(t) = \frac{1}{\sqrt{2}}(\psi^+(t) + \psi^-(t)) \qquad , \qquad \psi_2(t) = \frac{1}{\sqrt{2}}(\psi^+(t) - \psi^-(t)) \tag{3.83}$$

and for the *bar*[3] fields

$$\bar{\psi}_1(t) = \frac{1}{\sqrt{2}}(\bar{\psi}^+(t) - \bar{\psi}^-(t)) \qquad , \qquad \bar{\psi}_2(t) = \frac{1}{\sqrt{2}}(\bar{\psi}^+(t) + \bar{\psi}^-(t)). \tag{3.84}$$

Employing the field transformations, the Green's function or correlator between two fields becomes

$$\underline{G}(t,t') = \begin{bmatrix} G^R(t,t') & G^K(t,t') \\ 0 & G^A(t,t') \end{bmatrix}, \tag{3.85}$$

where the superscripts R, A, K, stand for **retarded, advanced** and **kinetic** or **Keldysh** component of the Green's function, respectively, and they are defined as

$$\begin{aligned} G^R(t,t') &= \frac{1}{2}(G^{\mathbb{T}}(t,t') - G^{\tilde{\mathbb{T}}}(t,t') + G^<(t,t') - G^<)(t,t') \\ &= \Theta(t-t')(G^>(t,t') - G^<(t,t') \qquad (3.86a) \\ G^A(t,t') &= \frac{1}{2}(G^{\mathbb{T}}(t,t') - G^{\tilde{\mathbb{T}}}(t,t') - G^<(t,t') + G^<)(t,t') \\ &= \Theta(t'-t)(G^<(t,t') - G^>(t,t')) \qquad (3.86b) \\ G^K(t,t') &= \frac{1}{2}(G^{\mathbb{T}}(t,t') + G^{\tilde{\mathbb{T}}}(t,t') + G^<(t,t') + G^<)(t,t') \\ &= G^>(t,t') + G^<(t,t')), \qquad (3.86c) \end{aligned}$$

[3]The reason of the different transformation for the *bar* fields is that $\bar{\psi}$ is not the conjugate of ψ, but rather a diferent field.

and consecuently

$$G^A(t,t') = [G^R(t,t')]^\dagger \qquad , \qquad G^K(t,t') = -[G^K(t,t')]^\dagger. \tag{3.87}$$

The components in Eq.(3.86a-3.86c) are often used to interpret the results of different calculations since they have an intuitive interpretation, which originates from their physical meaning in equilibrium: when the Hamiltonian $\mathcal{H}$ does not depend on time, real-time components of the Green's function G depend on time difference only and can be represented via their Fourier transform. The imaginary part of the retarded or advanced Green's function gives the single-particle spectral function

$$A(\omega) = -\frac{1}{\pi}\mathrm{Im}G^R(\omega) = \frac{1}{\pi}\mathrm{Im}G^A(\omega), \tag{3.88}$$

which represents the density of states of single-particle excitations at frequency ω of the many-body state. Out of equilibrium, one can still define the spectral function using Wigner transformation [52]

$$A(\omega,\bar{t}) = -\frac{1}{\pi}\mathrm{Im}\int d\delta_t e^{i\omega\delta_t}G^R(t,t'), \tag{3.89}$$

where $\bar{t} = \frac{1}{2}(t+t')$ and $\delta_t = t - t'$, which satisfies the sum rule

$$\int d\omega A(\omega,\bar{t}) = 1. \tag{3.90}$$

In equilibrium, all components of the matrix Green's function can be related to the spectral function

$$G(t,t') = -i\int d\omega e^{-i(t-t')}A(\omega)[\Theta(t-t') \pm f(\omega)], \tag{3.91}$$

where $f(\omega) = 1/(e^{\beta\omega} \mp 1)$ is the Bose (Fermi) distribution function. In particular, the imaginary part of the lesser (greater) Green's function thus yields the density of occupied

(unoccupied) states

$$\mp \mathrm{Im}G^{<}(\omega) = 2\pi A(\omega) f(\omega) \equiv 2\pi N(\omega) \tag{3.92a}$$

$$-\mathrm{Im}G^{>} = 2\pi A(\omega)[1 \pm f(\omega)]. \tag{3.92b}$$

In essence Eqs.(3.92a,3.92b) correspond to the *fluctuation-dissipation theorem* [53, 54] for single-particle excitations[4]

$$G^K(\omega) = [G^R(\omega) - G^A(\omega)]F(\omega), \tag{3.93}$$

where

$$F(\omega) = 1 \pm 2f(\omega) = \begin{cases} \coth\left(\frac{\beta\omega}{2}\right) & \text{bosons} \\ \tanh\left(\frac{\beta\omega}{2}\right) & \text{fermions} \end{cases} \tag{3.94}$$

For the toy example we are discussing in this section, the Green's function's component are given by

$$G^R(t,t') = -i\Theta(t-t')e^{-i\omega_0(t-t')} \xrightarrow{FT} \frac{1}{\omega - \omega_0 + i\eta^+} \tag{3.95a}$$

$$G^A(t,t') = i\Theta(t'-t)e^{-i\omega_0(t'-t)} \xrightarrow{FT} \frac{1}{\omega - \omega_0 - i\eta^+} \tag{3.95b}$$

$$G^K(t,t') = -i(2 - n_F(\omega))\exp[-i\epsilon_0(t-t')] \tag{3.95c}$$

$$\xrightarrow{FT} -2\pi i(1 - n_F(\omega_0))\delta(\epsilon - \epsilon_0) \tag{3.95d}$$

where $\eta^+ \to 0$ is a infinitesimal regulator. It follows that $G^K(\omega) \propto i\eta^+$ in equilibrium situations.

[4] If a statistical system in equilibrium is subjected to a small external force then the mean values of various random variables for the system exhibit a well defined response to this forcing. It turns out that such responses may be related to the equilibrium time lagged correlations of certain random variables within the system. This is of practical significance because often the equilibrium system may be observed over an extended period and so the time lag correlations of any observable random variables easily calculated. The Fluctuation-Dissipation theorem may then be used to deduce the response of the statistical system to an arbitrary but small perturbation.

3.4 Non-equilibrium Dyson equation

We conclude this chapter discussing very quickly the Dyson equation. In order to describe non-equilibrium correlated systems using Green's functions, one has to take account of self-energy corrections $\underline{\Sigma}$ to the non-interacting Green's function $\underline{G}_0$. In the Feynmann diagram language, the self-energy is defined as the sum of all one-particle irreducible diagrams of the interacting Green's function $\underline{G}$, i.e., diagrams that cannot be separated into two parts by cutting single $\underline{G}_0$ lines. It is important to note that the diagram rules are the same for the imaginary-time and contour-ordered Green's function when imaginary-time integrals over internal vertices are replaced by contour integrals. In the triagonal representation in Eq.(3.85), the matrix equation for the full interacting matrix Green's function $\underline{G}$ is

$$\underline{G} = \underline{G}_0 + \underline{G}_0 * \underline{\Sigma} * \underline{G}, \tag{3.96}$$

where the convolution $*$ signifies matrix multiplication in the spatial variable (as well as possible integral degrees of freedom) and time integration $A*B(t,t') \equiv \int_{-\infty}^{\infty} d\tilde{t} A(t,\tilde{t}B(\tilde{t},t))$. For each component it takes the form

$$\underline{G}^{R(A)} = \underline{G}_0^{R(A)} + \underline{G}_0^{R(A)} * \underline{\Sigma}^{R(A)} * \underline{G}^{R(A)} \tag{3.97a}$$

$$\underline{G}^{K} = \underline{G}_0^{K} + \underline{G}_0^{R} * \underline{\Sigma}^{R} * \underline{G}^{K} + \underline{G}_0^{R} * \underline{\Sigma}^{K} * \underline{G}^{A} + \underline{G}_0^{K} * \underline{\Sigma}^{A} * \underline{G}^{A}. \tag{3.97b}$$

To evaluate the self-energy in a realistic description of a physical system, we always need to implement a controlled approximation and additional techniques specifics of the problem. Equivalently, by iterating from the left gives a second matrix Dyson equation

$$\underline{G} = \underline{G}_0 + \underline{G} * \underline{\Sigma} * \underline{G}_0. \tag{3.98}$$

In equilibrium situations, we just need one of them, because the two equations are redundant, since the convolutions by Fourier transformation become simple products for which the order of the factors becomes irrelevant. However, in nonequilibrium scenarios the two matrix Dyson equations contain different information, and subtracting them is a useful

way of expressing nonequilibrium dynamics, for example, to derive the quantum kinetic equation [45].

Chapter 4

The model: A superconductor-semiconductor QD-Topological superconductor nano-junction

As we have already discussed Majorana fermions have recently received great interest in condensed matter physics due their possible existence in the form of a coherent superposition of zero energy electron-hole excitations [55] and various mechanisms have been proposed in order to search them. It is recognized that spinless Majorana bound states (MBS) can survive in p-wave superconductors [14, 56] which can be realized in a topological insulator in proximity to an s-wave superconductor. Recently the most popular topological quantum systems are the ordinary semiconductors with strong spin-orbit couplings, in proximity to an s-wave supercondutor and in the presence of Zeeman splitting. They support a pair of Majorana zero-energy modes (MZM) at the end of a 2D thin film of semiconductors [57, 58] or at the two ends of a 1D nanowire [59, 60].

Motivated by above findings, we consider a hybrid structure composed of a topological superconductor (TS), a Quantum Dot (QD) and a trivial s-wave superconductor lead (SC). We consider spinfull 1D TS realized by proximity-inducing superconductivity in a

spin-orbit-coupled semiconducting nanowire in a perpendicular magnetic field (which can also act on the dot). In this setup, the system can be tuned from a topologically trivial to a nontrivial regime by raising the Zeeman field above a certain critical value ($B > 0$) where, in the absence of interactions, the system undergoes a topological quantum phase transition with the effective induced superconductivity in the nanowire changing from a s-wave (trivial) character to a p-wave (topological) character. However, recent analyses [61] that incorporates strong repulsive interaction extend the parameter range over which the TS phase exists, achieving a topological phase even at zero magnetic field. Since the TS hosts two MBS on its ends, then within a reasonable approximation, the tunneling problem is reduced to that of transport in a SC-QD-MBS junction. We will consider large voltages V, such that $eV < \Delta$, which allows us to ignore a constant phase difference. Also we will consider a simple non-interacting model with $U = 0$. As the MZM exists as a zero-energy edge mode in the TS, tunneling conductance spectroscopy provides a simple way of detecting them.

In standard devices, like normal metal-superconductor junctions, it has been found that MZM mediates a perfect Andreev reflection (AR) at zero energy, which in turn gives rise to quantized $2e^2/h$ zero-bias conductance value [62, 63, 64, 65, 66], as long as the two MZMs at the wire ends are far from each other with exponentially small overlap between the MZM wavefunction, the so-called topologically protected regime. Nevertheless, the observed zero-bias conductance is substantially less than the MZM canonical quantized conductance value. A plausible source of discrepancy is thermal broadening in the normal metal lead, which reduces the zero-bias conductance value and widens the peak. The reason we are considering a SC lead instead of a normal metal lead is to mitigate this problem [67, 68, 69, 70]. In a SC lead, thermal quasi-particles excitations are exponentially suppressed by the superconducting gap, which grows as $\exp(-\Delta/T)$.

Following the last idea, an alternative way to detect MBS is to measure Majorana's nonlocal nature by, e.g., crossed AR[1]. The resulting nonlocal noise cross-correlations are studied extensively in lead-MBS directly coupling systems [63, 71, 72, 73]. It has reported

[1]Crossed Andreev reflection is the nonlocal conversion of an electron excitation into a hole excitation, each in a separate lead, while local AR converts an electron into a hole in the same lead. Equivalently, local AR injects a Cooper pair in a single lead, while crossed AR splits a Cooper pair over two lead.

[71] that large zero-mode splitting, the crossed AR process through a pair of MBSs dominates over the local AR, exhibiting maximally positive cross-correlations. On the other hand Law et al. [63] addressed that the currents from different leads can be maximally positively correlated or maximally negatively correlated, depending on the parity of the number of vortices. It is noticed that an injected electron, except for experiencing the crossed AR, can return to the same lead through local AR or enter the other lead by co-tunneling processes. Thus, different processes coexist simultaneously and probably confuse each other in these structures. To obtain the nonlocal information, a quantum dot is inserted between nanowires's ends and metal reservoirs. As a consequence, the local AR is heavily suppressed in favor of the observation of current cross-correlations, especially in the limit of weak dot-reservoir coupling.

The system we are investigating with is described in detail in section 4.1. As we have discussed above, it represents an excellent platform if one wants to study exotic correlation between different types of particles. In order to obtain the non-equilibrium transport current through the system, we make use of the mathematical framework discussed in the last chapter. In section 4.2 to introduce a source term, for later in section 4.3 we construct the central object we will deal with: the generating functional $\mathcal{Z}_{\mathcal{C}}$. We will show that it is necessary to define three different matrix Green's functions, one for each component of the system. In addition, due the bias voltage, the phase of the superconductor's order parameter depends on time, giving a Floquet representation of all Green's functions, described in detail in section 4.4. Once found all the relevant Keldysh-Floquet Green's functions, in section 4.5 the tunneling current is calculated by taking functional derivatives of $\mathcal{Z}_{\mathcal{C}}$ with respect to the sources.

Only calculation of the $\mathcal{Z}_{\mathcal{C}}$ and the tunneling current are given with all details in the present chapter. For the explicit calculation of others procedures, please refer to the appendices at the end of the thesis.

4.1 Our system

Our system consists on a hybrid structure composed of a topological superconductor (TS), a Quantum Dot (QD) and a trivial s-wave superconductor lead (L). The system is described by the second quantized Hamiltonian [74]

$$\hat{H} = \hat{H}_L + \hat{H}_d + \hat{H}_T. \tag{4.1}$$

The Hamiltonian is written in terms of spin matrices $\hat{s}$ and Nambu or particle-hole matrices $\hat{\tau}$, where $\hat{s}_0, \hat{\tau}_0, \hat{s}_i, \hat{\tau}_i$ with $i = x, y, z$ are unit and Pauli matrices in the respectively spaces. In this context, we define the lead and the dot electron operators as a 4-component spinor

$$\hat{c} = \begin{pmatrix} \hat{c}_\uparrow \\ \hat{c}_\downarrow \\ \hat{c}_\downarrow^\dagger \\ -\hat{c}_\uparrow^\dagger \end{pmatrix} \quad , \quad \hat{d} = \begin{pmatrix} \hat{d}_\uparrow \\ \hat{d}_\downarrow \\ \hat{d}_\downarrow^\dagger \\ -\hat{d}_\uparrow^\dagger \end{pmatrix} \tag{4.2}$$

and the Majorana fermion operator γ comes with the spinor

$$\bar{V}_\varphi = \begin{pmatrix} e^{i\varphi} \\ e^{i\varphi} \\ e^{-i\varphi} \\ -e^{-i\varphi} \end{pmatrix} \tag{4.3}$$

where φ is a constant topological phase [75]. Including the topological phase on the spinor we are considering an generalized Majorana fermion and as a consecuence, acting with an operator γ or $\gamma^\dagger$ differ only in a constant phase $e^{i\varphi}$.

Using this convention, the superconductor's Hamiltonian has the standard Bogoliubov-de Gennes form

$$\hat{H}_L = \frac{1}{2}\sum_k \hat{c}_k^\dagger \left[\left(\begin{bmatrix} \xi_k & \Delta \\ \Delta^* & -\xi_k \end{bmatrix} \right) \otimes \hat{s}_0 \right] \hat{c}_k, \tag{4.4}$$

where we have multiplied by the third Pauli matrix $\hat{\tau}_z$ in order to symmetrize the Hamilto-

nian [45] and Δ corresponds to the energy gap for the superconductor. The dot Hamiltonian reads

$$\hat{H}_d = \frac{1}{2}\hat{d}^\dagger \left(\varepsilon \hat{\tau}_z \otimes \hat{s}_0 + H\hat{\tau}_0 \otimes \hat{s}_z\right)\hat{d}, \tag{4.5}$$

where we consider a Zeeman component H, with a Larmor frequency given by $2H$, including the giromagnetic factor g. For the tunneling term

$$\hat{H}_T = \frac{1}{2}\left(t_L \hat{c}^\dagger(0)\hat{\tau}_z \otimes \hat{s}_0 + t_R \gamma \bar{V}^\dagger \hat{\tau}_z \otimes \hat{s}_0\right)\hat{d} + \text{h.c}, \tag{4.6}$$

we define the tunnel coupling between the normal superconductor and the dot, and between the dot and the topological superconductor as t_L, t_R respectively.

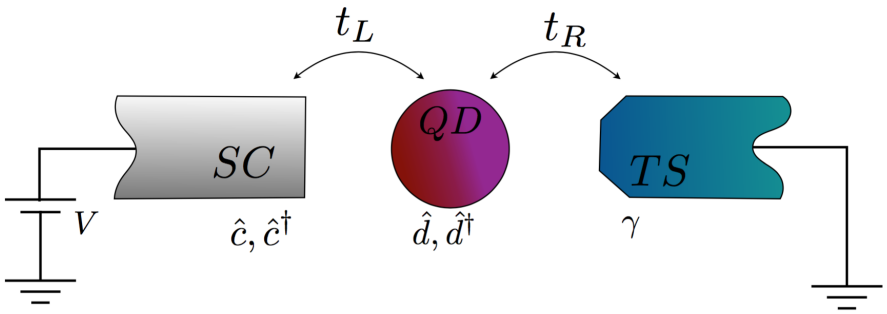

Figure 4.1: Structure of the nanojunction

The superconducting lead is placed at voltage bias V which is bigger compared to all other energy scales in the system, including Zeeman energy (although, V is less than the superconducting gap). For the topological superconductor we assume that the Majorana bound state (MBS) is well separated from other MBS's, i.e., at the other end of a TS wire, and therefore we are neglecting the couplings between them.

4.2 Current operator

The current is defined via continuity equation at the left SC lead[2]

$$\hat{J} = e\frac{d}{dt}\hat{N}_L = \frac{e}{i\hbar}[\hat{N}_L, \hat{H}], \tag{4.7}$$

where the number operator $\hat{N}_L$ for the superconductor has the form

$$\hat{N}_L = \frac{1}{2}\hat{c}^\dagger(0)\hat{\tau}_z \otimes \hat{s}_0\hat{c}(0). \tag{4.8}$$

We can immediately see that the only nonvanishing term that contributes to the current is the first term of H_T

$$\begin{aligned}
\hat{J} &= \frac{e}{2i\hbar}\big[\hat{c}^\dagger(0)\hat{\tau}_z \otimes \hat{s}_0\hat{c}(0), \frac{1}{2}t_L\hat{c}^\dagger(0)\hat{\tau}_z \otimes \hat{s}_0\hat{d} + \text{h.c}\big] \\
&= \frac{e}{4i\hbar}t_L\left(\big[\hat{c}^\dagger(0)\hat{\tau}_z \otimes \hat{s}_0\hat{c}(0), \hat{c}^\dagger(0)\hat{\tau}_z \otimes \hat{s}_0\hat{d}\big] - \text{h.c}\right) \\
&= -\frac{ie}{4\hbar}t_L\hat{c}^\dagger(0)_i\,(\hat{\tau}_z \otimes \hat{s}_0)_{ij}\underbrace{\big[\hat{c}(0)_j, \hat{c}^\dagger(0)_k\big]_+}_{\delta_{jk}}(\hat{\tau}_z \otimes \hat{s}_0)_{kl}\,\hat{d}_l + \text{h.c} \\
&= -\frac{ie}{4\hbar}t_L\left(c^\dagger(0)\hat{\tau}_z \otimes \hat{s}_0\hat{d} - \text{h.c}\right) \\
&= -\frac{ie}{4\hbar}\hat{j}_d
\end{aligned} \tag{4.9}$$

4.3 Keldysh Green's functions

According to Eq.(3.22) it is necessary to add a source term in order to construct the effective action. To this end we use the current in the Keldysh space $\hat{j}_d$. In the Keldysh theory the source field consists of two components: the classical α_{cl} and the quantum one α_q [41]. For simplicity we can set the classical contribution α_{cl} to the current to zero, because it is irrelevant for noise and current calculations. In the Keldysh space, the classical and

[2] In principle, one can argue that this kind of systems always obey the continuity equation for the currents $\hat{J}_R = -\hat{J}_L$. However, it is not possible to define a number operator $\hat{N}_R$ for Majorana fermions in the right lead, thus we analyze only the left current from the conventional superconductor.

quantum components for the current are proportional to the matrices

$$\hat{\sigma}^{cl} = \begin{pmatrix} 1 & 0 \\ 0 & 1 \end{pmatrix} = \hat{\sigma}_0 \quad , \quad \hat{\sigma}^{q} = \begin{pmatrix} 0 & 1 \\ 1 & 0 \end{pmatrix} = \hat{\sigma}_x, \tag{4.10}$$

where the Pauli matrices $\hat{\sigma}_i$ act on the Keldysh space. The source contribution is defined as

$$\hat{A}_{\rm s} = \frac{1}{4}\alpha\hat{j}_d, \tag{4.11}$$

which has only a quantum contribution. Now we will use the standard path-integral procedure shown in the Chapter 3 using coherent states. Implementing a continuum notation for the fields

$$\xi_i \longrightarrow \xi(t), \tag{4.12}$$

we can formally write the generating function as

$$\mathcal{Z}_{\mathcal{C}}[\alpha] = \int_{\mathcal{C}} \mathcal{D}[\bar{\xi}(t), \xi(t)] e^{i\mathcal{S}[\bar{\xi},\xi]}, \tag{4.13}$$

where $\mathcal{C}$ is the closed contour and the integration measure is the shorthand notation for $\mathcal{D}[\bar{\xi}(t), \xi(t)] = \prod_{i=1}^{2N} d[\bar{\xi}_i, \xi_i]/\mathrm{Tr}(\hat{\rho}(-\infty))$. With this source term the generating functional for our system will be

$$\mathcal{Z}_{\mathcal{C}}[\alpha] = \int_{\mathcal{C}} \mathcal{D}[\gamma(t)] \int_{\mathcal{C}} \mathcal{D}[\bar{\phi}(t), \phi(t)] \int_{\mathcal{C}} \mathcal{D}[\bar{f}(t), f(t)] e^{i[\mathcal{S}_0 + \mathcal{S}_{\rm s}]}, \tag{4.14}$$

where the action $\mathcal{S}_{\rm s}$ is due the presence of the source (4.11) and we have introduced an operator-field substitution via path-integral of fermionic coherent states

$$\hat{c}, \hat{c}^\dagger \quad \rightarrow \quad f, \bar{f} \tag{4.15a}$$

$$\hat{d}, \hat{d}^\dagger \quad \rightarrow \quad \phi, \bar{\phi} \tag{4.15b}$$

$$\gamma \quad \rightarrow \quad \gamma. \tag{4.15c}$$

Here, we have omited the time dependence of the coherent states. Splitting the fields in two components Ψ_+ and Ψ_-, as in Eq.(3.69) for the forward and backward contour, but

now taking account of the Nambu 4-component, we will have

$$\psi = \begin{pmatrix} \psi_{\uparrow} \\ \psi_{\downarrow} \\ \psi^{\dagger}_{\downarrow} \\ -\psi^{\dagger}_{\uparrow} \end{pmatrix} \Rightarrow \begin{pmatrix} \Psi_{+} \\ \Psi_{-} \end{pmatrix} = \begin{pmatrix} \begin{pmatrix} \psi_{\uparrow_{+}} \\ \psi_{\downarrow_{+}} \\ \psi^{\dagger}_{\downarrow_{+}} \\ -\psi^{\dagger}_{\uparrow_{+}} \end{pmatrix} \\ \begin{pmatrix} \psi_{\uparrow_{-}} \\ \psi_{\downarrow_{-}} \\ \psi^{\dagger}_{\downarrow_{-}} \\ -\psi^{\dagger}_{\uparrow_{-}} \end{pmatrix} \end{pmatrix} \tag{4.16}$$

and for the *bar* fields

$$\begin{aligned} \bar{\psi} &= \begin{pmatrix} \bar{\psi}^{\dagger}_{\uparrow} & \bar{\psi}^{\dagger}_{\downarrow} & \bar{\psi}_{\downarrow} & -\bar{\psi}_{\uparrow} \end{pmatrix} \\ &\Rightarrow \begin{pmatrix} \bar{\Psi}_{+} & \bar{\Psi}_{-} \end{pmatrix} = \left(\begin{pmatrix} \bar{\psi}^{\dagger}_{\uparrow_{+}} & \bar{\psi}^{\dagger}_{\downarrow_{+}} & \bar{\psi}_{\downarrow_{+}} & -\bar{\psi}_{\uparrow_{+}} \end{pmatrix} \begin{pmatrix} \bar{\psi}^{\dagger}_{\uparrow_{-}} & \bar{\psi}^{\dagger}_{\downarrow_{-}} & \bar{\psi}_{\downarrow_{-}} & -\bar{\psi}_{\uparrow_{-}} \end{pmatrix} \right) \\ . \end{aligned} \tag{4.17}$$

Note that now the integration is over the time axis and not over a contour $\mathcal{C}$. One of the consequences of splitting the fields is that we have to incorporate the relative minus sign to the $(-)$ fields due the backward contour. For this purpose, our previous structures transforms like

$$\bar{\psi}\hat{M}\psi \quad \Rightarrow \quad \begin{pmatrix} \bar{\Psi}_{+} & \bar{\Psi}_{-} \end{pmatrix} \left(\hat{\sigma}_z \otimes \hat{M} \right) \begin{pmatrix} \Psi_{+} \\ \Psi_{-} \end{pmatrix}, \tag{4.18}$$

where $\hat{M}$ is any 4×4 Hamiltonian term which only has spin and Nambu degrees of freedom and $\hat{\sigma}_z$ is the third Pauli matrix in the Keldysh space which incorporates the minus sign due the backward contour.

Our goal is to construct matrix Green's functions using the path-integral formalism. To obtain a more useful matrix structure, we have seen that is more convenient to use the triagonal representation Eq.(3.85), by making a Keldysh rotation Eq.(3.83, 3.84) and defining

new Keldysh fermionic fields labeled by the subindices $i = 1, 2$:

$$\begin{aligned} \Psi_+ &= \frac{1}{\sqrt{2}} (\Psi_1 + \Psi_2) \\ \Psi_- &= \frac{1}{\sqrt{2}} (\Psi_1 - \Psi_2) , \end{aligned} \tag{4.19}$$

such that

$$\begin{pmatrix} \Psi_+ \\ \Psi_- \end{pmatrix} = \frac{1}{\sqrt{2}} \begin{pmatrix} \mathbb{I}_{4\times4} & \mathbb{I}_{4\times4} \\ \mathbb{I}_{4\times4} & -\mathbb{I}_{4\times4} \end{pmatrix} \begin{pmatrix} \Psi_1 \\ \Psi_2 \end{pmatrix} = \hat{Q} \otimes (\hat{\tau}_0 \otimes \hat{s}_0) \begin{pmatrix} \Psi_1 \\ \Psi_2 \end{pmatrix}. \tag{4.20}$$

As we mentioned previously, the *bar* field transforms in a different manner. In this particular case, and following the above consideration, the transformation reads

$$\begin{aligned} \bar{\Psi}_+ &= \frac{1}{\sqrt{2}} \left(\bar{\Psi}_1 + \bar{\Psi}_2\right) \\ \bar{\Psi}_- &= \frac{1}{\sqrt{2}} \left(\bar{\Psi}_2 - \bar{\Psi}_1\right) \end{aligned} \tag{4.21}$$

and

$$\begin{pmatrix} \bar{\Psi}_+ \\ \bar{\Psi}_- \end{pmatrix} = \frac{1}{\sqrt{2}} \begin{pmatrix} \mathbb{I}_{4\times4} & \mathbb{I}_{4\times4} \\ -\mathbb{I}_{4\times4} & \mathbb{I}_{4\times4} \end{pmatrix} \begin{pmatrix} \bar{\Psi}_1 \\ \bar{\Psi}_2 \end{pmatrix} = \hat{Q}' \otimes (\hat{\tau}_0 \otimes \hat{s}_0) \begin{pmatrix} \bar{\Psi}_1 \\ \bar{\Psi}_2 \end{pmatrix}. \tag{4.22}$$

Then, the complete transformation is

$$\bar{\psi}\hat{H}\psi \quad \Rightarrow \quad \left(\bar{\Psi}_1 \quad \bar{\Psi}_2\right) \left(\hat{Q}'^T \otimes (\hat{\tau}_0 \otimes \hat{s}_0)\right) \left(\hat{\sigma}_z \otimes \hat{H}\right) \left(\hat{Q} \otimes (\hat{\tau}_0 \otimes \hat{s}_0)\right) \begin{pmatrix} \Psi_1 \\ \Psi_2 \end{pmatrix}. \tag{4.23}$$

Is important to note that only the matrices $\hat{Q}', \hat{\sigma}_z, \hat{Q}$ are in the Keldysh space. So this matrix product reduces to

$$\hat{Q}'^T \hat{\sigma}_z \hat{Q} = \hat{\sigma}_0, \tag{4.24}$$

and all the Keldysh degrees of freedom as a consequence of this transformation are incorporated into the identity matrix $\hat{\sigma}_0$. Then, the expression (4.23) acquires the form

$$\begin{aligned} \bar{\psi}\hat{M}\psi \quad &\Rightarrow \quad \bar{\psi}(\hat{\tau}_0 \otimes \hat{s}_0) \otimes \hat{\sigma}_0 \otimes \hat{M} \cdot (\hat{\tau}_0 \otimes \hat{s}_0)\psi \\ &= \quad \bar{\psi}\hat{\sigma}_0 \otimes (\hat{\tau}_0 \otimes \hat{s}_0) \cdot \hat{M} \cdot (\hat{\tau}_0 \otimes \hat{s}_0)\psi \\ &= \quad \bar{\psi}\hat{\sigma}_0 \otimes \hat{M}\psi \end{aligned} \tag{4.25}$$

In the last expression, the factor $\hat{\tau}_0 \otimes \hat{s}_0$ is just a 4 dimensional identity matrix, in the Nambu-spin space and is incorporated, without any effect, in the matrix $\hat{H}$.

The Majorana states have no spin and Nambu indices, they only have Keldysh indices. In this sense, we will consider that the Majorana fields split in two components like the other states, but they are a 2-component structures

$$\gamma^T \equiv \begin{pmatrix} \gamma_+ & \gamma_- \end{pmatrix} \quad \text{and} \quad \gamma = \begin{pmatrix} \gamma_+ \\ \gamma_- \end{pmatrix}. \tag{4.26}$$

Let us define

$$\gamma^T \bar{V}^\dagger = \begin{pmatrix} \gamma_+ \bar{V}^\dagger & \gamma_- \bar{V}^\dagger \end{pmatrix}_{(1\times 8)}. \tag{4.27}$$

So, after Keldysh rotations we will have for the coupling term

$$\begin{aligned} \gamma^T \bar{V}^\dagger \hat{M} \hat{d} \quad &= \quad \begin{pmatrix} \gamma_+ \bar{V}^\dagger & \gamma_- \bar{V}^\dagger \end{pmatrix}_{(1\times 8)} (\hat{\sigma}_0 \otimes \hat{M})_{(8\times 8)} \begin{pmatrix} d_+ \\ d_- \end{pmatrix}_{(8\times 1)} \\ &= \quad \begin{pmatrix} \gamma_+ \bar{V}^\dagger & \gamma_- \bar{V}^\dagger \end{pmatrix} \begin{pmatrix} \hat{M} & 0 \\ 0 & \hat{M} \end{pmatrix} \begin{pmatrix} d_+ \\ d_- \end{pmatrix} \\ &= \quad \begin{pmatrix} \gamma_+ & \gamma_- \end{pmatrix}_{(1\times 2)} \begin{pmatrix} \bar{V}^\dagger \cdot \hat{M} & 0 \\ 0 & \bar{V}^\dagger \cdot \hat{M} \end{pmatrix}_{(2\times 8)} \begin{pmatrix} d_+ \\ d_- \end{pmatrix}_{(8\times 1)} \\ &= \quad \gamma^T \hat{\sigma}_0 \otimes (\bar{V}^\dagger \cdot \hat{M}) \hat{d}. \end{aligned} \tag{4.28}$$

The same procedure must be applied for the hermitian conjugate.

Now we are able to work on the Keldysh action in the path integral. Returning to our

previous notation Eqs.(4.15a - 4.15c), but considering them as 8-component vectors, the action is

$$\mathcal{S}[\gamma,\phi,\bar{\phi},f,\bar{f}]=\mathcal{S}_d+\mathcal{S}_L+\mathcal{S}_T+\mathcal{S}_{\rm s}\equiv\mathcal{S}_0+\mathcal{S}_{\rm s}. \tag{4.29}$$

For the dot contribution, we have

$$\begin{aligned}\mathcal{S}_d &= \frac{1}{2}\int_{\mathbb{R}} dt\bar{\phi}\hat{\sigma}_0\otimes\left((i\partial_t-\varepsilon)\hat{\tau}_z\otimes\hat{s}_0-H\hat{\tau}_0\otimes\hat{s}_z\right)\phi\\ &= \frac{1}{2}\int_{\mathbb{R}} dt\bar{\phi}\underline{G}_{d0}^{-1}\phi,\end{aligned} \tag{4.30}$$

while the s-wave superconducting lead action is

$$\begin{aligned}\mathcal{S}_L &= \frac{1}{2}\int_{\mathbb{R}} dt\sum_k \bar{f}_k\hat{\sigma}_0\otimes\left(i\partial_t\left(\hat{\tau}_z\otimes\hat{s}_0\right)-\begin{pmatrix}\xi_k & -\Delta\\ \Delta^* & \xi_k\end{pmatrix}\otimes\hat{s}_0\right)f_k\\ &\equiv \frac{1}{2}\int_{\mathbb{R}} dt\bar{f}(0)\underline{g}^{-1}f(0).\end{aligned} \tag{4.31}$$

For the last term, which includes the coupling and the source terms, we write

$$\begin{aligned}\mathcal{S}_T+\mathcal{S}_{\rm s} &= \frac{1}{2}\int_{\mathbb{R}} dt\Big(\gamma^T\hat{\sigma}_0 i\partial_t\gamma+\frac{1}{2}t_L\bar{f}(0)\big[(\hat{\sigma}_0\otimes\hat{\tau}_z\otimes\hat{s}_0)+\alpha(\hat{\sigma}_x\otimes\hat{\tau}_0\otimes\hat{s}_0)\big]\phi\\ &\quad +t_R\gamma^T\hat{\sigma}_0\otimes(\bar{V}^\dagger\cdot(\hat{\tau_z}\otimes\hat{s}_0))\phi\Big)\\ &\quad +\frac{1}{2}\int_{\mathbb{R}} dt\Big(\frac{1}{2}t_L^*\bar{\phi}\big[(\hat{\sigma}_0\otimes\hat{\tau}_z\otimes\hat{s}_0)-\alpha(\hat{\sigma}_x\otimes\hat{\tau}_0\otimes\hat{s}_0)\big]f(0)\\ &\quad +t_R^*\bar{\phi}\hat{\sigma}_0\otimes((\hat{\tau}_z\otimes\hat{s}_0)\cdot\bar{V})\gamma\Big),\end{aligned} \tag{4.32}$$

where we have introduced the Keldysh matrix $\hat{\sigma}_x$ because we are considering the quantum source. Defining

$$\alpha_\pm=\frac{1}{2}\left[(\hat{\sigma}_0\otimes\hat{\tau}_z\otimes\hat{s}_0)\pm\alpha\left(\hat{\sigma}_x\otimes\hat{\tau}_0\otimes\hat{s}_0\right)\right], \tag{4.33}$$

the last equation adopts a more compact form

$$\begin{aligned}\mathcal{S}_T+\mathcal{S}_{\rm s} &= \frac{1}{2}\int_{\mathbb{R}} dt\left[\gamma^T(\hat{\sigma}_0(i\partial_t)\gamma+t_L\bar{f}(0)\alpha_+\phi+t_L^*\bar{\phi}\alpha_-f(0)\right.\\ &\left.+t_R\gamma^T\hat{\sigma}_0\otimes(\bar{V}^\dagger\cdot(\hat{\tau}_z\otimes\hat{s}_0))\phi+t_R^*\bar{\phi}\hat{\sigma}_0\otimes((\hat{\tau}_z\otimes\hat{s}_0)\cdot\bar{V})\gamma\right]. \quad (4.34)\end{aligned}$$

Adding all the contributions, the action reads

$$\begin{aligned}\mathcal{S}[\gamma,\phi,\bar{\phi},f,\bar{f}] &= \frac{1}{2}\int_{\mathbb{R}} dt\left[\gamma^T\hat{\sigma}_0(i\partial_t)\gamma\right.\\ &\left.+\bar{\phi}\underline{G}_{d0}^{-1}\phi+t_R\gamma^T\hat{\sigma}_0\otimes(\bar{V}^\dagger\cdot(\hat{\tau}_z\otimes\hat{s}_0))\phi+t_R^*\bar{\phi}\hat{\sigma}_0\otimes((\hat{\tau}_z\otimes\hat{s}_0)\cdot\bar{V})\gamma\right]\\ &+\frac{1}{2}\int_{\mathbb{R}} dt\left[\bar{f}(0)\underline{g}^{-1}f(0)+\bar{f}(0)\left(t_L\alpha_+\phi\right)+\left(t_L^*\bar{\phi}\alpha_-\right)f(0)\right]\\ &\equiv \mathcal{S}[\gamma,\phi,\bar{\phi}]+\mathcal{S}[\phi,\bar{\phi},f,\bar{f},\alpha]. \quad (4.35)\end{aligned}$$

At this point it is useful to remember the Gaussian identity for Grassmann variables [50]

$$\int\mathcal{D}[\bar{\xi}]\mathcal{D}[\xi]e^{-\bar{\xi}A\xi+J^\dagger\xi+J\bar{\xi}}=\det(A)e^{J^\dagger A^{-1}J}. \quad (4.36)$$

Using the Gaussian identity, we eliminate the superconductor degree of freedom by integrating at first the $\bar{f},f$ fields

$$\begin{aligned}\mathcal{Z}_{\mathcal{C}}[\alpha] &= \int\mathcal{D}[\gamma]\int\mathcal{D}[\phi,\bar{\phi}]e^{i\mathcal{S}[\gamma,\phi]}\int\mathcal{D}[f,\bar{f}]e^{i\mathcal{S}[f,\alpha]}\\ &= \mathcal{Z}_{\mathcal{C}}[\gamma,\phi,\bar{\phi}]\times\det\left(-\frac{i}{2}\underline{g}^{-1}\right)\exp\left[\frac{i}{2}\int_{\mathbb{R}}dt(t_L^*\bar{\phi}\alpha_-\left(-\underline{g}\right)t_L\alpha_+\phi)\right]\\ &= \mathcal{N}\times\mathcal{Z}_{\mathcal{C}}[\gamma,\phi,\bar{\phi}]\exp\left[-\frac{i}{2}\int_{\mathbb{R}}dt|t_L|^2\bar{\phi}\left(\alpha_-\underline{g}\alpha_+\right)\phi\right], \quad (4.37)\end{aligned}$$

with $\mathcal{N}$ a constant arising from the identity in Eq.(4.36). Using again the identity over the

last expression for integrating over the quantum dot degrees of freedom we get

$$\begin{aligned}
\mathcal{Z}_{\mathcal{C}}[\alpha] &= \mathcal{N}\int\mathcal{D}[\gamma]\int\mathcal{D}[\phi,\bar{\phi}]\exp\left\{\left[\frac{i}{2}\int_{\mathbb{R}}dt\bar{\phi}\left(\underline{G}_{d0}^{-1}-|t_L|^2\left(\alpha_-\underline{g}\alpha_+\right)\right)\phi\right.\right.\\
&\quad\left.\left.+\ (\gamma^T\hat{\sigma}_0(i\partial_t)\gamma+t_R\gamma^T\hat{\sigma}_0\otimes(\bar{V}^\dagger\cdot(\hat{\tau}_s\otimes\hat{s}_0))\phi+\bar{\phi}\left(t_R^*\hat{\sigma}_0\otimes((\hat{\tau}_z\otimes\hat{s}_0)\cdot\bar{V})\gamma\right)\right]\right\}\\
&= \mathcal{N}\times\det\left(-\frac{i}{2}(\underline{G}_{d0}^{-1}-|t_L|^2\left(\alpha_-\underline{g}\alpha_+\right))\right)\times\\
&\quad\int\mathcal{D}[\gamma]\exp\left\{\frac{i}{2}\int_{\mathbb{R}}dt\left[\gamma^T\hat{\sigma}_0(i\partial_t)\gamma\right.\right.\\
&\quad\left.\left.-\ |t_R|^2\gamma^T\left(\hat{\sigma}_0\otimes(\bar{V}^\dagger\cdot\hat{\tau}_z\otimes\hat{s}_0)\right)\left[\underline{G}_{d0}^{-1}-|t_L|^2\left(\alpha_-\underline{g}\alpha_+\right)\right]^{-1}\left(\left(\hat{\sigma}_0\otimes(\hat{\tau}_z\otimes\hat{s}_0)\cdot\bar{V}\right)\gamma\right]\right\}\\
&= \mathcal{C}\int\mathcal{D}[\gamma]\exp\left\{\frac{i}{2}\int_{\mathbb{R}}dt\gamma^T\hat{\sigma}_0(i\partial_t)\gamma-|t_R|^2\gamma^T\hat{\sigma}_0\otimes(\bar{V}^\dagger\cdot(\hat{\tau}_z\otimes\hat{s}_0))\underline{G}_d(\hat{\sigma}_0(\otimes\hat{\tau}_z\otimes\hat{s}_0)\cdot\bar{V})\gamma\right\}
\end{aligned}\tag{4.38}$$

As the topological phase φ is an arbitrary constant, we can consider $\varphi=0$ to simplify calculations. With this assumption, the $\bar{V}-$ spinor is

$$\bar{V}_{\varphi=0}=\begin{pmatrix}1 & 1 & 1 & -1\end{pmatrix}^T.\tag{4.39}$$

Then, the effective generating function is

$$\begin{aligned}
\mathcal{Z}_{\mathcal{C}}[\alpha] &= \mathcal{C}\int\mathcal{D}[\gamma]\exp\left\{\frac{i}{2}\int_{\mathbb{R}}dt\gamma^T\hat{\sigma}_0(i\partial_t)\gamma-|t_R|^2\gamma^T\left(\hat{\sigma}_0\otimes(\bar{V}^\dagger\cdot(\hat{\tau}_z\otimes\hat{s}_0)\right)\right.\\
&\qquad\left.\times\quad\underline{G}_d\left(\hat{\sigma}_0\otimes((\hat{\tau}_z\otimes\hat{s}_0)\cdot\bar{V}\right)\gamma\right\}\\
&= \mathcal{C}\int\mathcal{D}[\gamma]\exp\left\{\frac{i}{2}\int_{\mathbb{R}}dt\gamma^T(\underline{G}_{M0}^{-1}-\underline{\Sigma}_M)\gamma\right\}\\
&= \mathcal{C}\int\mathcal{D}[\gamma]\exp\left\{\frac{i}{2}\int_{\mathbb{R}}dt\gamma^T\underline{G}_M^{-1}\gamma\right\}\\
&= \mathcal{C}\int\mathcal{D}[\gamma]e^{i\mathcal{S}_{\text{eff}}[\alpha]}.
\end{aligned}\tag{4.40}$$

From the previous calculation we can identify three Green's functions. Using the energy representation, the superconductor lead Keldysh Green's function is

$$\underline{g}(E) = \begin{pmatrix} \underline{g}^R(E) & \underline{g}^K(E) \\ 0 & \underline{g}^A(E) \end{pmatrix}. \tag{4.41}$$

Each of the Green's functions $g^{(R,K,A)}$ is a 4×4 matrix and they include the dimension from the Keldysh rotation. Following Ref.[45] and after some convenient rotations (see Appendix B) the superconductor Green's function in equilibrium ($V = 0$) has the form

$$\underline{g}^{(R,A)}(E) = A^{(R,A)}(E)\hat{\tau}_0 \otimes \hat{s}_z + iB^{(R,A)}(E)\hat{\tau}_z \otimes \hat{s}_y. \tag{4.42}$$

As we showed, due to the fluctuation-dissipation theorem, the Keldysh or Kinetic Green's function satisfies

$$\boxed{\underline{g}^K(E) = \left[\underline{g}^R(E) - \underline{g}^A(E)\right] \tanh\left(\frac{E}{2T}\right)}. \tag{4.43}$$

The second Green's function is given by

$$\underline{G}_d(E,\alpha) = \left[\underline{G}_{d0}^{-1}(E) - |t_L|^2 \left(\alpha_- \underline{g}(E) \alpha_+\right)\right]^{-1}, \tag{4.44}$$

corresponding to the quantum dot's Green's function and where the retarded Green's function of the noninteracting dot in a magnetic field H has the form

$$\underline{G}_{d0}^{(R,A)}(E) = \left[(E \pm i\eta)\hat{\tau}_0 \otimes \hat{s}_0 - \varepsilon\hat{\tau}_z \otimes \hat{s}_0 - H\hat{\tau}_0 \otimes \hat{s}_z\right]^{-1} \quad \text{and} \quad \underline{G}_{d0}^{K}(E) = 0, \tag{4.45}$$

with $\eta \to 0$ a regulator. Finally, the Majorana Green's function is

$$\underline{G}_M(E,\alpha) = \left[\underline{G}_{M0}^{-1} - |t_R|^2(\hat{\sigma}_0 \otimes (\bar{V}^\dagger \cdot (\hat{\tau}_z \otimes \hat{s}_0)))\underline{G}_d(E,\alpha)(\hat{\sigma}_0 \otimes ((\hat{\tau}_z \otimes \hat{s}_0) \cdot \bar{V}))\right]^{-1}, \tag{4.46}$$

or in the Dyson Equation form

$$\underline{G}_M^{-1}(E,\alpha) = \underline{G}_{M0}^{-1}(E) - \underline{\Sigma}_M(E,\alpha), \tag{4.47}$$

where

$$\underline{\Sigma}_M(E,\alpha) = |t_R|^2(\hat{\sigma}_0 \otimes (\bar{V}^\dagger \cdot (\hat{\tau}_z \otimes \hat{s}_0)))\hat{\underline{G}}_d(E,\alpha)(\hat{\sigma}_0 \otimes ((\hat{\tau}_z \otimes \hat{s}_0) \cdot \bar{V}). \tag{4.48}$$

Here $\hat{G}^{-1}_{M0}(E)$ is the noninteracting Majorana Green's function, which in momentum space takes the form

$$\underline{G}_{M0}(E) = \begin{pmatrix} \underline{G}^R_{M0}(E) & \underline{G}^K_{M0}(E) \\ 0 & \underline{G}^A_{M0}(E) \end{pmatrix}, \tag{4.49}$$

where its components are

$$\underline{G}^{(R,A)}_{M0}(E) = \frac{1}{E \pm i\eta} \quad \text{and} \quad \underline{G}^K_{M0}(E) = 0. \tag{4.50}$$

The total Majorana Green's function, although, it depends on the dot Green's function G_d, *has no spin and particle-hole representation.* Indeed, it is a 2×2 matrix, representing only the Keldysh degrees of freedom. The noninteracting kinetic Dot and Majorana Green's functions, $\underline{G}^K_{d0}(E)$ and $\underline{G}^K_{M0}(E)$, are zero because they are proportional to the regulator $i\eta$ and vanish in the limit $\eta \to 0$, since noninteracting systems are dissipationless.

4.4 Green's functions in Floquet space

Now we will obtain the non-equilibrium Green's functions of the superconductor, the Majorana, and the dot as matrices in Floquet space.

Green's functions in the Floquet basis

Note that if we replace in Eq. (C.20) for Appendix (C) E, E' by $E + 2eVm$, $E + 2eVn$, the delta functions in Eq. (C.20) will have the form

$$\begin{aligned} \delta(E,E') &\implies \delta(m,n) \\ \delta(E,E'+2eV) &\implies \delta(m,n+1) \\ \delta(E,E'-2eV) &\implies \delta(m,n-1) \end{aligned} \tag{4.51}$$

then it is convenient to introduce the matrix notation

$$g^{\alpha}(E+2eVm, E+2eVn) \equiv g^{\alpha}_{m,n}(E), \tag{4.52}$$

with $\alpha =$ R,A,K. Because g^{α} for every m, n is a 4×4 matrix itself, we use the new indices i, k to designate the actual matrix element. The definitions (C.20) and (4.51) show that the energy difference between the initial and the final states is an integer multiple of $2eV$. To simplify notations we define the Floquet-states indices

$$I = \text{integer}\left[\frac{i-1}{4}\right] \quad , \quad K = \text{integer}\left[\frac{k-1}{4}\right], \tag{4.53}$$

and $E_K = E - 2eV(N-K)$ where $i, k = 1, \ldots, 4(2N+1)$. Using this new indices, then

$$\delta(E, E') \rightarrow \delta_{I,K} \tag{4.54}$$

$$\delta(E, E'+2eV) \rightarrow \delta_{I,K+1} \tag{4.55}$$

$$\delta(E, E'-2eV) \rightarrow \delta_{I,K-1}. \tag{4.56}$$

For the superconductor Green's function in the Floquet space we have

$$\boxed{\underline{g}^{\alpha}_{i,k}(E) = \underline{g}^{\text{diag}}_{i,k}(E) + \underline{g}^{+}_{i,k}(E) + \underline{g}^{-}_{i,k}(E).} \tag{4.57}$$

Superconductor Green function

According with Eq. (C.20) we have

$$\underline{g}^{\text{diag}}_{ik}(E) = \delta_{I,K}\begin{pmatrix} A(E_K-eV) & & & \\ & -A(E_K+eV) & & \\ & & A(E_K+eV) & \\ & & & -A(E_K-eV) \end{pmatrix}_{i-4K,k-4K} \tag{4.58}$$

$$\underline{g}^{-}_{ik}(E) = \delta_{I,K+1} \left(\begin{array}{cc|cc} 0 & B(E_K+eV) & & \\ 0 & 0 & & \\ \hline & & 0 & 0 \\ & & -B(E_K+eV) & 0 \end{array} \right)_{i-4(K+1),k-4K} \tag{4.59}$$

$$\underline{g}^{+}_{ik}(E) = \delta_{I,K-1} \left(\begin{array}{cc|cc} 0 & 0 & & \\ B(E_K-eV) & 0 & & \\ \hline & & 0 & -B(E_K-eV) \\ & & 0 & 0 \end{array} \right)_{i-4(K-1),k-4K} , \tag{4.60}$$

where α in Eq. (4.57) refers to the components R,A,K of the matrix Green's function $\underline{g}$. The matrix structure of the $4(2N+1)\times 4(2N+1)$ matrix $\underline{g}^{\alpha}_{i,k}(E)$ consists of 4×4 diagonal boxes $\underline{g}^{\text{diag}}_{ik}$ and of 4×4 blocks $\underline{g}^{\pm}_{ik}$ on each side of the diagonal. The others Keldysh Green's functions have a similar representation. The dot Green's function includes the superconductor Green's function $\underline{g}$ as a non-equilibrium part, therefore we can write the total dot Green's function such as $\underline{g}$. The total Majorana Green's function is a matrix in the Floquet space $(2N+1)\times(2N+1)$. Using the definition of the spinor $\bar{V}_{\varphi=0}$ we find

$$\boxed{G^{-1R}_{M_{i,k}}(E) = G^{-1R}_{M0}(E) - \Sigma^{R}_{M_{p,q}}(E,\alpha)}, \tag{4.61}$$

Majorana Green function

where the zero-order Majorana Green Function consists of only diagonal matrix elements in Floquet space

$$G^{-1R}_{M0_{p,q}}(E) = \delta_{p,q}(E - 2eVN + 2eVp). \tag{4.62}$$

In the Floquet basis, with $p, q = 0, 1, 2, \ldots, 2N$ (such as the indices I, K), we have for the Dot Green's function

$$G^R_{d_{p,q}} = \begin{bmatrix} G^R_{d_{4p+1,4q+1}} & G^R_{d_{4p+1,4q+2}} & G^R_{d_{4p+1,4q+3}} & G^R_{d_{4p+1,4q+4}} \\ G^R_{d_{4p+2,4q+1}} & G^R_{d_{4p+2,4q+2}} & G^R_{d_{4p+2,4q+3}} & G^R_{d_{4p+2,4q+4}} \\ G^R_{d_{4p+3,4q+1}} & G^R_{d_{4p+3,4q+2}} & G^R_{d_{4p+3,4q+3}} & G^R_{d_{4p+3,4q+4}} \\ G^R_{d_{4p+4,4q+1}} & G^R_{d_{4p+4,4q+2}} & G^R_{d_{4p+4,4q+3}} & G^R_{d_{4p+4,4q+4}} \end{bmatrix}_{(4\times 4)},$$

where we have considered the structures of the suprconductor Green's function in Eq.(4.41).

Using the explicit form of the Majorana self-energy, we obtain

$$\begin{aligned} \underline{\Sigma}_{M_{pq}}(E,\alpha) &= |t_R|^2(\hat{\sigma}_0 \otimes (\bar{V}^\dagger \cdot (\hat{\tau}_z \otimes \hat{s}_0)))\underline{G}_{d_{pq}}(\hat{\sigma}_0 \otimes ((\hat{\tau}_z \otimes \hat{s}_0) \cdot \bar{V}) \\ &= |t_R|^2(\hat{\sigma}_0 \otimes (\bar{V}^\dagger \cdot (\hat{\tau}_z \otimes \hat{s}_0))) \begin{pmatrix} \underline{G}^R_{d_{pq}} & \underline{G}^K_{d_{pq}} \\ 0 & \underline{G}^A_{d_{pq}} \end{pmatrix} (\hat{\sigma}_0 \otimes ((\hat{\tau}_z \otimes \hat{s}_0) \cdot \bar{V})) \\ &\equiv |t_R|^2 \hat{\Lambda}^T \underline{G}_{d_{pq}}(E,\alpha)\hat{\Lambda}. \end{aligned} \tag{4.63}$$

4.5 The tunneling current

If we want to evaluate the current, we have to take derivatives of the effective action with respecto to α:

$$\begin{aligned} \langle \hat{j}(t) \rangle &= \left. \frac{\delta \mathcal{Z}_{\mathcal{C}}[\alpha]}{\delta\alpha(t)} \right|_{\alpha\to 0} = \left. \frac{\delta}{\delta\alpha(t)} \left(\int \mathcal{D}[\gamma] e^{i\mathcal{S}_{\text{eff}}[\alpha]} \right) \right|_{\alpha\to 0} = \left. \frac{\delta}{\delta\alpha(t)} \left(\int \mathcal{D}[\gamma] e^{\frac{i}{2}\int dt \gamma^T \underline{G}_M^{-1} \gamma} \right) \right|_{\alpha\to 0} \\ &= -\frac{1}{2}\text{Tr} \int dt_1 \int dt_2 \underline{G}_M[t_1, t_2, \alpha] \left(\frac{\delta \underline{G}_M^{-1}[t_2, t_1\alpha]}{\delta\alpha(t)} \right) \mathcal{Z}_{\mathcal{C}}[\alpha] \Big|_{\alpha\to 0} \\ &= -\frac{1}{2}\text{Tr} \int dt_1 \int dt_2 \underline{G}_M[t_1, t_2, \alpha] \left(\frac{\delta}{\delta\alpha(t)} \left[\underline{G}_{M0}^{-1}[t_2, t_1] - t_R^2 \hat{\Lambda}^T \underline{G}_d[t_2, t_1, \alpha]\hat{\Lambda} \right] \right) \Big|_{\alpha\to 0} \\ &= -\frac{1}{2}\text{Tr} \int dt_1 \int dt_2 \underline{G}_M[t_1, t_2, \alpha] \left(-t_R^2 \hat{\Lambda}^T \left(\frac{\delta}{\delta\alpha(t)} \underline{G}_d[t_2, t_1, \alpha] \right) \hat{\Lambda} \right) \Big|_{\alpha\to 0}. \end{aligned} \tag{4.64}$$

For any inverse operator $\hat{A}^{-1}(x)$, its derivative is given by

$$\begin{aligned}
&\frac{d}{dx}\left(\hat{A}^{-1}(x)\hat{A}(x)\right) = 0 \\
\Leftrightarrow\quad &\left(\frac{d}{dx}\hat{A}(x)\right)\hat{A}^{-1}(x) + \hat{A}(x)\left(\frac{d}{dx}\hat{A}^{-1}(x)\right) = 0 \\
\Leftrightarrow\quad &\frac{d}{dx}\hat{A}^{-1}(x) = -\hat{A}^{-1}(x)\left(\frac{d}{dx}\hat{A}(x)\right)\hat{A}^{-1}(x). \qquad (4.65)
\end{aligned}$$

Therefore

$$\frac{\delta \underline{G}_d[t_2,t_1,\alpha]}{\delta\alpha(t)} = -\int dt_3 \int dt_4 \underline{G}_d[t_2,t_3,\alpha]\left(\frac{\delta}{\delta\alpha(t)}\underline{G}_d^{-1}[t_3,t_4,\alpha]\right)\underline{G}_d[t_4,t_1,\alpha],$$

where

$$\begin{aligned}
\frac{\delta}{\delta\alpha(t)}\underline{G}_d^{-1}[t_3,t_4,\alpha] &= \frac{\delta}{\delta\alpha(t)}\left(\underline{G}_{d0}^{-1} - t_L^2\alpha_-\underline{g}\alpha_+\right)[t_3,t_4,\alpha] \\
&= -\frac{t_L^2}{2}\big[\delta(t-t_4)(\hat{\sigma}_0\otimes\hat{\tau}_z\otimes\hat{s}_0))\underline{g}(t_3,t_4)(\hat{\sigma}_x\otimes\hat{\tau}_0\otimes\hat{s}_0)) \\
&\qquad \delta(t-t_3)(\hat{\sigma}_x\otimes\hat{\tau}_0\otimes\hat{s}_0))\underline{g}(t_4,t_3)(\hat{\sigma}_0\otimes\hat{\tau}_z\otimes\hat{s}_0)) - \mathcal{O}(\alpha)\big]. \qquad (4.66)
\end{aligned}$$

In the limit $\alpha \to 0$ we obtain for the quantum dot Green's function

$$\underline{G}_d[E,\alpha]|_{\alpha\to 0} = \left[\underline{G}_{d0}^{-1} - t_L^2(\hat{\sigma}_0\otimes\hat{\tau}_z\otimes\hat{s}_0)\underline{g}(\hat{\sigma}_0\otimes\hat{\tau}_z\otimes\hat{s}_0)\right]^{-1}, \qquad (4.67)$$

and the Majorana Green's function is

$$\underline{G}_M[E,\alpha]|_{\alpha\to 0} = \left[\underline{G}_{M0}^{-1} - t_R^2\hat{\Lambda}^T\left(\underline{G}_{d0}^{-1} - t_L^2(\hat{\sigma}_0\otimes\hat{\tau}_z\otimes\hat{s}_0)\underline{g}(\hat{\sigma}_0\otimes\hat{\tau}_z\otimes\hat{s}_0)\right)^{-1}\hat{\Lambda}\right]^{-1}. \qquad (4.68)$$

Collecting all the terms, and after integrating the delta functions, we have the final expression for the current

$$\begin{aligned}\langle\hat{j}\rangle \quad = \quad & \frac{(t_R t_L)^2}{4}\mathrm{Tr}\int dt_1 \int dt_2 \underline{G}_M(t_1,t_2,\alpha=0)\hat{\Lambda}^T \\ & \left\{\int dt_3 \underline{G}_d(t_2,t_3,\alpha=0)\hat{M}_{0z0}\underline{g}(t_3,t)\hat{M}_{x00}\underline{G}_d(t,t_1,\alpha=0)\right. \\ & \left.\int dt_4 \underline{G}_d(t_2,t,\alpha=0)\hat{M}_{x00}\underline{g}(t,t_4)\hat{M}_{0z0}\underline{G}_d(t_4,t_1,\alpha=0)\right\}\hat{\Lambda}, \end{aligned} \tag{4.69}$$

where, for convenient reasons, we have defined the matrices

$$(\hat{\sigma}_0 \otimes \hat{\tau}_z \otimes \hat{s}_0) \equiv \hat{M}_{0z0} \quad \text{and} \quad (\hat{\sigma}_x \otimes \hat{\tau}_0 \otimes \hat{s}_0) \equiv \hat{M}_{x00}. \tag{4.70}$$

Note that in our case, the Green's functions actually depend on time differences, i.e.

$$G(t,t') \equiv G(t-t'), \tag{4.71}$$

then they admit a single-variable Fourier transform. Using the convolution theorem, we have for example:

$$\begin{aligned}\int dt_1 \int dt_2 \quad \int dt_3 \quad & f(t_1-t_2)g(t_2-t_3)h(t_3-t)j(t-t_1) \\ & \Rightarrow \int d\tau_1 \int d\tau_2 \int d\tau_3 f(\tau_1)g(\tau_2)h(\tau_3)j(-(\tau_1+\tau_2+\tau_3))\end{aligned}$$

where we have defined a new set of variables

$$\tau_1 = t_1 - t_2 \quad , \quad \tau_2 = t_2 - t_3 \quad , \quad \tau_3 = t_3 - t. \tag{4.72}$$

Making a Fourier transformation we have

$$\begin{aligned}
\xrightarrow{\text{F.T}} \quad & \int dE_1 \int dE_2 \int dE_3 \int dE_4 \int d\tau_1 \int d\tau_2 \int d\tau_3 \\
& \times \exp\big[-iE_1\tau_1 - iE_2\tau_2 - iE_3\tau_3 + iE_4(\tau_1+\tau_2+\tau_3)\big] \tilde{f}(E_1)\tilde{g}(E_2)\tilde{h}(E_3)\tilde{j}(E_4) \\
= \quad & \int dE_1 \int dE_2 \int dE_3 \int dE_4 \underbrace{\int d\tau_1 e^{-i(E_1-E_4)\tau_1}}_{\delta(E_1-E_4)} \\
& \times \underbrace{\int d\tau_2 e^{-i(E_2-E_4)\tau_2}}_{\delta(E_2-E_4)} \underbrace{\int d\tau_3 e^{-i(E_3-E_4)\tau_3}}_{\delta(E_3-E_4)} \tilde{f}(E_1)\tilde{g}(E_2)\tilde{h}(E_3)\tilde{j}(E_4) \\
= \quad & \int dE \tilde{f}(E)\hat{g}(E)\tilde{h}(E)\tilde{j}(E)
\end{aligned}$$

where we have called $E = E_4$. According to this, in what follows we will omit time arguments and integrals and we will use only the energy representation

$$\begin{aligned}
\langle \hat{j} \rangle \quad &= \quad \mathcal{C}\mathrm{Tr} \int dE \underline{G}_M(E)\hat{\Lambda}^T \Big\{ \underline{G}_d(E)\hat{M}_{0z0}\underline{g}(E)\hat{M}_{x00}\underline{G}_d(E) - \underline{G}_d(E)\hat{M}_{x00}\underline{g}(E)\hat{M}_{0z0}\underline{G}_d(E) \Big\} \hat{\Lambda} \\
&\equiv \quad \int dE j(E,V,T) \\
&\equiv \quad J(V,T), \qquad (4.73)
\end{aligned}$$

where Tr implies taking the trace over Keldysh and Floquet spaces.

Chapter 5

Results and discussion

In the present chapter we show the I-V characteristic of the tunneling current through the system for different setups. Thermoelectric transport coefficients discussed in section 2.4 are also studied.

5.1 Electric current

We have evaluated numerically the non-equilibrium transport current Eq. (4.73) using the Numpy package for scientific computing with Python. Even though the energy domain of the integral is the complete real axis, because of the quasi-classical approximation discussed in Appendix A, only a finite region around the Fermi energy is relevant. That is why we have used the Gaussian Quadrature integration method in order to evaluate the energy integral, where the weights of large energy-contributions allow us to consider the relevant region and neglect the energy contributions that do not play any important role in transport processes.

To calculate the $I-V$ characteristic, the number of Floquet states is adjusted until the result is insensitive to a further increase in n. In figure 5.1 the first six modes are shown, and the resulting current is the result of the addition of all modes. It can be seen that the contribution of the $n = 2$ mode is dominant while the contribution of the following modes decreases as n increases. It is important to note that the contribution of the $n = 0$ mode is notoriously small because the $n = 0$ block-matrices Green's functions are diagonal and

the non-diagonal contributions are present starting from the $n = 1$ Floquet mode.

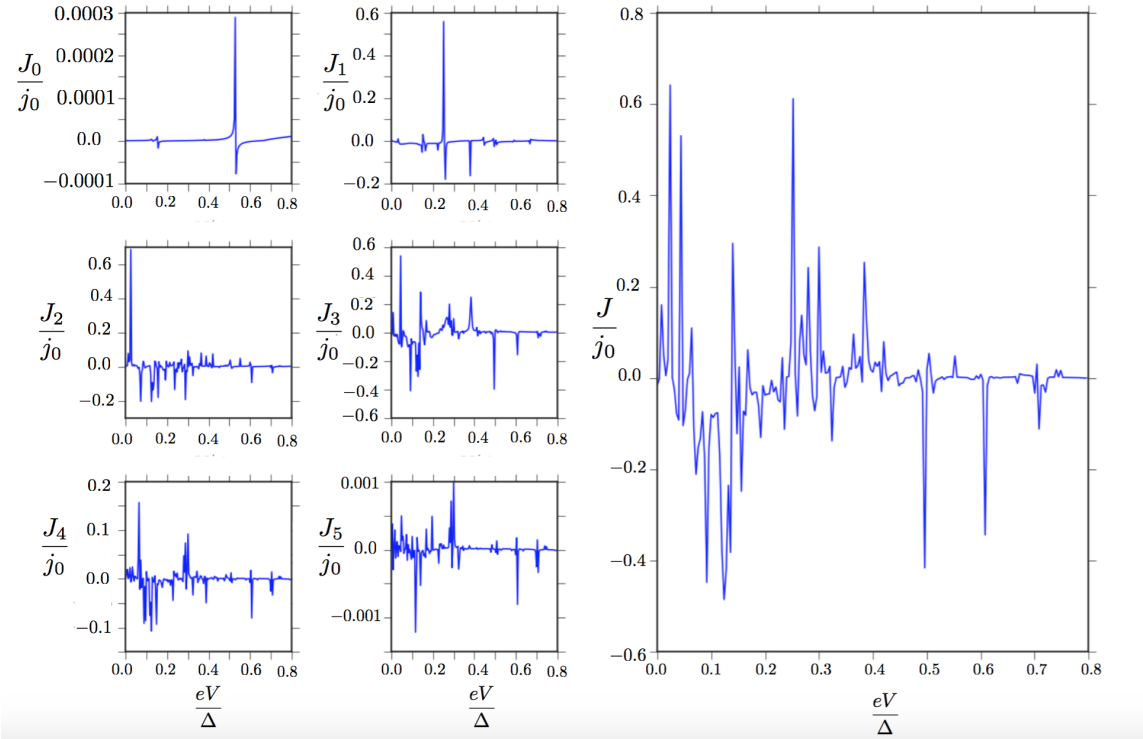

Figure 5.1: First six Floquet modes and the resulting transport current through the nano junction. We have set the dot energy $\epsilon = -0.01\Delta$, the temperature $T = 0.1\Delta$, magnetic field $H = 0.0$, and the tunneling constants $t_L = 0.7\Delta$ and $t_R = 0.05\Delta$ and $j_0 = e\Delta/2\hbar$.

The oscillating behavior of the current is a signature of Floquet modes, but most importantly, the inversion of the sign in the transport current and the positive peak are hallmarks of the processes already discussed in chapter 2: Andreev reflections (AR), that constitute the key mechanism for the superconducting proximity effect (PE). It was understood in the sixties that superconducting correlations could extend over large length scale in a normal metal, even in the absence of attractive electron-electron interactions. In this context the PE is the emergence of superconducting-like properties in a non-superconducting material placed in electrical contact with a superconductor. The role of AR is central to this process since it provides the elementary mechanism for converting single electron states from normal metal to Cooper pairs in the superconducting condensate. When a Cooper pair leaves the superconductor, because of multiple AR, different processes can occur in the way to the MBS.

Consider for instance that in the interface of the quantum dot the Cooper pair suffers an AR and it splits into one electron traveling to the right and a backscattered hole traveling to the superconducting lead. Let's study what happens with the reflected hole: when the hole scatters the superconducting interface, a Cooper pair is absorbed into the superconducting ground state, and an electron is reflected to the right, producing a second AR. After this process we have two additional contribution to the electric current between the superconductor-quantum dot: the hole carrying a charge e moving to the left and an extra electron with charge $-e$ traveling to the right, doubling the net charge to the right. On the other hand, the first electron originated from the Cooper pair splitting traveling to the right can occupy the dot's level (without any AR because there is no superconductor-metal interface) and then continue his way to the topological superconductor, in whose interface a MBS is located. As we discussed previously, in an adequate approximation, the Majorana fermion acts as effective lead, so we can consider that the (quasi-)particles traveling from the left interact only with the MBS. When an incoming electron has energy that matches an energy level of the quantized Majorana mode, then the incident electron is converted into a backscattered hole with probability of unity, independent of the coupling strength. This processes is known as resonant Andreev reflection (RAR) [63], which has a sharp contrast to the AR present in normal metal-insulator-superconductor systems, where it has been reported that amplitude of normal AR at fixed subgap energy decreases with decreasing coupling strength. So, because of RAR processes, there will be an second hole traveling to the left. This hole can occupy the dot's level as the electron did, and later it will scatter the superconductor interface, producing an extra absorbed Cooper pair and an additional reflected electron. This processes is described in Fig. 5.2 a).

The other virtual process is shown in Fig. 5.2b): suppose that the Cooper pair from the superconductor does not suffer any AR. It splits in two electrons of opposite spin in the interface of the quantum dot. Because of the Pauli exclusion principle, these two electrons can occupy the dot's level without any restriction (nevertheless, if there is a magnetic field, there will be a Zeeman splitting in the dot's energy level and the electrons will occupy different levels according their spin values) and continue traveling to the topological superconducting interface. As we describe earlier, because of the MBS, there will be two

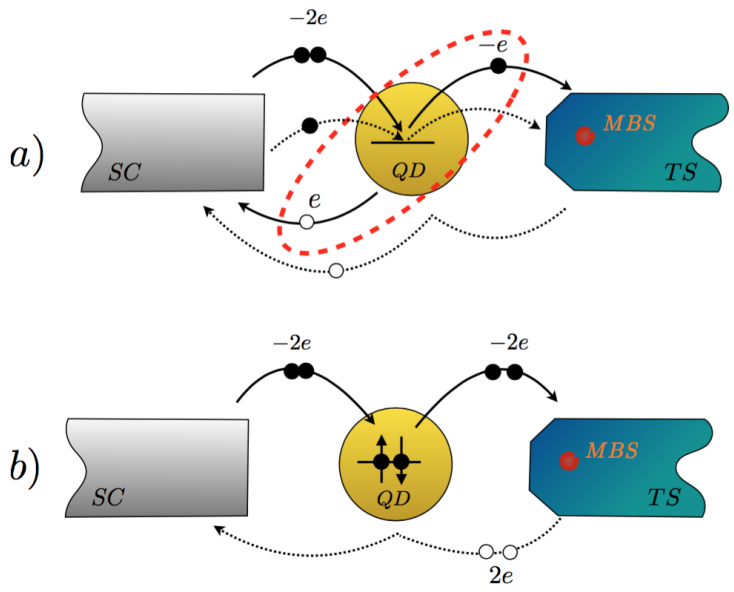

Figure 5.2: a) First procces in which the Copper pair suffers an AR in the interface with the QD (red dashed line) and the other two AR in the TS interface and in the SC interface (dotted line), generating Andreev bound states; **b)** The Cooper pair splits in two electron of opposite spin, in order to occupy the dot's level, producing two backscattered holes in the TS interface. The AR of an electron (hole) is equivalent to the transfer of a single Cooper pair in (out) of the superconducting condensate.

RAR, one for each electron, producing two hole traveling to the left. These quasi-particles will occupy the dot's level and will reach the superconducting lead, where they will suffer a second AR, producing an absorption of two Cooper pairs and two backscattered holes, contributing with a $2e$ charge-flux to the right transport current through the nano junction.

Because of the self-Hermitian property Eq.(2.3) the Majorana fermion is ensured to couple with electron and holes with equal amplitude. Therefore, when a lead is coupled to a Majorana fermion mode, the lead plays the role of both an electron lead and a hole lead. If our system had two lead coupled to the MBS, there would be a resonant tunneling from the electron lead to the hole lead.

If AR processes do not dominate the transport current, Cooper pairs at the quantum dot interface can admit not only AR, but normal reflections too. In this case, a backscattered electron reaches to the superconducting interface. Depending on its energy, it can enter to the superconductor or it can be Andreev reflected as hole, moving to the right. In

both cases, there is an inversion of the current due this process, because in this scenario, electron and holes will move in the opposite direction to that mentioned in the previous cases. Figure 5.1 shows that the shape of the current is predominantly positive, which is in agreement with the fact that Andreev reflections dominate the transport processes, as we expect due to the presence of a superconductor and a topological superconductor lead. Even though there may be no AR at the topological superconductor lead, MBS will remain after normal reflections because they are topologically protected against electron-like quasiparticles scattering or backscattering at non-magnetic impurities and defects.

As we discussed in chapter 2, when a bias voltage V is applied, the situation is more complicated, because the quasi-particles increase their kinetic energy. As a consequence the transport current may be benefited if the increment in energy does not break the quantum correlations. In particular if an electron-like quasi-particle can be exited from a state below the gap to a state above the gap due multiple AR, it will contribute to the transport current without any kind of reflection, behaving as a classical particle, and therefore having no role in the tunneling scenario. In order to avoid these situations, and keeping in the linear response regime, small voltages were applied, such that $eV < \Delta$. With all these considerations, we can see that the transport current has a peaks near to zero bias voltage and in the regime between $eV = 0.2\Delta$ and $eV = 0.3\Delta$. In that region the multiple AR dominates the transport processes and the quasi-particles couple to the MBS with maximal amplitude. On the other hand, in the region $0.1\Delta < eV < 0.2\Delta$ normal reflected electrons dominate the behavior of the current, inverting the sign in that energy regime. This behavior coincide with different coupling strengths, only the position of the principal peak varies smoothly.

For higher energies it can be seen that normal reflections appear as relevant processes, inverting the sign of the current and indicating that correlation between quasi-particles become weaker.

The Zeeman contribution to the energy increases with the magnetic field (modifying the dot's energy scale) and electrons with grater energies are required to occupy the dot's energy level. Therefore at non-zero magnetic field, electrons in regions of higher voltages will dominate the transport processes, as is shown in Fig.(5.3). There is a peak at $0.05eV$,

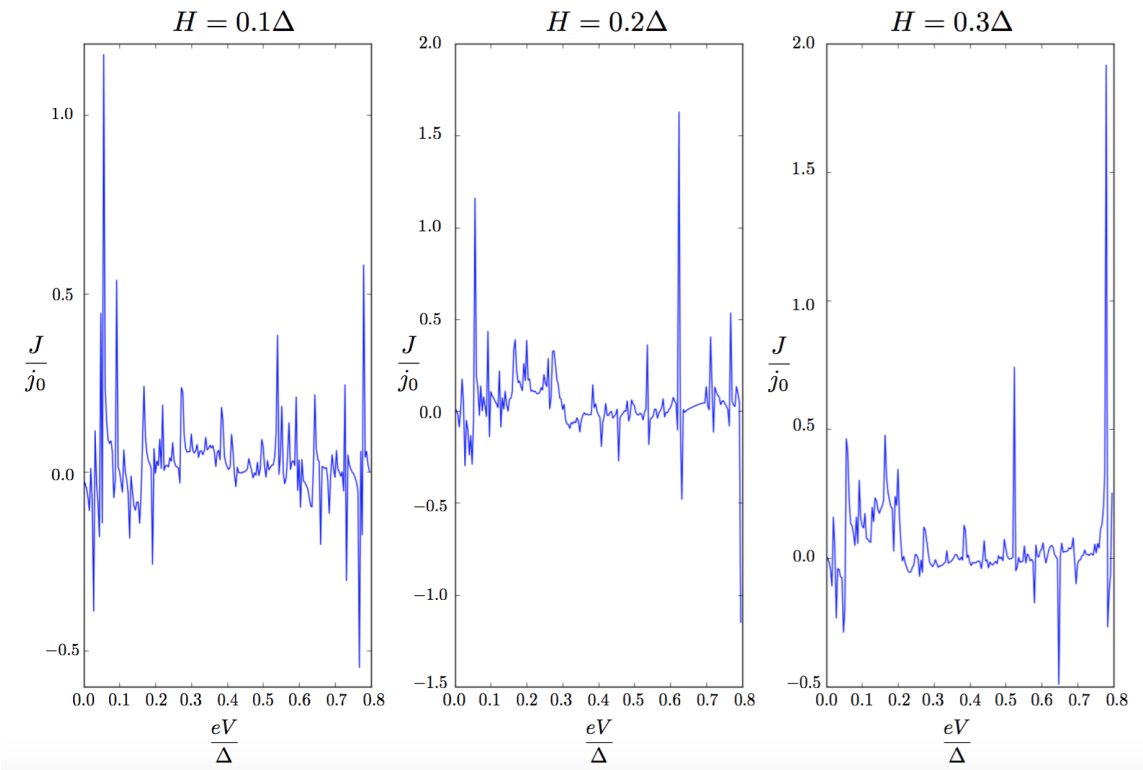

Figure 5.3: Currents for different magnetic fields. It can be seen that higher energy electrons becomes relevant for transport processes. The set of parameters are the same as before.

whose position coincides for different values of the magnetic field. This behavior is an important criterion which helps to identify MBS.

In order to elucidate which process dominates for each configuration, we have calculated the occupation number $\hat{n}_d = \hat{n}_{d\uparrow} + \hat{n}_{d\downarrow}$ for the electrons in the dot according to

$$\langle \hat{n}_d \rangle = \mathrm{Tr} \int dE n_F(E, V, T) \left(-\frac{1}{\pi} \mathrm{Im} \left\{ G_d^R(E, V, T) \right\} \right) \tag{5.1}$$

where the fermionic distribution function is

$$n_F(E, V, T) = \frac{1}{\exp\left\{ \frac{E-V}{k_B T} \right\} + 1}. \tag{5.2}$$

Figure (5.4) shows the occupation number of electrons in the dot. We can see that at zero Zeeman splitting there is practically no localized electron in the dot because elec-

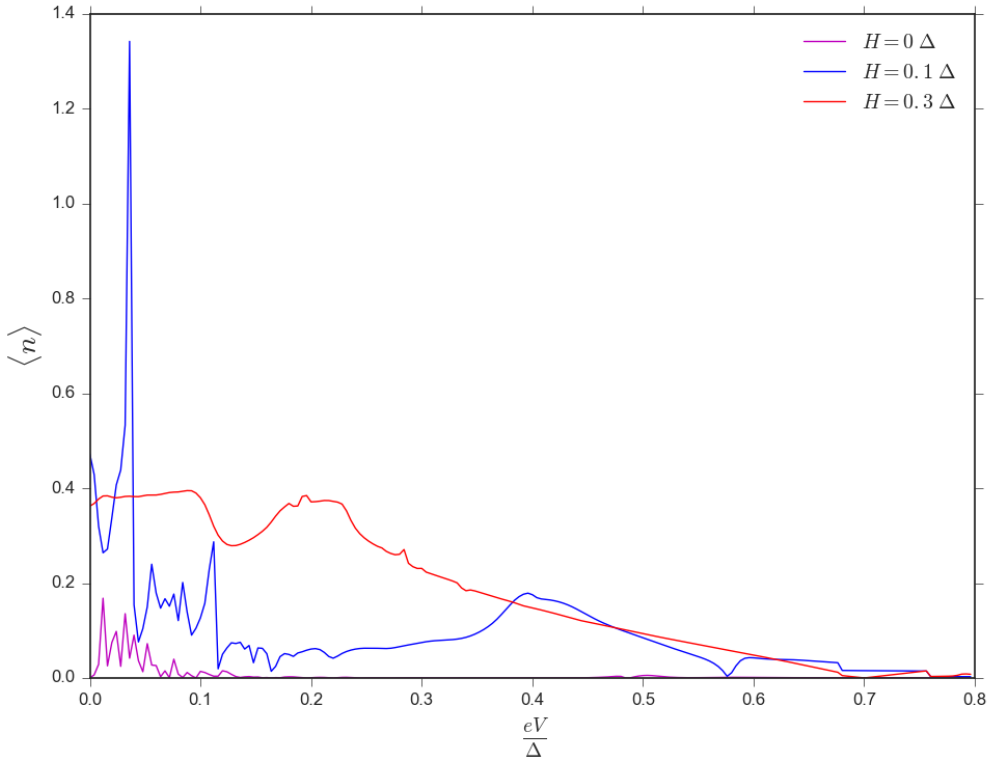

Figure 5.4: Occupation number for different magnetic fields. We have used the same set of parameters ss before.

trons can occupy easily the dot level and then continue traveling to the topological lead. However, when we consider a finite non-zero magnetic field, the energy transport barrier represented by the dot's energy increases because of the Zeeman energy contribution. Thus electrons with higher energies (accelerated due non-zero bias) are responsible for the electrical conduction.

However, the most important conclusion we get from figure (5.4) is that the contribution of the first virtual process described in figure (5.2) dominates the tunneling current because double occupation in the dot are practically suppressed (except for the very low voltage regime, where the second process seems to be dominant at $H = 0.1\Delta$). It means that at the superconductor-quantum dot interface there are multiple one-particle Andreev reflections, producing several Andreev bound states, being the current carried by individuals (retro)-reflected (holes)-electrons.

5.2 Thermoelectric performance

In order to study the thermoelectric properties of our system, we have to consider the temperature dependence of the electric current in the linear response regime, which is presented in figure 5.5. We have assumed that the s-wave superconductor is in thermal equilibrium at temperature T (as before), and the topological superconductor is at zero temperature. Therefore the thermal flux is generated by the temperature difference $\Delta T = T - 0 = T$.

As we did before, we have set T/k_B less than the superconducting gap. In this regime, we can see that, independently of the magnetic field value, the temperature dependence of the electric current is very low, which coincides with the fact that our model is lattice-independent (phonons are present only in the BCS description of the superconductor Hamiltonian). As a consequence, this system does not dissipate a great amount of thermal energy due to the current flow and, at first sight, it may be represent a good candidate for a dissipationless thermoelectric nano device.

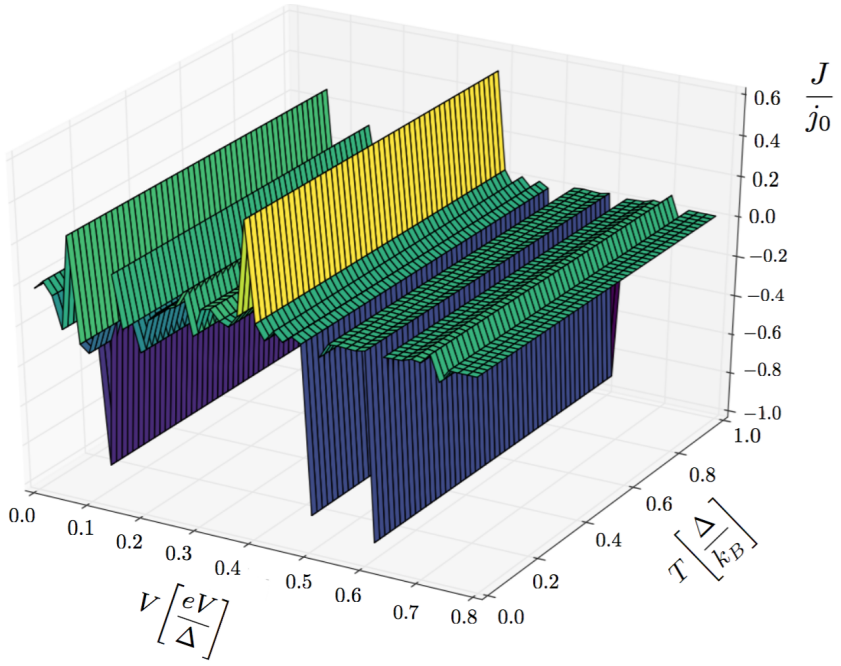

Figure 5.5: Voltage and temperature dependence of the electric current for zero magnetic field. We have considered the same setup as in the previous plot.

Even though the current does not dependent strongly on the temperature, in order to elucidate the thermoelectric performance of the of the system, we have to study the figure of merit Eq.(2.16). The Seebeck coefficient Eq.(2.14) was calculated according to

$$S = -\left.\frac{\Delta V}{\Delta T}\right|_{J=0} = -\left.\frac{\frac{\partial J}{\partial T}}{\frac{\partial J}{\partial V}}\right|_{J=0} \tag{5.3}$$

and the thermal current as

$$J_Q(V,T) = \int j(E,V,T)E\,dE. \tag{5.4}$$

The electric and thermal conductivities , σ and κ respectively, can be obtained from the electric and thermal currents through

$$\sigma = \left.\frac{\partial J(V,T)}{\partial V}\right|_{J=0}; \quad \kappa = \left.\frac{\partial J_Q(V,T)}{\partial T}\right|_{J=0}. \tag{5.5}$$

The thermoelectric figure of merit is presented in figure 5.6 for different voltages.

Our results show different thermoelectric performance according to the intensity of the applied magnetic field. In figure (5.6) the highest values of the figure of merit are shown for different fields, reaching the maximum at $0.7eV/\Delta$ when the magnetic field has a value of 0.3Δ. Until now it has very hard to achieve high ZT, because σ, S and κ cannot be independently controlled, namely, a material with large electrical conductivity σ has a large thermal conductivity κ. Particularly, the small values of ZT is a consequence of the TEP of the device, as is presented in figure (5.7): small values of the Seebeck coefficient means that this is not an efficient system in converting temperature differences in electric voltages. This behavior is anticipated from figure (5.5), in which the temperature does not play an important role in the electrical current. It is important to note that the change of sign in the Seebeck coefficient is due to the inversion of the current, which it is another signature of multiple Andreev reflections in this system.

In contrast to normal metals (which have a small ZT) and semiconductors (that have demonstrated to be better thermoelectric materials than normal metals), where the thermoelectric figure of merit reaches its maximum values after a large variation in temperature,

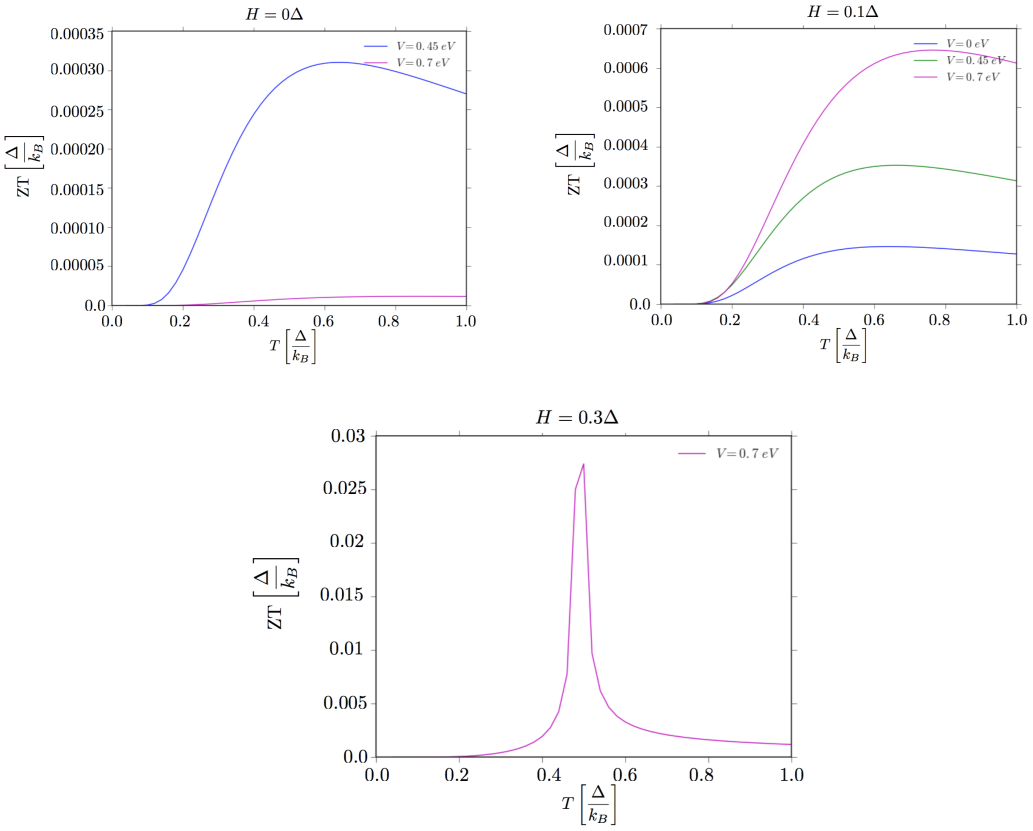

Figure 5.6: Thermoelectric figure of merit as a function of temperature for differentes voltages and magnetic fields using the same parameters.

we can see that in this case both, Seebeck coefficient and thermoelectric figure of merit, saturate in the low temperature regime, which might give some information about the quality factor of this particular hybrid system.

Andreev reflections give also an explanation to the low heat transport through the structure: low energy electrons (energy below the superconducting gap) hit a barrier (such as the quantum dot barrier) and convert into retroreflected holes, carrying the same energy back in the opposite direction. Thus, the subgap thermal flow through the superconductor is blocked, and only quasi-particles with energy $E > \Delta$ participate in the heat transport. However, in order to analyze the role of correlations between quasi-particles in the electrical transport current, we have set all the relevant parameters, such as the energy of electrons and bias voltages, less than the superconducting gap and thus suppressing thermal flow.

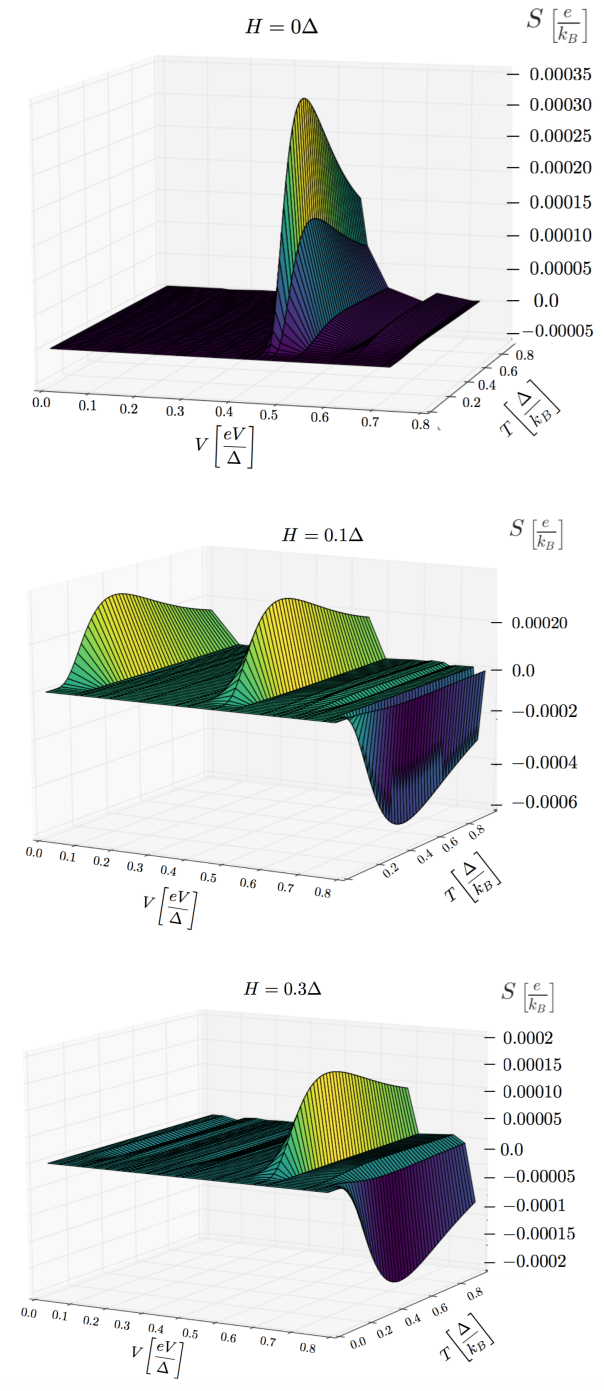

Figure 5.7: Seebeck coefficients as a function of temperature and applied vias voltage for different magnetic fields.

The high value of the figure of merit presented in figure (5.6) for $H = 0.3\Delta$ is a consequence of the high value of voltage combined with the magnitude of the magnetic field. With those values, electrons are very close to the threshold characteristic energy value of the system.

Even though the figure of merit does not reach high values, it is interesting to discuss the role of the magnetic field in the system. Due to spin degrees of freedom present in the model, electrons are sensitive to the applied magnetic field. This field breaks the symmetry between electrons, giving different energy contributions for spin up or spin down fermions: electrons that have a spin parallel to the magnetic field dominate in the whole transport process compared to those with anti-parallel spin. Therefore, some electrons will gain more energy due to the magnetic field, increasing the electrical conductivity, whereas the thermal conductivity will not be affected. This behavior is presented in the evaluation of the Lorenz number L, which is defined as the ratio of the electronic thermal conductivity to the electrical conductivity. This ratio is proportional to the temperature

$$L = \frac{\kappa}{\sigma T}, \tag{5.6}$$

and takes lower values for higher magnetic field. Figure (5.8) shows the Lorenz number in the whole temperature and bias voltage regime.

Multiple Andreev reflections also play a role in the evaluation of the Wiedemann-Franz (WF) law. For Fermi liquids the Lorenz number do not differ strongly from the Sommerfeld value

$$L_0 = \frac{\pi^2}{3}\left(\frac{k_B}{e}\right)^2 = 2.44 \times 10^{-8} W\Omega K^{-2}. \tag{5.7}$$

In our case, the WF law is violated (figure 5.8): the Lorenz number has significant variations, having minimum and maximum values far apart from those obtained for typical Fermi liquids. Breakdown of WF law have been recently theoretically predicted [76, 77] and experimentally observed in different electronic systems at cryogenic temperature and arise from unconventional phases of matter, strong inelastic scattering of quasi-particles, semimetal physics [78, 79, 80] or low dimensionallity [81]. However, it was found recently a violation of the WF law at high temperature in metallic vanadium dioxide in the vecinity of its metal-insulator transition [82].

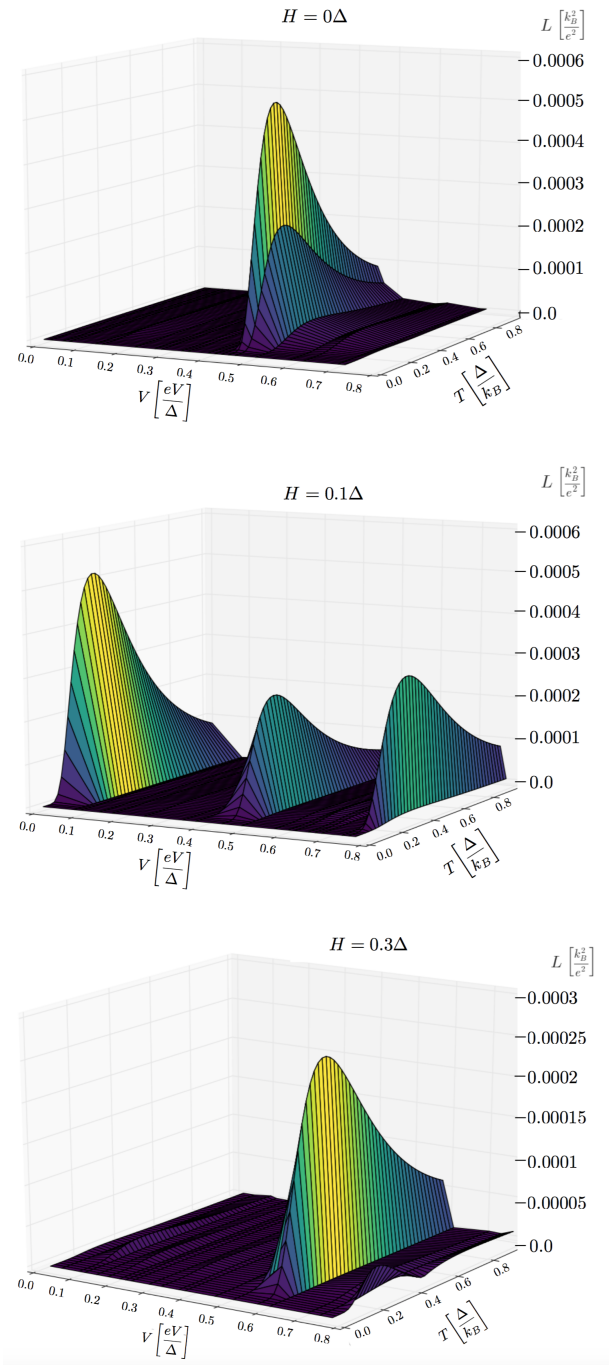

Figure 5.8: Lorenz numbers as function of temperature and voltages. At higher magnetic field, the electrical conductivity increases, whereas the thermal conductivity remains practically constant, given a lower Lorenz number. We have used the same setup of parameter as before .

Heat conduction in topological superconductors can be achieved by introducing disorder or defects in the system. It has been reported that the addition of disorder and defects to a 2D topological superconductor makes it start to conduct [83] because Majorana fermions bound to defects are responsible for the heat conduction. Defects create bound states within the superconducting gap. An isolated MBS must have $E = 0$ and it is this mind-gap alignment of MBS that allows for resonant conduction if the density of defects is sufficiently large [84]. This disorder driven phase transition from a thermal insulator to a thermal metal has not yet been observed experimentally, but it is evident in computer simulations, making this an interesting research focus.

Chapter 6

Conclusions and further work

6.1 Conclusions

Using the non-equilibrium Green's function methods and Floquet theory we have calculated the non-equilibrium transport current in a normal superconductor-topological superconductor nano junction and we have studied its thermoelectric perfomance.

We found that the conduction properties of the systems are highly mediated by virtual processes, known as Andreev reflections (AR), which is evidenced by studying the occupation number in figure (5.4). These processes are responsible for the proximity effect in nano-junctions involving superconductors interfaces. Particularly, we found a non-linear electrical current, which oscillates strongly due the presence of AR and because of the time-dependent Floquet driving perturbation as a result of a an finite applied bias voltages. The electrical current shows several peaks, whose positions do not change with different applied magnetic field, giving signatures of Majorana bound states.

Our thermoelectric results show that this system has a weak thermoelectric performance, represented by a figure of merit which maximum value of 0.02 k_B/Δ is reported at a magnetic field $H = 0.3\Delta$ and at bias voltage $0.7eV/\Delta$. It is important to emphasize that this system breaks the Wiedemann-Franz law, reporting values of the Lorenz number different for typical bulk materials, and that its values varying with different applied magnetic field. Magnetic fields higher than 0.3Δ were not studied in this work, but we think they might improve the thermoelectric performance of these kind of systems. In spite

of the small values of the figure of merit, the low temperature dependence of the system might be harnessed as a dissipationless device.

Even though the figure of merit is small compared with other materials such as semiconductors, it is important to note that this system can be improved in different ways, some alternatives include adding alloys to the superconductor or considering others interactions in the dot in order to increase the many-body quantum correlations.

6.2 Further work

The first step in order to go deeper in the study of this system is including a Coulomb interaction between electrons in the quantum Dot. The most direct way to do that is incorporating an Anderson interaction term to the Hamiltonian and proceed with the mean field approximation. The theoretical calculations are presented in Appendix (F), where it is shown that the dot's Hamiltonian depends explicitly on the expectation value of the number operator for each spin value. This is a self-consistent problem, whose solution requires a more complicated computational solver. Variations of this proposal include the study of the Kondo regime, considering a localized magnetic moment in the dot, or adding phonon contributions in the dot via Anderson-Holstein model.

Other interesting focus of research is incorporating more topological superconductor terminals, increasing the channels of current transmissions and analyze more carefully the role played by resonant Andreev reflections, in which retroreflected holes can go from one to another topological terminal.

Appendix A

Superconductor Green's function in the quasiclassical approximation

Superconductivity was discovered in 1911 by H. Kamerlingh Onnes, but his microscopic understanding was elucidated by Bardeen, Cooper and Schrieffer in 1957 [85]. The microscopic mechanism which leads to a superconducting state is known as BCS theory and it is easily understood if one assumes an attractive interaction between electrons in a superconductor. In this appendix, we will derive the BCS Green's function for a superconductor in the quasi-classical approximation.

BCS theory and Gor'kov equations for a s-wave superconductor.

The BCS theory considers an effective attractive interaction between electrons. This attraction is a consequence of the crucial role played by the lattice of ion cores, i.e. nuclei with tightly bound inner electrons. The electrons need this interaction to form Cooper pairs which then condense into superconducting states. Considering a spin-independent interaction, the superconducting states will be spin-singlet (or zero-spin) states, which are characteristic in real superconductors. The anti-symmetric property of the fermionic wave function requires a spin-singlet state to have an even parity under transposition of

particle coordinates or with respect to inversion of relative momentum of the particles. This means that the superconducting states should be of either s-wave or d-wave (or of other higher-order even) symmetry in the relative momentum of particles.

The attractive interaction between electrons is mediated by the exchange of phonons and it is attractive in the low frequency regime, particularly for frequencies below a threshold value, the characteristic Debye frequency Ω_D, and vanishes for energy transfer larger than some cut-off value $\Omega_{\rm BCS}$. If the interaction is relatively weak, the characteristic energies of particles participating in the superconducting phenomena, are much smaller than both the Fermi energy and the cut-off frequency $\Omega_{\rm BCS}$. The BCS Hamiltonian is

$$\mathcal{H}_{BCS} = \int d^3r \left[-\psi_\alpha^\dagger \frac{\nabla^2}{2m} \psi_\alpha + \frac{g}{2} \psi_\beta^\dagger \psi_\alpha^\dagger \psi_\alpha \psi_\beta \right], \tag{A.1}$$

with $g < 0$ for an attractive interaction.

In order to incorporate the effect of the temperature of the system, we will work with the imaginary-time or Matsubara Green function defined for imaginary time

$$t = -i\tau \tag{A.2}$$

within the interval

$$-\frac{1}{T} < \tau_1 - \tau_2 < \frac{1}{T}, \tag{A.3}$$

with T the temperature of the system in thermal equilibrium. The Heisenberg particle operator in this notation are

$$\psi_\alpha(\mathbf{r}, \tau) = e^{(\hat{\mathcal{H}} - \mu\hat{\mathcal{N}})\tau} \tilde{\psi}_\alpha(\mathbf{r}) e^{-(\hat{\mathcal{H}} - \mu\hat{\mathcal{N}})\tau} \tag{A.4}$$

$$\psi_\alpha^\dagger(\mathbf{r}, \tau) = e^{(\hat{\mathcal{H}} - \mu\hat{\mathcal{N}})\tau} \tilde{\psi}_\alpha^\dagger(\mathbf{r}) e^{-(\hat{\mathcal{H}} - \mu\hat{\mathcal{N}})\tau} \tag{A.5}$$

and the Matsubara Green's function is defined as

$$G_{\alpha\beta}(\mathbf{r}_1, \tau_1; \mathbf{r}_2, \tau_2) = \left\langle \hat{T}_\tau \left(\psi_\alpha(\mathbf{r}_1, \tau_1) \psi_\beta^\dagger(\mathbf{r}_2, \tau_2) \right) \right\rangle \tag{A.6}$$

where $\hat{T}_\tau$ means ordering in τ. For fermionic particles

$$\hat{T}_\tau\left(\psi_1\psi_2^\dagger\right) = \begin{cases} \psi_1\psi_2^\dagger & \tau_2 > \tau_2 \\ -\psi_2^\dagger\psi_1 & \tau_1 < \tau_2 \end{cases}$$

According to these definitions, the time-derivatives of the Heisenberg operator are given by

$$\frac{\partial}{\partial}\psi_\alpha(x) = \left(\frac{\nabla^2}{2m} - \mu\right)\psi_\alpha(x) - g\psi_\gamma^\dagger(x)\psi_\gamma(x)\psi_\alpha(x) \tag{A.7}$$

$$\frac{\partial}{\partial t}\psi_\alpha^\dagger(x) = -\left(\frac{\nabla^2}{2m} - \mu\right)\psi_\alpha^\dagger(x) + g\psi_\alpha^\dagger(x)\psi_\gamma^\dagger(x)\psi_\gamma(x), \tag{A.8}$$

where $x \equiv (\tau, \mathbf{r})$ and we have considered the commutation relations between the Heisenberg operator and the Hamiltonian (A.1) and the particle-number operator. For the Green function its time-derivatives looks like

$$\begin{aligned} \frac{\partial}{\partial\tau_1}G_{\alpha\beta}(x_1,x_2) &= \frac{\partial}{\partial\tau_1}\left[\delta_{\alpha\beta}\Theta(\tau_1-\tau_2)\right] + \left\langle \hat{T}_\tau \frac{\partial\psi_\alpha(x_1)}{\partial\tau_1}\psi_\beta^\dagger(x_2)\right\rangle \\ &= \delta_{\alpha\beta}\delta(\mathbf{r}_1-\mathbf{r}_2)\delta(\tau_1-\tau_2) \\ &\quad + \left\langle \hat{T}_\tau\left[\left(\frac{\nabla^2}{2m}+\mu\right)\psi_\alpha(x_1)\psi_\beta^\dagger(x_2)\right.\right. \\ &\quad \left.\left. -g\psi_\gamma^\dagger(x_1)\psi_\gamma(x_1)\psi_\alpha(x_1)\psi_\beta^\dagger(x_2)\right]\right\rangle \\ &= \delta_{\alpha\beta}\delta(\mathbf{r}_1-\mathbf{r}_2)\delta(\tau_1-\tau_2) + \left(\frac{\nabla^2}{2m}+\mu\right)G_{\alpha\beta}(x_1,x_2) \\ &\quad -g\left\langle \hat{T}_\tau\left(\psi_\gamma^\dagger(x_1)\psi_\gamma(x_1)\psi_\alpha(x_1)\psi_\beta^\dagger(x_2)\right)\right\rangle, \end{aligned} \tag{A.9}$$

where the delta term comes from the fact that the Green function at $\tau = \tau_1 - \tau_2 = 0$ is

$$\left[G(\tau) - G(-\tau)\right]_{\tau\to 0^+} = \left\langle \psi_\alpha(\mathbf{r}_1)\psi_\beta^\dagger(\mathbf{r}_2) + \psi_\beta^\dagger(\mathbf{r}_2)\psi_\alpha(\mathbf{r}_1)\right\rangle = \delta_{\alpha\beta}\delta(\mathbf{r}_1-\mathbf{r}_2). \tag{A.10}$$

In order to simplify the last term in Eq.(A.9) we employ the Wick's theorem and we get

$$\begin{aligned}\left\langle \hat{T}_\tau \left(\psi^\dagger_\gamma(x_1)\psi_\gamma(x_1)\psi_\alpha(x_1)\psi^\dagger_\beta(x_2)\right)\right\rangle &= -\left\langle \hat{T}_\tau \left(\psi_\gamma(x_1)\psi^\dagger_\gamma(x_1)\right)\right\rangle \left\langle \hat{T}_\tau \left(\psi_\alpha(x_1)\psi^\dagger_\beta(x_2)\right)\right\rangle \\ &+\left\langle \hat{T}_\tau \left(\psi_\alpha(x_1)\psi^\dagger_\gamma(x_1)\right)\right\rangle \left\langle \hat{T}_\tau \left(\psi_\gamma(x_1)\psi^\dagger_\beta(x_2)\right)\right\rangle \\ &-\left\langle \hat{T}_\tau \left(\psi_\alpha(x_1)\psi_\gamma(x_1)\right)\right\rangle \left\langle \hat{T}_\tau \left(\psi^\dagger_\gamma(x_1)\psi^\dagger_\beta(x_2)\right)\right\rangle .\end{aligned}$$

The last expression corresponds to a generalized form of the Wick's theorem, because we are including the one essentially feature of superconductors, i.e., the possibility that two electrons of opposite spin can form a self-bound Cooper pair. As a consequence, the equation of motion for the Heisenberg operators $\psi^\dagger, \psi$ are coupled and therefore the theory no longer conserves the number of particles. In this sense, the first and second line in Eq.(A.11) represents interaction such that do not result in a superconducting behavior and we can neglect them. Indeed this consideration is not always true (particularly for a strongly correlated electron system) but for a s-wave superconductor this approximation leads to very realistic results. The first two term of Eq.(A.11) represent a Hartree-Fock contribution and we can neglect entirely, thereby treating the normal state as a free electron gas. This approximation considers that these terms are the same in both normal and superconducting phases and do not affect the comparison between the two states. According to this, we can rewrite the equation for the Green function as

$$\begin{aligned}\delta_{\alpha\beta}\delta(x_1-x_2) &= \left(\frac{\partial}{\partial\tau_1}-\frac{\nabla_1^2}{2m}-\mu\right)G_{\alpha\beta}(x_1,x_2) \\ &-g\left\langle \hat{T}_\tau\psi_\alpha(x_1)\psi_\gamma(x_1)\right\rangle \left\langle \hat{T}_\tau\psi^\dagger_\gamma(x_1)\psi^\dagger_\beta(x_2)\right\rangle . \qquad \text{(A.11)}\end{aligned}$$

At this point we define the Gor'kov functions as

$$\begin{aligned}F^\dagger_{\alpha\beta}(x_1,x_2) &= \left\langle \hat{T}_\tau\psi^\dagger_\alpha(x_1)\psi^\dagger_\beta(x_2)\right\rangle \\ F_{\alpha\beta}(x_1,x_2) &= \left\langle \hat{T}_\tau\psi_\alpha(x_1)\psi_\beta(x_2)\right\rangle \end{aligned} \qquad \text{(A.12)}$$

and

$$\Delta_{\alpha\beta} = |g| F_{\alpha\beta}(x,x). \tag{A.13}$$

Using these definition the equation for the Green function becomes

$$\delta_{\alpha\beta}\delta(x_1 - x_2) = \left(\frac{\partial}{\partial\tau_1} - \frac{\nabla_1^2}{2m} - \mu\right) G_{\alpha\beta}(x_1,x_2) + \Delta_{\alpha\gamma} F^{\dagger}_{\gamma\beta}(x_1,x_2). \tag{A.14}$$

Because of the fermionic statistic, the function $F_{\alpha\beta}(x_1,x_2)$ is odd under transposition of the particle coordinates and spin indices. In the case of a s-wave, the paring interaction as an even parity in the orbital space, therefore the Cooper paring can only occur between electrons with opposite spin projection into a singlet state and the pair wave function is anti-symmetric in spin indices:

$$\Delta_{\alpha\beta}(x) = -\Delta_{\beta\alpha}(x). \tag{A.15}$$

In a matrix notation

$$\Delta_{\alpha\beta} = i\sigma_y^{\alpha\beta}\Delta(x) \quad , \quad \Delta^{\dagger}_{\alpha\beta} = -i\sigma_y^{\alpha\beta}\Delta^*(x), \tag{A.16}$$

where $\sigma_y^{\alpha\beta}$ is the second Pauli matrix. As a result we obtain

$$\left(\frac{\partial}{\partial\tau_1} - \frac{\nabla_1^2}{2m} - \mu\right) G(x_1,x_2) + \Delta(x_1) F^{\dagger}(x_1,x_2) = \delta(x_1 - x_2) \tag{A.17}$$

Noting that the Green function is proportional to the unity matrix because the interaction does not depend on spin indices

$$G_{\alpha\beta}(x_1,x_2) = \delta_{\alpha\beta} G(x_1,x_2).$$

Considering the second equation in Eq.(A.8) we have an equation for the function $F^{\dagger}(x_1,x_2)$

$$\left(\frac{\partial}{\partial\tau_1} + \frac{\nabla_1^2}{2m} + \mu\right) F^{\dagger}(x_1,x_2) + \Delta^*(x_1) G(x_1,x_2) = 0. \tag{A.18}$$

Because of the fact that $\Delta(x_1)$ depend on the function F we have to incorporate to more

equations. Proceeding in an analogous way we can find

$$\begin{aligned} -\left(\frac{\partial}{\partial\tau_1}+\frac{\nabla_1^2}{2m}+\mu\right)\bar{G}(x_1,x_2)+\Delta^*(x_1)F(x_1,x_2) &= \delta(x_1-x_2) \\ \left(-\frac{\partial}{\partial\tau_1}+\frac{\nabla_1^2}{2m}+\mu\right)F(x_1,x_2)+\Delta(x_1)\bar{G},(x_1,x_2) &= 0 \end{aligned} \tag{A.19}$$

where $\bar{G}_{\alpha\beta}(x_1,x_2)=-\left\langle \hat{T}_\tau\psi_\alpha^\dagger(x_1)\psi_\beta(x_2)\right\rangle=\delta_{\alpha\beta}\bar{G}(x_1,x_2)$. The four equation (A.17-A.19) are known as the Gor'kov equations[86] and Δ corresponds to the order parameter. Note that $G(x_1,x_2)$ describes a moving particles from x_1 to x_2 while $\bar{G}(x_1,x_2)$ represents a particle moving from x_2 to x_1 or, equivalently, a hole. The fact that $\bar{G}(x_1,x_2)=G(x_2,x_1)$ is a manifestation of the particle-hole symmetry in the BCS model.

It is convenient to introduce a matrix notation for the four coupled equations as

$$\check{G}^{-1}(x_1)\check{G}(x_1,x_2)=\check{1}\delta(x_1-x_2) \tag{A.20}$$

where

$$\check{G}(x_1,x_2)=\begin{pmatrix} G(x_1,x_2) & F(x_1,x_2) \\ -F^\dagger(x_1,x_2) & \bar{G}(x_1,x_2)\end{pmatrix} \tag{A.21}$$

and the matrix operator

$$\check{G}^{-1}=\tau_z\frac{\partial}{\partial\tau}+\check{\mathcal{H}} \tag{A.22}$$

with[1]

$$\check{\mathcal{H}}=\begin{pmatrix} -\frac{\nabla^2}{2m}-\mu & -\Delta \\ \Delta^* & -\frac{\nabla^2}{2m}-\mu\end{pmatrix} \tag{A.24}$$

It is convenient to work in the momentum representation of the Green's function

$$\check{G}(\mathbf{r}_1,\mathbf{r}_2)=\int\frac{d^3p}{(2\pi)^3}\frac{d^3k}{(2\pi)^3}\check{G}(\mathbf{p},\mathbf{p}-\mathbf{k})e^{i\mathbf{p}\mathbf{r}_1-i(\mathbf{p}-\mathbf{k})\mathbf{r}_2}. \tag{A.25}$$

[1]If we add a magnetic field, the Hamiltonian operator reads

$$\check{\mathcal{H}}=\begin{pmatrix} -\frac{1}{2m}\left(\nabla-\frac{ie}{c}\mathbf{A}\right)^2-\mu & -\Delta \\ \Delta^* & -\frac{1}{2m}\left(\nabla+\frac{ie}{c}\mathbf{A}\right)^2-\mu\end{pmatrix} \tag{A.23}$$

and $\check{G}^{-1}$ remains unchanged.

Particularly, for a homogeneous state we have

$$\check{G}_{\omega_n}(\mathbf{r}_1,\mathbf{r}_2)=\int\frac{d^3p}{(2\pi)^3}e^{i\mathbf{p}(\mathbf{r}_1-\mathbf{r}_2)}\check{G}_{\omega_n}(\mathbf{p}). \tag{A.26}$$

After a Fourier transformation for the other Green's functions we obtain

$$\begin{aligned}(-i\omega_n+\xi_{\mathbf{p}})\,G+\Delta F^{\dagger} &= 1 &\text{(A.27)}\\ (-i\omega_n-\xi_{\mathbf{p}})\,F^{\dagger}+\Delta^{*}G &= 0 &\text{(A.28)}\end{aligned}$$

where $\xi_{\mathbf{p}}=\frac{p^2}{2m}-\mu=E(\mathbf{p})-E_F$, while $E_n(\mathbf{p})$ is the electronic spectrum in the normal state and E_F is the Fermi energy. Solving Gor'kov equations in the momentum representation we have

$$G=\frac{\xi_{\mathbf{p}}+i\omega_n}{\xi_{\mathbf{p}}^2+\omega_n^2+|\Delta|^2} \quad , \quad F^{\dagger}=\frac{\Delta^{*}}{\xi_{\mathbf{p}}^2+\omega_n^2+|\Delta|^2} \tag{A.29}$$

$$\bar{G}=\frac{\xi_{\mathbf{p}}-i\omega_n}{\xi_{\mathbf{p}}^2+\omega_n^2+|\Delta|^2} \quad , \quad F=\frac{\Delta}{\xi_{\mathbf{p}}^2+\omega_n^2+|\Delta|^2}. \tag{A.30}$$

We can define a retarded(advanced) real-time Green function which corresponds to an analytical function of $\epsilon=i\omega_n$ in the upper(lower) half-plane of complex ϵ. In our case, these function take the form

$$G^{R(A)}=\frac{\xi_{\mathbf{p}}+\epsilon}{\xi_{\mathbf{p}}^2-(\epsilon\pm i\delta)^2+|\Delta|^2} \quad , \quad F^{\dagger R(A)}=\frac{\Delta^{*}}{\xi_{\mathbf{p}}^2-(\epsilon\pm i\delta)^2+|\Delta|^2} \tag{A.31}$$

$$\bar{G}^{R(A)}=\frac{\xi_{\mathbf{p}}-\epsilon}{\xi_{\mathbf{p}}^2-(\epsilon\pm i\delta)^2+|\Delta|^2} \quad , \quad F^{R(A)}=\frac{\Delta}{\xi_{\mathbf{p}}^2-(\epsilon\pm i\delta)^2+|\Delta|^2}. \tag{A.32}$$

We can also write

$$G^{R(A)}=-\frac{\xi_{\mathbf{p}}+\epsilon}{(\epsilon-\epsilon_{\mathbf{p}}\pm i\delta)\,(\epsilon+\epsilon_{\mathbf{p}}\pm i\delta)}, \tag{A.33}$$

where $\epsilon_{\mathbf{p}}=\sqrt{\xi_{\mathbf{p}}^2+|\Delta|^2}$. This says that the energy spectrum of a clean superconductor in absence of currents and magnetic field has a gap, such that all excitations have energies above $|\Delta|$ as we expected. The Green function have poles at $\epsilon=\pm\epsilon_{\mathbf{p}}$, which means that excitations in a superconductor have energies $\pm\epsilon_{\mathbf{p}}$.

Quasi-classical approximation

The Green's functions in Eq. (A.21) and Eq.(A.26) oscillates as a function of relative coordinate $|\mathbf{r}_1 - \mathbf{r}_2|$ on a scale of the Fermi wave-length λ_F, which os much shorter than the characteristic length scale of variations of the order parameter. This implies that the Fermi momentum p_F is much larger that the order parameter variation $\hbar/\xi_0$, with $\xi_0 = \hbar v_F/2\pi T_C$ the zero-temperature coherence length. Moreover, in this kind of problems, it is important to study the phase of two-electron wave function which depend on the center of mass coordinate. For this reason it is possible to integrate out the dependence of the relative coordinate. The possibility to separate and then exclude fast oscillating parts in the quasi-particle wave functions, known as the quasi-classical approximation, is provided by the relations between the magnitudes of superconducting and normal sates characteristic parameter of the superconducting material $p_F\xi_0 \gg 1$. The accuracy of this approximation depends on how well the inequality

$$\frac{\hbar}{p_F\xi_0} \sim \frac{\Delta}{E_F} \ll 1 \tag{A.34}$$

is satisfied.

The Green's function in the momentum representation is a function of $\xi_{\mathbf{p}}$, and because the condition (A.34) it varies strongly near the Fermi surface when $\xi_{\mathbf{p}}$ changes by an amount $\delta\xi_{\mathbf{p}} \sim \Delta$. Since $\delta\xi_{\mathbf{p}} \ll E_F$, the magnitude of the quasi-particle momentum $\mathbf{p}$ remains close to the Fermi momentum, therefore we can considered that the momentum dependence of the Green's function can be taken as a dependence of the momentum at the Fermi surface. As a consequence we can parameterize the momentum-space integral as

$$\frac{d^3p}{(2\pi)^3} = \frac{d\xi_{\mathbf{p}}}{v_F}\frac{dS_F}{(2\pi)^3}, \tag{A.35}$$

with $d\xi_{\mathbf{p}}/dv_F$ the momentum increment in the direction perpendicular to the Fermi surface and $dS_F = p_F^2 d\Omega_{\mathbf{p}}$ is the Fermi-surface area element. Integrating over the energy near the

Fermi surface we define the first group of quasiclassical Green's function[87, 38, 88] as

$$\begin{aligned} f_{\omega_n}(\hat{\mathbf{p}},\mathbf{k}) &= \int \frac{d\xi_{\mathbf{p}}}{i\pi} F_{\omega_n}(\mathbf{p}_+,\mathbf{p}_-) = \oint \frac{d\xi_{\mathbf{p}}}{i\pi} F_{\omega_n}(\mathbf{p}_+,\mathbf{p}_-) \\ f^{\dagger}_{\omega_n}(\hat{\mathbf{p}},\mathbf{k}) &= \int \frac{d\xi_{\mathbf{p}}}{i\pi} F^{\dagger}_{\omega_n}(\mathbf{p}_+,\mathbf{p}_-) = \oint \frac{d\xi_{\mathbf{p}}}{i\pi} F^{\dagger}_{\omega_n}(\mathbf{p}_+,\mathbf{p}_-), \end{aligned} \tag{A.36}$$

which only exist in the superconducting state. The quasi-particles states corresponds to the poles of the Green's function and the contour integration shows that we are taking contributions from poles close to the Fermi surface, while the particle momentum lies at the Fermi surface. Therefore the only variable is the momentum direction, denoted by $\hat{\mathbf{p}}$. The second group of Green's function incorporates the normal states and take the form

$$g_{\omega_n} = \oint \frac{d\xi_{\mathbf{p}}}{i\pi} G_{\omega_n}(\mathbf{p}_+,\mathbf{p}_-) \tag{A.37}$$

$$\bar{g}_{\omega_n} = \oint \frac{d\xi_{\mathbf{p}}}{i\pi} G_{\omega_n}(\mathbf{p}_+,\mathbf{p}_-). \tag{A.38}$$

The quasi-classical Green's function are defined in a symmetric way with respect to the incoming $\mathbf{p}_+ = \mathbf{p} + \mathbf{k}/2$ and outgoing $\mathbf{p}_- = \mathbf{p} - \mathbf{k}/2$ momenta.

The coordinate dependence of the Green's function after the $\xi_{\mathbf{p}}$-integration contains

$$e^{i(\mathbf{p}+\frac{\mathbf{k}}{2})\mathbf{r_1} - i(\mathbf{p}-\frac{\mathbf{k}}{2})\mathbf{r_2}} = e^{i\mathbf{p}(\mathbf{r}_1-\mathbf{r}_2)+i\mathbf{k}(\mathbf{r}_1+\mathbf{r}_2)/2}. \tag{A.39}$$

As we mentioned above, the fast oscillations of the Green function associated with the relative coordinate $|\mathbf{r}_1-\mathbf{r}_2|$ are excluded and remains only contributions of slow dependence on the center-of-mass coordinate $(\mathbf{r}_1 + \mathbf{r}_2)/2 \equiv \mathbf{r}$. The quasi-classical matrix Green's function will be denote as

$$\check{g}_{\omega_n}(\hat{\mathbf{p}},\mathbf{k}) = \begin{pmatrix} g_{\omega_n} & f_{\omega_n} \\ -f^{\dagger}_{\omega_n} & \bar{g}_{\omega_n} \end{pmatrix}. \tag{A.40}$$

Let's calculate these functions for a homogeneous superconductor, using the contour

indicated in figure A.1 a):

$$\begin{aligned} f_{\omega_n} &= \int \frac{d\xi_{\mathbf{p}}}{i\pi} \frac{\Delta}{\left(\xi_{\mathbf{p}} + i\sqrt{\omega_n^2 + |\Delta|^2}\right)\left(\xi_{\mathbf{p}} - i\sqrt{\omega_n^2 + |\Delta|^2}\right)} \\ &= \frac{\Delta}{i\sqrt{\omega_n^2 - |\Delta|^2}}, \end{aligned} \tag{A.41}$$

and similarly

$$f_{\omega_n}^{\dagger} = \frac{\Delta^*}{i\sqrt{\omega_n^2 - |\Delta|^2}}. \tag{A.42}$$

For the second group of quasi-classical Green's function we have

$$\begin{aligned} g_{\omega_n} &= \oint \frac{d\xi_{\mathbf{p}}}{i\pi} \frac{\xi_{\mathbf{p}} + i\omega_n}{\left(\xi_{\mathbf{p}} + i\sqrt{\omega_n^2 + |\Delta|^2}\right)\left(\xi_{\mathbf{p}} - i\sqrt{\omega_n^2 + |\Delta|^2}\right)} \\ &= \frac{1}{2}\oint \frac{d\xi_{\mathbf{p}}}{i\pi}\left[\frac{1}{\xi_{\mathbf{p}} - i\sqrt{\omega_n^2 + |\Delta|^2}} + \frac{1}{\xi_{\mathbf{p}} + i\sqrt{\omega_n^2 + |\Delta|^2}}\right] \\ &\quad + \oint \frac{d\xi_{\mathbf{p}}}{i\pi} \frac{i\omega_n}{\left(\xi_{\mathbf{p}} + i\sqrt{\omega_n^2 + |\Delta|^2}\right)\left(\xi_{\mathbf{p}} - i\sqrt{\omega_n^2 + |\Delta|^2}\right)} \\ &= \frac{\omega_n}{\sqrt{\omega_n^2 + |\Delta|^2}}, \end{aligned} \tag{A.43}$$

where we have considered that the terms inside the parenthesis cancel each other. Analogously for the fourth function

$$\bar{g}_{\omega_n} = -\frac{\omega_n}{\sqrt{\omega_n^2 + |\Delta|^2}}. \tag{A.44}$$

From these four results we can easily note that

$$g_{\omega_n} + \bar{g}_{\omega_n} = 0 \tag{A.45}$$

$$g_{\omega_n}^2 - f_{\omega_n} f_{\omega_n}^{\dagger} = 1, \tag{A.46}$$

and they can be combined in the matrix equation

$$\check{g}_{\omega_n}^2 = \begin{pmatrix} g_{\omega_n}^2 - f_{\omega_n} f_{\omega_n}^{\dagger} & (g_{\omega_n} + \bar{g}_{\omega_n}) f_{\omega_n} \\ -f_{\omega_n}^{\dagger}(g_{\omega_n} + \bar{g}_{\omega_n}) & \bar{g}_{\omega_n}^2 - f_{\omega_n} f_{\omega_n}^{\dagger} \end{pmatrix} = \check{1}. \tag{A.47}$$

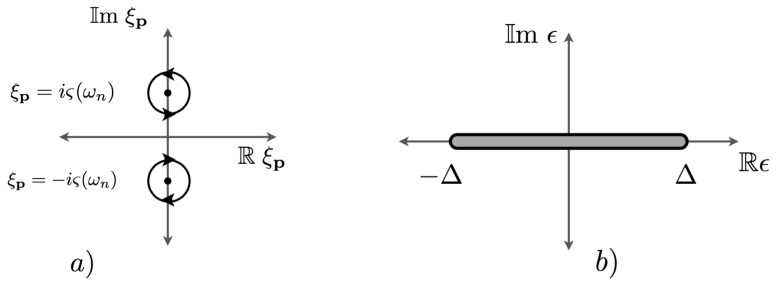

Figure A.1: a) Contour integration over $d\xi_{\mathbf{p}}$. We have denoted $\varsigma(\omega_n) = \sqrt{\omega_n^2 + |\Delta|^2}$, **b)** The plane of complex ϵ indicating the connecting points.

If we want to find the retarded and advanced function for each component of the matrix Green's function we have to make a analytical continuation $i\omega_n \to \epsilon$ and be careful with the range of possible values of ϵ. After the analytical continuation

$$g_\epsilon^R = \frac{\epsilon}{\sqrt{(\epsilon + i\delta)^2 - |\Delta|^2}} \quad , \quad g_\epsilon^A = -\frac{\epsilon}{\sqrt{(\epsilon - i\delta)^2 - |\Delta|^2}} \tag{A.48}$$

$$f_\epsilon^R = \frac{\Delta}{\sqrt{(\epsilon + i\delta)^2 - |\Delta|^2}} \quad , \quad f_\epsilon^A = -\frac{\Delta}{\sqrt{(\epsilon - i\delta)^2 - |\Delta|^2}}, \tag{A.49}$$

where the δ is a infinitesimal number introduced in order perform the analytical continuation correctly. The function $\sqrt{\epsilon^2 - |\Delta|^2}$ is defined on the plane of the complex variable ϵ with $-|\Delta|$ and $|\Delta|$ as cut connecting points. For $|\epsilon| > |\Delta|$ we have

$$g_\epsilon^R = \frac{\epsilon}{\sqrt{\epsilon^2 - |\Delta|^2}} = -g_\epsilon^A \tag{A.50}$$

$$f_\epsilon^R = \frac{\Delta}{\sqrt{\epsilon^2 - |\Delta|^2}} = -f_\epsilon^A. \tag{A.51}$$

In order to get the retarded functions in the region $|\epsilon| < |\Delta|$ we have to continue $\sqrt{\epsilon^2 - |\Delta|^2}$ to the upper edge of the cut, i.e. it becomes $i\sqrt{|\Delta|^2 - \epsilon^2}$ while for the advanced components the square root has to be continue to the lower edge, becoming $-i\sqrt{|\Delta|^2 - \epsilon^2}$, as is

presented in figure A.1 b). Therefore, for $|\epsilon| < |\Delta|$ we have

$$g_\epsilon^R = \frac{-i\epsilon}{\sqrt{|\Delta|^2 - \epsilon^2}} = g_\epsilon^A \tag{A.52}$$

$$f_\epsilon^R = \frac{-i\Delta}{\sqrt{|\Delta|^2 - \epsilon^2}} = f_\epsilon^A. \tag{A.53}$$

The other components can be found using Eqs.(A.46). The matrix Green's function for $|\epsilon| < |\Delta|$ is then

$$\check{g}_\epsilon^R = \frac{-i}{\sqrt{|\Delta|^2 - \epsilon^2}} \begin{pmatrix} \epsilon & \Delta \\ -\Delta & -\epsilon \end{pmatrix} = \frac{-i}{\sqrt{|\Delta|^2 - \epsilon^2}} \left[\epsilon\tau_z + i\Delta\tau_y\right] = \check{g}_\epsilon^A \tag{A.54}$$

while for the region $|\epsilon| > |\Delta|$

$$\check{g}_\epsilon^R = \frac{1}{\sqrt{\epsilon^2 - |\Delta|^2}} \begin{pmatrix} \epsilon & \Delta \\ -\Delta & -\epsilon \end{pmatrix} = \frac{1}{\sqrt{\epsilon^2 - |\Delta|^2}} \left[\epsilon\tau_z + i\Delta\tau_y\right] = -\check{g}_\epsilon^A. \tag{A.55}$$

Appendix B

Superconductor Green's function rotation

In order to write the BCS Hamiltonian as a quadratic standard form, it is useful to introduce the Nambu pseudo-spinor field

$$\Psi = \begin{pmatrix} \psi_\uparrow \\ \psi_\downarrow^\dagger \end{pmatrix}. \tag{B.1}$$

In a 4-term notation, the field takes the form

$$\Psi = \begin{pmatrix} \psi_\uparrow \\ \psi_\downarrow^\dagger \\ \psi_\downarrow \\ \psi_\uparrow^\dagger \end{pmatrix}. \tag{B.2}$$

Using the 4-component pseudo-spinor field, the superconductor Green's function is [89, 45]

$$\underline{\mathbb{G}}^{(R,A)} = A^{(R,A)}(E)\hat{\tau}_z \otimes \hat{s}_0 + iB^{(R,A)}(E)\hat{\tau}_y \otimes \hat{s}_0, \tag{B.3}$$

where the function $A^{(R,A)}$ and $B^{(R,A)}$ were determined in the appendix A

The notation (B.2) is not the same as we have used in Eq. (4.2). In order to work with

the definition of $\underline{\mathbb{G}}$ in our notation, we have to perform a linear transformation, such that

$$\psi = \hat{S}\hat{c} \Leftrightarrow \hat{c} = \hat{S}^{-1}\psi, \tag{B.4}$$

where the transformation is given by the matrix

$$\hat{S} = \begin{pmatrix} 1 & 0 & 0 & 0 \\ 0 & 0 & 1 & 0 \\ 0 & 1 & 0 & 0 \\ 0 & 0 & 0 & -1 \end{pmatrix} = \hat{S}^{-1} = \hat{S}^{T}. \tag{B.5}$$

Using the triagonal form of the matrix Green's function

$$\underline{\mathbb{G}}(E) = \begin{pmatrix} \underline{\mathbb{G}}^{R}(E) & \underline{\mathbb{G}}^{K}(E) \\ 0 & \underline{\mathbb{G}}^{A}(E) \end{pmatrix} \tag{B.6}$$

the corresponding rotation is

$$\hat{S} \longrightarrow \underline{\hat{S}} = \begin{pmatrix} \hat{S} & 0 \\ 0 & \hat{S} \end{pmatrix}_{8\times 8} \tag{B.7}$$

and the resulting Green's function is

$$\begin{aligned} \underline{g}(E) &= \begin{pmatrix} \hat{S} & 0 \\ 0 & \hat{S} \end{pmatrix} \begin{pmatrix} \underline{\mathbb{G}}^{R}(E) & \underline{\mathbb{G}}^{K}(E) \\ 0 & \underline{\mathbb{G}}^{A}(E) \end{pmatrix} \begin{pmatrix} \hat{S} & 0 \\ 0 & \hat{S} \end{pmatrix} \\ &= \begin{pmatrix} \hat{S}\underline{\mathbb{G}}^{R}(E)\hat{S} & \hat{S}\underline{\mathbb{G}}^{K}(E)\hat{S} \\ 0 & \hat{S}\underline{\mathbb{G}}^{A}(E)\hat{S} \end{pmatrix} = \begin{pmatrix} \underline{g}^{R}(E) & \underline{g}^{K}(E) \\ 0 & \underline{g}^{A}(E) \end{pmatrix} \end{aligned} \tag{B.8}$$

where

$$\underline{g}^{\alpha}(E) = \left(\begin{array}{cc|cc} A^{\alpha}(E) & B^{\alpha}(E) & & \\ -B^{\alpha}(E) & -A^{\alpha}(E) & & \\ \hline & & A^{\alpha}(E) & -B^{\alpha}(E) \\ & & B^{\alpha}(E) & -A^{\alpha}(E) \end{array}\right) = A^{\alpha}(E)\hat{\tau}_0 \otimes \hat{s}_z + iB^{\alpha}(E)\hat{\tau}_z \otimes \hat{s}_y \quad \text{(B.9)}$$

with $\alpha = R, A, K$.

Appendix C

Fourier Transform of the Keldysh Green's Functions

Any field operator representing charged particles $\psi(\mathbf{x},t)$ transforms according to

$$\psi(\mathbf{x},t) \longrightarrow \tilde{\psi}(\mathbf{x},t) = e^{ie\chi(\mathbf{x},t)}\psi(\mathbf{x},t), \tag{C.1}$$

under the gauge transformation

$$\varphi(\mathbf{x},t) \longrightarrow \varphi(\mathbf{x},t) + \frac{\partial}{\partial t}\chi(\mathbf{x},t) \tag{C.2}$$

$$\mathbf{A}(\mathbf{x},t) \longrightarrow \mathbf{A}(\mathbf{x},t) - \nabla_{\mathbf{x}}\chi(\mathbf{x},t). \tag{C.3}$$

As we know, Quantum Mechanics is gauge invariant, therefore both probability and current density of particles will be invariant under this transformation. If we have a 2×2 matrix, say, $\underline{G}^{<}(t,t')$, it transforms according to

$$\tilde{\underline{G}}^{<}(1,1') = i\begin{pmatrix} e^{ie(\chi(1)-\chi(1'))}\langle\psi^{\dagger}_{\uparrow}(1')\psi_{\uparrow}(1)\rangle & e^{ie(\chi(1)+\chi(1'))}\langle\psi_{\downarrow}(1')\psi_{\uparrow}(1)\rangle \\ -e^{-ie(\chi(1)+\chi(1'))}\langle\psi^{\dagger}_{\uparrow}(1')\psi^{\dagger}_{\downarrow}(1)\rangle & -e^{-ie(\chi(1)-\chi(1'))}\langle\psi_{\downarrow}(1')\psi^{\dagger}_{\downarrow}(1)\rangle \end{pmatrix} \tag{C.4}$$

$$= e^{ie\chi(1)\hat{\tau}_z}\underline{G}^{<}e^{-ie\chi(1')\hat{\tau}_z}, \tag{C.5}$$

where we have called $1 \equiv (\mathbf{x}, t)$ and we have used the fact that

$$e^{i\alpha\hat{\tau}_3} = \cos(\alpha)\mathrm{I} + i\sin(\alpha)\hat{\tau}_z = \begin{pmatrix} e^{i\alpha} & 0 \\ 0 & e^{-i\alpha} \end{pmatrix}. \tag{C.6}$$

In our case, the Green function is in Keldysh-Nambu-Spin spaces, but each component of the Superconductor Green's function is in the Nambu-spin 4×4 space

$$\underline{g}^{\alpha} = A^{\alpha}\hat{\tau}_0 \otimes \hat{s}_z + iB^{\alpha}\hat{\tau}_z \otimes \hat{s}_y \tag{C.7}$$

where the index α denotes R, A, K. The off-diagonal Green's function on a s-wave superconductor depends on the phase of the order parameter $\exp(\pm i\phi(t))$ where

$$\phi(t) = \phi_0 + 2e\int_0^t d\bar{t}V(\bar{t}) \tag{C.8}$$

and $V(t)$ is the electric potential of the electrode. Therefore, at nonzero voltages V we have a Floquet periodic time-dependent problem with a basic frequency $\omega_0 = \frac{d\phi(t)}{dt} = 2eV$. In this sence, at constant applied voltage V, the tunneling between two superconductors is described by a GF's which depends on time via a phase of the order parameter[90]. The non-equilibrium Green's function of the superconductor $\tilde{g}^{\alpha}$ acquires a form

$$\underline{\tilde{g}}^{\alpha}(t-t') = \exp\left[i\frac{\phi(t)\hat{\tau}^z}{2}\right]\underline{g}^{\alpha}(t-t')\exp\left[-i\frac{\phi(t')\hat{\tau}^z}{2}\right], \tag{C.9}$$

where

$$\hat{\tau}^z = \begin{pmatrix} \hat{\tau}_z & \\ & \hat{\tau}_z \end{pmatrix} \tag{C.10}$$

In a matrix form

$$\begin{aligned}
\underline{\tilde{g}}^{\alpha}(t-t') &= \begin{pmatrix} e^{\frac{i}{\hbar}eV\hat{\tau}_3 t} & 0 \\ 0 & e^{-\frac{i}{\hbar}eV\hat{\tau}_3 t} \end{pmatrix} \begin{pmatrix} \underline{\Gamma}_{2\times 2}(t-t') & 0 \\ 0 & \underline{\Omega}_{2\times 2}(t-t') \end{pmatrix} \begin{pmatrix} e^{-\frac{i}{\hbar}eV\hat{\tau}_3 t'} & 0 \\ 0 & e^{\frac{i}{\hbar}eV\hat{\tau}_3 t'} \end{pmatrix} \\
&= \begin{pmatrix} e^{\frac{i}{\hbar}eV\hat{\tau}_3 t}\underline{\Gamma}(t-t')_{2\times 2}e^{-\frac{i}{\hbar}eV\hat{\tau}_3 t'} & 0 \\ 0 & e^{-\frac{i}{\hbar}eV\hat{\tau}_3 t}\underline{\Omega}(t-t')_{2\times 2}e^{\frac{i}{\hbar}eV\hat{\tau}_3 t'} \end{pmatrix} \qquad \text{(C.11)} \\
&= \begin{pmatrix} \underline{\tilde{\Gamma}}(t-t') & 0 \\ 0 & \underline{\tilde{\Omega}}(t-t') \end{pmatrix} \qquad \text{(C.12)}
\end{aligned}$$

with $\underline{\tilde{\Gamma}}, \underline{\tilde{\Omega}}$ are 2-dimensional matrices in Nambu space given by Eq. (C.7). For $\underline{\tilde{\Gamma}}$ we have

$$\underline{\tilde{\Gamma}}(t-t') = \begin{pmatrix} e^{\frac{i}{\hbar}eVt} & 0 \\ 0 & e^{-\frac{i}{\hbar}eVt} \end{pmatrix} \begin{pmatrix} A^{\alpha}(t-t') & B^{\alpha}(t-t') \\ -B^{\alpha}(t-t') & -A^{\alpha}(t-t') \end{pmatrix} \begin{pmatrix} e^{-\frac{i}{\hbar}eVt'} & 0 \\ 0 & e^{\frac{i}{\hbar}eVt'} \end{pmatrix}. \quad \text{(C.13)}$$

The Fourier transform for each elements is

$$\begin{aligned}
\underline{\tilde{\Gamma}}_{11}(E,E') &\equiv \langle E|A^{\alpha}(t-t')|E'\rangle \\
&= \int_{\mathbb{R}} dt \int_{\mathbb{R}} dt' e^{-\frac{i}{\hbar}Et+\frac{i}{\hbar}E't'} e^{\frac{i}{\hbar}eVt} A^{\alpha}(t-t') e^{-\frac{i}{\hbar}eVt'} \\
&= \int_{\mathbb{R}} dt \int_{\mathbb{R}} dt' A^{\alpha}(t-t') e^{\frac{i}{\hbar}eV(t-t')} e^{-\frac{i}{\hbar}E(t-t')} e^{-\frac{i}{\hbar}(E-E')t'} \\
&= \int_{\mathbb{R}} dt' e^{-\frac{i}{\hbar}(E-E')t'} \int_{\mathbb{R}} d(t-t') e^{-\frac{i}{\hbar}(E-eV)(t-t')} A^{\alpha}(t-t') \\
&= \delta(E,E') A^{\alpha}(E-eV) \qquad \text{(C.14)}
\end{aligned}$$

$$\begin{aligned}
\underline{\tilde{\Gamma}}_{12}(E,E') &\equiv \langle E|B^{\alpha}(t-t')|E'\rangle \\
&= \int_{\mathbb{R}} dt \int_{\mathbb{R}} dt' e^{-\frac{i}{\hbar}Et+\frac{i}{\hbar}E't'} e^{\frac{i}{\hbar}eVt} B^{\alpha}(t-t') e^{\frac{i}{\hbar}eVt'} \\
&= \int_{\mathbb{R}} d(t-t') e^{-\frac{i}{\hbar}(E-eV)(t-t')} B^{\alpha}(t-t') \int_{\mathbb{R}} dt' e^{-\frac{i}{\hbar}(E-E'-2eV)t'} \\
&= \delta(E,E'+2eV) B^{\alpha}(E-eV) \qquad \text{(C.15)}
\end{aligned}$$

$$\begin{aligned}\underline{\tilde{\Gamma}}_{21}(E,E') &\equiv -\langle E|B^{\alpha}(t-t')|E'\rangle \\ &= -\int_{\mathbb{R}} dt \int_{\mathbb{R}} dt' e^{-\frac{i}{\hbar}Et+\frac{i}{\hbar}E't'} e^{-\frac{i}{\hbar}eVt} B^{\alpha}(t-t') e^{-\frac{i}{\hbar}eVt'} \\ &= -\int_{\mathbb{R}} d(t-t') e^{-\frac{i}{\hbar}(E+eV)(t-t')} B^{\alpha}(t-t') \int_{\mathbb{R}} dt' e^{-\frac{i}{\hbar}(E-E'+2eV)t'} \\ &= -\delta(E,E'-2eV) B^{\alpha}(E+eV) \end{aligned} \tag{C.16}$$

$$\begin{aligned}\underline{\tilde{\Gamma}}_{22}(E,E') &\equiv -\langle E|A^{\alpha}(t-t')|E'\rangle \\ &= -\int_{\mathbb{R}} dt \int_{\mathbb{R}} dt' e^{-\frac{i}{\hbar}Et+\frac{i}{\hbar}E't'} e^{-\frac{i}{\hbar}eVt} A^{\alpha}(t-t') e^{\frac{i}{\hbar}eVt'} \\ &= -\int_{\mathbb{R}} d(t-t') e^{-\frac{i}{\hbar}(E+eV)(t-t')} A^{\alpha}(t-t') \int_{\mathbb{R}} dt' e^{-\frac{i}{\hbar}(E-E')t'} \\ &= -\delta(E,E') A^{\alpha}(E+eV). \end{aligned} \tag{C.17}$$

Therefore, the matrix $\underline{\tilde{\Gamma}}(E,E')$ is giving by

$$\underline{\tilde{\Gamma}}(E,E') = \begin{pmatrix} \delta(E,E')A^{\alpha}(E-eV) & \delta(E,E'+2eV)B^{\alpha}(E-eV) \\ -\delta(E,E'-2eV)B^{\alpha}(E+eV) & -\delta(E,E')A^{\alpha}(E+eV) \end{pmatrix}. \tag{C.18}$$

Proceeding in the same way for the matrix $\underline{\tilde{\Omega}}(t-t')$ we obtain

$$\underline{\tilde{\Omega}}(E,E') = \begin{pmatrix} \delta(E,E')A^{\alpha}(E+eV) & -\delta(E,E'-2eV)B^{\alpha}(E+eV) \\ \delta(E,E'+2eV)B^{\alpha}(E-eV) & -\delta(E,E')A^{\alpha}(E-eV) \end{pmatrix}. \tag{C.19}$$

The 4×4 matrix becomes after the Fourier transform

$$\tilde{g}^{\alpha}(E,E') = \delta(E,E') \begin{bmatrix} A^{\alpha}(E-eV) & & & \\ & -A^{\alpha}(E+eV) & & \\ & & A^{\alpha}(E+eV) & \\ & & & -A^{\alpha}(E-eV) \end{bmatrix}$$

$$+ \quad \delta(E,E'+2eV) \begin{bmatrix} 0 & B^{\alpha}(E-eV) & 0 & 0 \\ 0 & 0 & 0 & 0 \\ 0 & 0 & 0 & 0 \\ 0 & & B^{\alpha}(E-eV) & 0 \end{bmatrix}$$

$$+ \quad \delta(E,E'-2eV) \begin{bmatrix} 0 & 0 & 0 & 0 \\ -B^{\alpha}(E+eV) & 0 & 0 & 0 \\ 0 & 0 & 0 & -B^{\alpha}(E+eV) \\ 0 & 0 & 0 & 0 \end{bmatrix}$$

Due to off-diagonal terms in $\underline{\tilde{g}}^{\alpha}$ the phase exponent does not commute with $\underline{\tilde{g}}^{\alpha}$. Therefore, the Fourier transform $\underline{\tilde{g}}$, which depends on two energies, includes energies shifted by a period of $2eV$. The lead Green's function $\underline{\tilde{g}}^{\alpha}$ may be any function (R,A or K). Then, the Green function can be written as

$$g = g(E,E) + g(E,E-2eV) + g(E,E+2eV), \tag{C.20}$$

It is important to note that we have dropped the constant phase $e^{\pm i\phi_0}$ which is justified for not very small voltages. Note that all of these Green Functions are 4×4 matrices. To recover the 8×8 superconductor Green function we have to consider the complete Green's function in the Keldysh space as we showed in Eq. (4.41).

Appendix D

The Structure of the Keldysh component

subsectionThe structure of the Keldysh component Note that from the matrix Dyson Equation

$$\begin{aligned} G &= \left[\left(G_0^{-1}\right) - \Sigma\right]^{-1} \\ &\Leftrightarrow \begin{pmatrix} G^R & G^K \\ 0 & G^A \end{pmatrix} = \begin{bmatrix} \left(G_0^{-1}\right)^R - \Sigma^R & \left(G_0^{-1}\right)^K - \Sigma^K \\ 0 & \left(G_0^{-1}\right)^A - \Sigma^A \end{bmatrix}^{-1} \\ &= \frac{1}{\underbrace{\left[\left(G_0^{-1}\right)^R - \Sigma^R\right]}_{(G^R)^{-1}} \underbrace{\left[\left(G_0^{-1}\right)^A - \Sigma^A\right]}_{(G^A)^{-1}}} \begin{bmatrix} \left(G_0^{-1}\right)^A - \Sigma^A & -\left[\left(G_0^{-1}\right)^K - \Sigma^K\right] \\ 0 & \left(G_0^{-1}\right)^R - \Sigma^R \end{bmatrix} \end{aligned} \tag{D.1}$$

Therefore, the Keldysh component is

$$\boxed{G^K = G^R\left[-\left(G_0^{-1}\right)^K + \Sigma^K\right]G^A,} \tag{D.2}$$

while the explicit form for $\left(G_0^{-1}\right)^K$ is:

$$\begin{aligned}
\left(G_0^{-1}\right) &= \begin{pmatrix} G_0^R & G_0^K \\ 0 & G_0^A \end{pmatrix}^{-1} = \frac{1}{G_0^R G_0^A} \begin{pmatrix} G_0^A & -G_0^K \\ 0 & G_0^R \end{pmatrix} \\
\Rightarrow \left(G_0^{-1}\right)^K &= \left(G_0^{-1}\right)^R (-G_0)^K \left(G_0^{-1}\right)^A \\
&= -\left(G_0^R\right)^{-1} (G_0)^K \left(G_0^A\right)^{-1}. \qquad \text{(D.3)}
\end{aligned}$$

It is important to remember that $\left(G_0^{-1}\right)^K$ contains information about the initial condition. In general, $\left(G_0^{-1}\right)^K$ is proportional to $i\eta$ in frequency space, and vanishes in the limit $\eta \to 0$, since the non-interacting system is dissipationless. Thus we have

$$\left(G_0^{-1}\right)^K = 0 \quad \Rightarrow \quad G^K = G^R \Sigma^K G^A. \qquad \text{(D.4)}$$

Appendix E

Real part of the Current

Starting with our previous result of the electric current

$$\langle\hat{j}\rangle = \mathcal{C}\mathrm{Tr}\int dE\underline{G}_M(E)\hat{\Lambda}^T\left\{\underline{G}_d(E)\hat{M}_{0z0}\underline{g}(E)\hat{M}_{x00}\underline{G}_d(E) - \underline{G}_d(tE)\hat{M}_{x00}\underline{g}(E)\hat{M}_{0z0}\underline{G}_d(E)\right\}\hat{\Lambda}, \tag{E.1}$$

it is possible to demonstrate that it corresponds to a real quantity. Indeed for the first contribution we have

$$\begin{aligned}
\underline{G}_d\hat{M}0z0\underline{g}\hat{M}_{x00}\underline{G}_d &= \underline{G}_d\hat{M}_{0z0}\underline{g}\begin{pmatrix} 0 & \hat{T}_{00}\underline{G}_d^A \\ \hat{T}_{00}\underline{G}_d^R & \hat{T}_{00}\underline{G}_d^K \end{pmatrix} \\
&= \underline{G}_d\hat{M}_{0z0}\begin{pmatrix} \underline{g}\hat{T}_{00}\underline{G}_d^R & \underline{g}^K\hat{T}_{00}\underline{G}_d^K + \underline{g}^R\hat{T}_{00}\underline{G}_d^A \\ \underline{g}^A\hat{T}_{00}\underline{G}_d^R & \underline{g}^A\hat{T}_{00}\underline{G}_d^K \end{pmatrix} \\
&= \underline{G}_d\begin{pmatrix} \hat{T}_{z0}\underline{g}\hat{T}_{00}\underline{G}_d^R & \hat{T}_{z0}\underline{g}^K\hat{T}_{00}\underline{G}_d^K + \hat{T}_{z0}\underline{g}^R\hat{T}_{00}\underline{G}_d^A \\ \hat{T}_{z0}\underline{g}^A\hat{T}_{00}\underline{G}_d^R & \hat{T}_{z0}\underline{g}^A\hat{T}_{00}\underline{G}_d^K \end{pmatrix} \\
&= \begin{pmatrix} \underline{G}_d^R\hat{T}_{z0}\underline{g}^K\underline{G}_d^R + \underline{G}_d^K\hat{T}_{z0}\underline{g}^A\underline{G}_d^R & \underline{G}_d^R\hat{T}_{z0}\underline{g}^K\underline{G}_d^K + \underline{G}_d^R\hat{T}_{z0}\underline{g}^R\underline{G}_d^A + \underline{G}_d^K\hat{T}_{z0}\underline{g}^A\underline{G}_d^K \\ \underline{G}_d^A\hat{T}_{z0}\underline{g}^A\underline{G}_d^R & \underline{G}_d^A\hat{T}_{z0}\underline{g}^A\underline{G}_d^K \end{pmatrix}
\end{aligned} \tag{E.2}$$

where we have called $\hat{T}_{z0} \equiv \hat{\tau}_z \otimes \hat{s}_0$ and the 4×4 identity matrix $\hat{T}_{00} \equiv \hat{\tau}_0 \otimes \hat{s}_0 = \mathbb{I}$ has been omitted in the last step because it is irrelevant. For the second contribution we have

$$\underline{G}_d \hat{M} x 00 \underline{g} \hat{M}_{0z0} \underline{G}_d = \begin{pmatrix} \underline{G}_d^K \underline{g}^R \hat{T}_{z0} \underline{G}_d^R & \underline{G}_d^R \underline{g}^A \hat{T}_{z0} \underline{G}_d^A + \underline{G}_d^K \underline{g}^K \hat{T}_{z0} \underline{G}_d^A + \underline{G}_d^K \underline{g}^R \hat{T}_{z0} \underline{G}_d^K \\ \underline{G}_d^A \underline{g}^R \hat{T}_{z0} \underline{G}_d^R & \underline{G}_d^A \underline{g}^K \hat{T}_{z0} \underline{G}_d^A + \underline{G}_d^A \underline{g}^R \hat{T}_{z0} \underline{G}_d^K \end{pmatrix} \tag{E.3}$$

Noting that

$$\hat{\Lambda}^T = \begin{pmatrix} 1 & 1 & -1 & 1 & 0 & 0 & 0 & 0 \\ 0 & 0 & 0 & 0 & 1 & 1 & -1 & 1 \end{pmatrix} \equiv \begin{pmatrix} \tilde{V}^\dagger & 0 \\ 0 & \tilde{V}^\dagger \end{pmatrix} \tag{E.4}$$

and

$$\underline{G}_M = \begin{pmatrix} G_M^R & G_M^K \\ 0 & G_M^A \end{pmatrix}_{2\times 2} \tag{E.5}$$

we can express the explicit form of the current in term of the dot and Majorana Green's functions. As we are only interested in the trace of the final matrix, we will consider only the diagonal terms. After multiplying by the matrices $\hat{\Lambda}^T$ and $\hat{\Lambda}$ for the left and right sides respectively, multiplying by $\bar{G}_M$ and taking the trace, the current is

$$\begin{aligned} \langle \hat{j} \rangle &= \mathcal{C} \int dE \left\{ G_M^R \tilde{V}^\dagger \left(\underline{G}_d^R \hat{T}_{z0} \underline{g}^K \underline{G}_d^R + \underline{G}_d^K \hat{T}_{z0} \underline{g}^A \underline{G}_d^R - \underline{G}_d^K \underline{g}^R \hat{T}_{z0} \underline{G}_d^R \right) \tilde{V} \right. \\ &+ G_M^K \tilde{V}^\dagger \left(\underline{G}_d^A \hat{T}_{z0} \underline{g}^A \underline{G}_d^R - \underline{G}_d^A \underline{g}^R \hat{T}_{z0} \underline{G}_d^R \right) \tilde{V} \\ &+ \left. G_M^A \tilde{V}^\dagger \left(\underline{G}_d^A \hat{T}_{z0} \underline{g}^A \underline{G}_d^K - \underline{G}_d^A \underline{g}^K \hat{T}_{z0} \underline{G}_d^A - \underline{G}_d^A \underline{g}^R \hat{T}_{z0} \underline{G}_d^K \right) \tilde{V} \right\}. \end{aligned} \tag{E.6}$$

We can rewrite the last expression and defining three sub-currents:

$$\begin{aligned} \tilde{j}_1 &= G_M^R \tilde{V}^\dagger \underline{G}_d^R \hat{T}_{z0} \underline{g}^K \underline{G}_d^R \tilde{V} - G_M^A \tilde{V}^\dagger \underline{G}_d^A \underline{g}^K \hat{T}_{z0} \underline{G}_d^A \tilde{V} \\ &= G_M^R \tilde{V}^\dagger \underline{G}_d^R \hat{T}_{z0} \underline{g}^K \underline{G}_d^R \tilde{V} - \left[G_M^R \tilde{V}^\dagger \underline{G}_d^R \hat{T}_{z0} (-\underline{g}^K) \underline{G}_d^R \tilde{V} \right]^\dagger \\ &= 2\mathbb{R}\{ G_M^R \tilde{V}^\dagger \underline{G}_d^R \hat{T}_{z0} \underline{g}^K \underline{G}_d^R \tilde{V} \} \end{aligned} \tag{E.7}$$

where we have considered that $(G^R)^* = G^A$ and $(G^K)^* = -G^K$. Is important to note that the operation $(\cdot)^\dagger$ acts over the Nambu space, so the Majorana Green's functions is

not affected when we transpose the matrices and we only conjugate them (that is because the components of the Majorana Green's functions are scalars in this case). The second current is

$$\begin{aligned}\tilde{j}_2 &= G_M^K \tilde{V}^\dagger \underline{G}_d^A \hat{T}_{z0} \underline{g}^A \underline{G}_d^R \tilde{V} - G_M^K \tilde{V}^\dagger \underline{G}_d^A \underline{g}^R \hat{T}_{z0} \underline{G}_d^R \tilde{V} \\ &= \mathbb{R}\{G_M^K \tilde{V}^\dagger \underline{G}_d^A (\hat{T}_{z0} \underline{g}^A - \underline{g}^R \hat{T}_{z0}) \underline{G}_d^R \tilde{V}\} \\ &= |t_R|^2 |t_L|^2 \mathbb{R}\{G_M^R \tilde{V}^\dagger \underline{G}_d^R \hat{T}_{z0} \underline{g}^K \hat{T}_{z0} \underline{G}_d^A \tilde{V} G_M^A \tilde{V}^\dagger \underline{G}_d^A (\hat{T}_{z0} \underline{g}^A - \underline{g}^R \hat{T}_{z0}) \underline{G}_d^R \tilde{V}\} \quad \text{(E.8)}\end{aligned}$$

and the third sub-current is

$$\begin{aligned}\tilde{j}_3 &= G_M^R \tilde{V}^\dagger \underline{G}_d^K (\hat{T}_{z0} \underline{g}^A - \underline{g}^R \hat{T}_{z0}) \underline{G}_d^R \tilde{V} + G_M^A \tilde{V}^\dagger \underline{G}_d^A (\hat{T}_{z0} \underline{g}^A - \underline{g}^R \hat{T}_{z0}) \underline{G}_d^K \tilde{V} \\ &= 2\mathbb{R}\{G_M^R \tilde{V}^\dagger \underline{G}_d^K (\hat{T}_{z0} \underline{g}^A - \underline{g}^R \hat{T}_{z0}) \underline{G}_d^R \tilde{V}\} \\ &= 2\mathbb{R}|t_L|^2 \{G_M^R \tilde{V}^\dagger \underline{G}_d^R \hat{T}_{z0} \underline{g}^K \hat{T}_{z0} \underline{G}_d^A (\hat{T}_{z0} \underline{g}^A - \underline{g}^R \hat{T}_{z0}) \underline{G}_d^R \tilde{V}\}. \quad \text{(E.9)}\end{aligned}$$

In the second and third sub-current we have used the definitions for the Majorana and Dot's Green's function

$$\begin{aligned}G_M^K &= G_M^R \Sigma_M^K G_M^A \\ &= |t_R|^2 G_M^R \tilde{V}^\dagger G_{\underline{d}}^K \tilde{V} G_M^A \quad \text{(E.10)}\end{aligned}$$

and

$$\begin{aligned}G_d^K &= G_d^R \Sigma_d^K G_d^A \\ &= |t_L|^2 \underline{G}_d^R \left[\alpha_- \underline{g}^K \alpha_+\right] \underline{G}_d^A \\ &\xrightarrow{\alpha \to 0} |t_L|^2 \underline{G}_d^R \hat{T}_{z0} \underline{g}^K \hat{T}_{z0} \underline{G}_d^A, \quad \text{(E.11)}\end{aligned}$$

which are consequences of the final expression of the Appendix (D).

Inserting $\tilde{j}_1, \tilde{j}_2, \tilde{j}_3$ into (4.73) we have the real quantity

$$\langle \hat{j} \rangle = \frac{1}{4} t_R^2 t_L^2 \mathrm{tr} \int dE \left(\tilde{j}_1 + \tilde{j}_2 + \tilde{j}_3\right) \quad \text{(E.12)}$$

where tr stands for the trace over Floquet states and t_R, t_L real constants.

Appendix F

Coulomb interaction

The Coulomb interaction for the dot's electrons has the form

$$\hat{H}_I = U\hat{n}_\uparrow\hat{n}_\downarrow \tag{F.1}$$

where the number operator of spin σ is $\hat{n}_\sigma = \hat{d}^\dagger_\sigma\hat{d}_\sigma$ with $\sigma = \{\uparrow,\downarrow\}$. We know that

$$(\hat{n}_\uparrow + \hat{n}_\downarrow)^2 = \hat{n}^2_\uparrow + \hat{n}^2_\downarrow + \hat{n}_\uparrow\hat{n}_\downarrow + \hat{n}_\downarrow\hat{n}_\uparrow, \tag{F.2}$$

but

$$\begin{aligned}\hat{n}_\uparrow\hat{n}_\downarrow &= \hat{d}^\dagger_\uparrow\hat{d}_\uparrow\hat{d}^\dagger_\downarrow\hat{d}_\downarrow = \hat{d}^\dagger_\uparrow(\delta_{\uparrow\downarrow} - \hat{d}^\dagger_\downarrow\hat{d}_\uparrow)\hat{d}_\downarrow \\ &= -\hat{d}^\dagger_\uparrow\hat{d}^\dagger_\downarrow\hat{d}_\uparrow\hat{d}_\downarrow = -\hat{d}^\dagger_\downarrow\hat{d}^\dagger_\uparrow\hat{d}_\downarrow\hat{d}_\uparrow \\ &= \hat{n}_\uparrow\hat{n}_\downarrow. \end{aligned} \tag{F.3}$$

Therefore

$$(\hat{n}_\uparrow + \hat{n}_\downarrow)^2 = \hat{n}^2_\uparrow + \hat{n}^2_\downarrow + 2\hat{n}_\uparrow\hat{n}_\downarrow. \tag{F.4}$$

However, the $\hat{d}^{(\dagger)}$ operators are actually fermion operators, so they satisfy

$$(\hat{d}^\dagger\hat{d})^2 = \hat{d}^\dagger\hat{d} \qquad \text{and} \qquad (\hat{d}^\dagger)^2 = (\hat{d})^2 = 0. \tag{F.5}$$

Using these relations we have finally

$$\boxed{\hat{n}_\uparrow \hat{n}_\downarrow = \frac{1}{2}\left[(\hat{n}_\uparrow + \hat{n}_\downarrow)^2 - (\hat{n}_\uparrow + \hat{n}_\downarrow)\right].} \tag{F.6}$$

The next step is to obtain $(\hat{n}_\uparrow + \hat{n}_\downarrow)$ using the 4-component spinors (4.2). It is easy to verify that

$$(\hat{n}_\uparrow + \hat{n}_\downarrow) = \frac{1}{2}\hat{d}^\dagger \left(\hat{\tau}_z \otimes \hat{s}_0\right) \hat{d}. \tag{F.7}$$

So, the Coulomb interaction in terms od the spinors has the form

$$\hat{H}_I = \frac{U}{2}\left[\left(\frac{1}{2}\hat{d}^\dagger \left(\hat{\tau}_z \otimes \hat{s}_0\right) \hat{d}\right)^2 - \frac{1}{2}\hat{d}^\dagger \left(\hat{\tau}_z \otimes \hat{s}_0\right) \hat{d}\right] \tag{F.8}$$

Mean Field Approximation

In the mean field approximation we replace the product between two operator $\hat{A}, \hat{B}$ according to

$$\hat{A}\hat{B} \cong \langle \hat{A} \rangle \hat{B} + \hat{A}\langle \hat{B} \rangle - \langle \hat{A} \rangle \langle \hat{B} \rangle. \tag{F.9}$$

According to this, the Coulomb interaction will be

$$U\hat{n}_\uparrow \hat{n}_\downarrow \cong U\langle \hat{n}_\uparrow \rangle \hat{n}_\downarrow + U\hat{n}_\uparrow \langle \hat{n}_\downarrow \rangle - U\langle \hat{n}_\uparrow \rangle \langle \hat{n}_\downarrow \rangle. \tag{F.10}$$

Noting that

$$\hat{d}^\dagger \left(\hat{\tau}_z \otimes \hat{s}_0\right) \hat{d} = 2\hat{n}_\uparrow + 2\hat{n}_\downarrow \tag{F.11}$$

$$\hat{d}^\dagger \left(\hat{\tau}_0 \otimes \hat{s}_z\right) \hat{d} = 2\hat{n}_\uparrow - 2\hat{n}_\downarrow, \tag{F.12}$$

so, we can write the number operators in a convenient form

$$\hat{n}_\uparrow = \frac{1}{4}\left[\hat{d}^\dagger \left(\hat{\tau}_z \otimes \hat{s}_0\right) \hat{d} + \hat{d}^\dagger \left(\hat{\tau}_0 \otimes \hat{s}_z\right) \hat{d}\right] \tag{F.13}$$

$$\hat{n}_\downarrow = \frac{1}{4}\left[\hat{d}^\dagger \left(\hat{\tau}_z \otimes \hat{s}_0\right) \hat{d} - \hat{d}^\dagger \left(\hat{\tau}_0 \otimes \hat{s}_z\right) \hat{d}\right]. \tag{F.14}$$

Then, in the Mean Field Approximation, the Coulomb interaction reads

$$H_I^{\mathrm{MF}} = \frac{U}{4}\left[\hat{d}^\dagger\left(\hat{\tau}_z\otimes\hat{s}_0\right)\hat{d} + \hat{d}^\dagger\left(\hat{\tau}_0\otimes\hat{s}_z\right)\hat{d}\right]\langle\hat{n}_\downarrow\rangle \tag{F.15}$$

$$+ \frac{U}{4}\left[\hat{d}^\dagger\left(\hat{\tau}_z\otimes\hat{s}_0\right)\hat{d} - \hat{d}^\dagger\left(\hat{\tau}_0\otimes\hat{s}_z\right)\hat{d}\right]\langle\hat{n}_\uparrow\rangle - U\langle\hat{n}_\uparrow\rangle\langle\hat{n}_\downarrow\rangle. \tag{F.16}$$

Including the mean field term into the dot's Hamiltonian, we have

$$H_d = \frac{1}{2}\hat{d}^\dagger\left[\left(\varepsilon + \frac{U}{2}[\langle\hat{n}_\uparrow\rangle + \langle\hat{n}_\downarrow\rangle]\right)\hat{\tau}_z\otimes\hat{s}_0 + \left(H - \frac{U}{2}\left[\langle\hat{n}_\uparrow\rangle - \langle\hat{n}_\downarrow\rangle\right]\right)\hat{\tau}_0\otimes\hat{s}_z\right]\hat{d} - U\langle\hat{n}_\uparrow\rangle\langle\hat{n}_\downarrow\rangle \tag{F.17}$$

$$= \frac{1}{2}\hat{d}^\dagger\begin{pmatrix} \varepsilon + H + U\langle\hat{n}_\downarrow\rangle & 0 & 0 & 0 \\ 0 & \varepsilon - H + U\langle\hat{n}_\uparrow\rangle & 0 & 0 \\ 0 & 0 & -\varepsilon + H - U\langle\hat{n}_\uparrow\rangle & 0 \\ 0 & 0 & 0 & -\varepsilon - H - U\langle\hat{n}_\downarrow\rangle \end{pmatrix}\hat{d} - U\langle\hat{n}_\uparrow\rangle\langle\hat{n}_\downarrow\rangle \tag{F.18}$$

Bibliography

[1] Hasan M. Z. and C. L. Kane, 2010, Rev. Mod, Phys. **82**, 3045.

[2] Xiao-Lang Qi and Shou-Cheng Zhang, 2011, Rev. Mod. Phys. **83**, 1057.

[3] Knig M, S. Wiedman, C. Brne, A. Roth, H. Buhmann, L. W. Molenkamp, X. -L. Qi, and S. -C. Zhang, 2008, Science, **318**, 766.

[4] Moore J. E., 2010, Nature **464**, 194.

[5] Qi, X.L. and S.C. Zhang, 2010, Phys. Today **63**, 33.

[6] Egger, R., Zazunov, A. and Yeyati, A. L. (2015) *Interaction Effects on Transport in Majorana Nanowires, in Topological Insulators*, Fundamentals and Perspectives (eds F. Ortmann, S. Roche and S. O. Valenzuela), Wiley-VCH Verlag GmbH & Co. KGaA, Weinheim, Germany.

[7] Takahashi R. and S. Murakami, 2010, Phys. Rev. B **81**, 161302.

[8] Majorana, E. 1937, Nuovo Cimento **14**, 171.

[9] Di Bari, P. 2012, Contemp. Phys. **53**, 315.

[10] Fukugita, M. and T. Yanagida, 1986, Phys. Rev. Lett. **174**, 45.

[11] Beenakker, C. W. J., 2013, Annu. Rev. Condens. Matter Phys. **4**, 113.

[12] Elliot, S. R. and M. Franz, 2015, Rev. Mod. Phys. **87**, 137.

[13] Moore, G., and N. Read, 1991, Nucl. Phys. B **360**, 362.

[14] Nayak, C., S. H. Simon, A. Stern, M. Freedman, and S. Das Sarma, 2008, Rev. Mod. Phys. **80**, 1083.

[15] Stern, A. 2010, Nature **464**, 187.

[16] Ivanov,D. A., 2001, Phys. Rev. Lett. **86**, 268.

[17] Kitaev A. Yu, 2001, Phys. Usp. **44**, 131.

[18] Mourik, V. 2012, Science **336**, 6084.

[19] Das, A., Y. Ronen, Y. Most, Y. Oreg, M. Heiblum, and H. Shtrikman, 2012, Nat. Phys. **8**, 887.

[20] Alicea, J., 2012, Rep. Prog. Phys. **75**, 076501.

[21] Andreev, A. F., 1964, Zh. Esxp. Teor. Fiz. **46**, 1823 [Sov. Phys. JETP **19**, 1228 (1964)]

[22] Beenakker, C.W.J., 2000, *Why Does a Metal-Superconductor Junction Have a Resistance?* in *Quantum Mesoscopic Phenomena and Mesoscopic Devices in Microelectronics* (Springer, Germany)

[23] Dubi, Y. and M. Di Ventra, 2011, Rev. Mod. Phys. **83**, 131.

[24] Ziman, J. M. 1960 *Electrons and Phonons* (Oxford University Press, Cambridge, England).

[25] Ashcroft N. W and N. Mermin 1976 *Solid State Physics* (Cengage Learning, USA.)

[26] Bulusu A. and D.G. Walker, 2008, Superlattuces and Microstructures, **44**, 1.

[27] Peskin, M.E. and D.V. Schroeder 1995 *An Introduction to Quantum Field Theory* (Westview Press, Boulder, USA).

[28] Zinn-Justin J. 2002 *Quantum Field Theory and Critical Phenomena* 4th ed. (Oxford University Press, Oxford, England).

[29] Bonitz, M., 2016. *Quantum Kinetic Theory* (Springer, Berlin, Germany), 2nd Ed.

[30] Kadanoff, L.P. and G. Baym, 1962, *Quantum Statistical Mechanics* (Benjamin, New York, USA).

[31] Abrikosov, A.A, L.P. Gorkov, and I.E. Dzyaloshinski, 1975, *Methods of Quantum Field Theory in Statistical Physics* (Dover, New York)

[32] Martin P.C and J.Schwinger 1959, Phys.Rev. **115**,1342.

[33] Schwinger, J. 1961, J. Math. Phys. **2**, 407.

[34] Konstantinov, O.V, and V.I. Perel' 1960, Zh.Eksp. Teor. Fiz **39**,197 [Sov.Phys. JETP **12**, 142 (1961)].

[35] Stefanucci, G. and R. Van Leeuwen, 2013, *Non-Equilibrium Many-Body Theory of Quantum Systems* (Cambridge University Press, Cambridge, England).

[36] Dzyaloshiski, I.E. 1962, Zh. Eskp. Teor. Fiz. **42**, 1126 [Sov. Phys.JETP **15**, 778 (1962)].

[37] Keldysh, L.V., P. 1964, Zh.Eksp. Teor. Fiz **47**,1515 [Sov.Phys. JETP **20**, 1018 (1965)].

[38] Eliashberg, G.M, 1971, Zh. Eskp. Teor. Fiz. **61**, 1254 [Sov. Phys.-JETP **34**, 668 (1972)].

[39] Altland A. and B. Simons *Condensed Matter Field Theory*, 2010 (Cambridge University Press, Cambridge, England).

[40] Calzetta, E.A. and Hu B-L, B. 2011, *Nonequilibrium Quantum Field Theory* (Cambridge University Press, Cambridge, England).

[41] Kamenev, A., 2011. *Field theory of Non-Equilibrium Systems* (Cambridge University Press, Cambridge, England).

[42] Sieberer, L.M, M. Buchhold and S. Diehl, 2016, Rep. Prog. Phys. **79** 096001.

[43] Haug, H. and A.P. Jauho, 2008, *Quantum Kinetics in Transport and Optics of Semiconductors* (Springer, Berlin, Germany), 2nd Ed.

[44] Rammer, J. and H. Smith, 1986, Re. Mod. Phys. **58**, 323.

[45] Rammer J. 2007, *Quantum Field Theory of Non-equilibrium States* (Cambridge University Press, Cambridge, England).

[46] Gell-Mann, M. and F. Low, 1951, Phys. Rev. **84**, 350.

[47] Fetter, A.L. and J.D. Walecka, 2003, *Quantum Theory of Many-Particle Systems* (Dover, New York).

[48] Aoki, N.T, M. Eckstein, M. Kollar, T. Oka and P. Werner, 2014, Rev. Mod. Phys. **86**, 779.

[49] Itzykson, C. and J.M. Drouffe, 1989, *Statistical Field Theory, Vol.1* (Cambridge University Press, Cambridge, England).

[50] Negele, J.W and H. Orland 1998, *Quantum Many-Particle Systems* (Westview Press, Boulder, USA).

[51] Larkin A. I. and Yu. N. Ovchinnikov 1975, Zh.Eksp. Teor. Fiz **68**,1915 [Sov.Phys. JETP **46**, 155 (1977)].

[52] Wigner, E., 1932, Phys. Rev. **40**, 749.

[53] Kubo, R. 1957, J. Phys.. Soc. J. **12**, 57.

[54] Mahan, G.D, 2000, *Many-Particle Physics* (Plenum, New York, USA) 3rd ed.

[55] Qi, X.L. and S.C. Zhang, 2011, Rev. Mod. Phys. **83**, 1057.

[56] Read M. and D. Green 2000, Phys. Rev. B **61**, 10267.

[57] Sau, J.D., L.M. Lutchyn, S. Tewari, S. Das Sarma 2010, Phys. Rev. Lett. **104**, 040502.

[58] Alicea, J. 2010, Phys. Rev. B, **81**, 125318.

[59] Sau, S. Tewari, J.D., L.M. Lutchyn,T.D. Stanescu , S. Das Sarma, 2010, Phys. Rev. B. **82**, 214509.

[60] Oreg Y., G. Rafael, F. von Oppen, 2010, Phys. Rev. Lett. **105**, 177002.

[61] Stoudenmire, E.M, J. Alicea, O.A. Starykh, M.P.A. Fisher, 2011, Phys. Rev. B **84**, 014503.

[62] Sengupta K., I. Zutic, H. L. Kwon, V. M. Yakovenko, S. Das Sarma, 2001, Phys. Rev. B **63**, 144531.

[63] Law K. T., P. A. Lee, T. K. Ng, 2009, Phys. Rev. Lett. **103**, 237001.

[64] Flensberg K., 2010, Phys. Rev. B, **82**, 180516.

[65] Wimmer M., A. R. Akhmerov, J. P. Dahlhaus, C. W. J. Beenakker, 2011, New J. Phys. **13**, 053016.

[66] Setiawan F., P. M. Brydon, Jay D. Sau, S. Das Sarma 2014, Phys. Rev. B **91**, 214513.

[67] Peng Y., F. Pientka, Y. Vinkler-Aviv, L. I. Glazmann and F. von Oppen, 2015, Phys. Rev. Lett. **115**, 266804.

[68] Setiawan F., W. S. Cole, Jay D. Sau, S. Das Sarma 2017, Phys. Rev. B **95**, 020501 (R).

[69] Zazunov A., R. Egger, A. Levy Yeyati, 2016, Phys. Rev. B, **94**, 014502.

[70] Chevallier D. and J. Klinovaja 2016, Phys. Rev. B **94**, 035417.

[71] Nilsson, J., A. R. Akhmerov, C. W. J. Beenakker, 2008, Phys. Rev. Lett **101**, 120403.

[72] Bolech, C. J., E. Demler, 2007, Phys. Rev. Lett **98**, 237002.

[73] Chung, S. B., X. L. Qi, J. Maciejko, S. C. Zhang, 2011, Phys. Rev. B **83**, 100512.

[74] Golub, A., 2015, Phys. Rev. B **91**, 205105.

[75] Leijnse M. and K. Flensberg. 2012, Semicond. Sci. Technol. **27**, 124003.

[76] Kane C. L and M. P. A. Fisher 1996, Phys. Rev. Lett. **76**, 3192.

[77] Kim K. S. and C. Pépin 2009, Phys. Rev. Lett. **102**, 156404.

[78] Machida Y., K. Tomokuni, K. Izawa, G. Lapertort, G. Knebel, J.-P. Brison and J. Flouquet. 2013, Phys. Rev. Lett. **110**, 236402.

[79] Dong J. K., Y. Tokiwa, S. L. Bud'ko, P. C. Canfield, P. Gegenwart 2013, Phys. Rev. Lett. **110**, 176402.

[80] Crossno J. et al. 2016, Science **351**, 1058.

[81] Wakeham et al. 2011, Nat. Comm. **2**, 396.

[82] Lee S. et al. 2017, Science **355**, 371.

[83] Senthil T. and M. P. A. Fisher 2000, Phys. Rev. B **61**, 9690.

[84] Beenakker C. W. J and L. Kouwenhoven 2016, Nature **12**, 618.

[85] Bardeen, J., L. N. Cooper and J. R. Schrieffer, 1957, Phys. Rev. **108**, 1175.

[86] Gor'kov, L.P., 1958, Zh. Eskp. Teor. Fiz **34**, 735 [Sov. Phys. JETP **7**, 505, (1958)].

[87] Eilenberger, G. 1968, Z. Phys. **214**, 195.

[88] Larkin A. I. and Yu. N. Ovchinnikov 1977, Zh.Eksp. Teor. Fiz **73**, 299 [Sov.Phys. JETP **41**, 960 (1975)].

[89] Kopnin, N, 2001, *Theory of Nonequilibrium Superconductivity* (Oxford University Press, England.)

[90] Arnold, G. B., 1987, J. Low Temp. Phys. **68**.